

The Significance of Shear Zones
Within the Plutonic Section of North Arm Mountain,
Bay of Islands Ophiolite Complex, Newfoundland

A thesis presented to the Faculty
of the State University of New York
at Albany
in partial fulfillment of the requirements
for the degree of
Master of Science

College of Science and Mathematics
Department of Geological Sciences

Katrina A. J. Idleman

1985

The Significance of Shear Zones
Within the Plutonic Section of North Arm Mountain,
Bay of Islands Ophiolite Complex, Newfoundland

Abstract of
A thesis presented to the Faculty
of the State University of New York
at Albany
in partial fulfillment of the requirements
for the degree of
Master of Science

College of Science and Mathematics
Department of Geological Sciences

Katrina A. J. Idleman

1985

ABSTRACT

The most commonly observed structures in studies of the ocean floor in the vicinity of mid-ocean ridges are inward- and outward-facing, axis-parallel and axis-oblique normal faults. The characteristics of these faults at depth is not well known due to the limitations inherent in marine geological work. Shear zones within the plutonic portion of the North Arm Mountain massif, Bay of Islands Ophiolite Complex, western Newfoundland, are likely to have formed as deep level expressions of mid-ocean ridge bounding normal faults.

The mineral assemblage of the shear zones is hornblende + calcic plagioclase, with minor clinopyroxene, sphene, chlorite, opaques, and quartz. Plagioclase and hornblende compositions suggest that shear zone formation took place under lower amphibolite conditions. A minimum temperature of formation of 420 °C is estimated.

The shear zones are S-C mylonites in which the c-surfaces form the main mylonitic foliation. The sense of shear across each of the shear zones was determined, mainly using microstructural criteria. This sense of offset information, combined with reconstruction of the massif to its pre-obduction configuration, suggests that the shear zones formed as mid-ocean ridge related axis-parallel and axis-oblique normal faults. Some of these faults formed dipping towards the spreading axis, while others dipped away from the axis.

ACKNOWLEDGEMENTS

This project could not have been completed without the help and support of many people. Dr. J.F. Casey of University of Houston suggested the problem, provided funding, and generously agreed to be a member of my thesis committee.

Dr. W.S.F. Kidd, as advisor, willingly provided advice, encouragement, and careful thesis editing. Discussions with Bill have helped clarify my views of many topics.

I would like to thank Drs. A. Miyashiro and W.D. Means for their guidance in the areas of metamorphic petrology and structural geology, respectively, and for taking the time to carefully review portions of this thesis.

Many thanks go to Steve Komor and to the Boys of Halibut Head. They helped to make my time on North Arm Mountain not just tolerable, but enjoyable.

I would like to thank my parents, Hans and Anne-Marie Jensen, for instilling in me the love of the outdoors which first prompted me to study geology. The support and encouragement of all of the members of the Jensen and Idleman families have been a great help to me throughout my time as a graduate student.

Thanks also go to thank all of my friends and fellow graduate students for helping to make my time at Albany as enjoyable as it has been. Without various parties, potlucks, and excursions, life as a graduate student would have been quite dull. Susan Coughlin, in particular, has been a great provider of a balanced point of view of life.

Special thanks go to my husband, Bruce. Along the way, Bruce has

provided support, encouragement, time, advice, cajoling, and more support, without which completion of this thesis would have been impossible.

Funding for field work done during this study was provided by NSF Grant EAR 8309535.

TABLE OF CONTENTS

	Page
ABSTRACT	
ACKNOWLEDGEMENTS	
TABLE OF CONTENTS	
LIST OF FIGURES	
LIST OF TABLES	
CHAPTER 1: INTRODUCTION	1
A. Purpose	1
B. Previous Work	1
C. Location and Physiography	3
D. Field Methods	6
CHAPTER 2: THE EARLY PALEOZOIC GEOLOGY OF WESTERN NEWFOUNDLAND .	7
A. Introduction	7
B. Basement and Autochthon	9
C. The Allochthonous Terrain	12
1. The Sedimentary Allochthon	12
2. The Neoautochthon	14
3. The Ophiolitic Allochthon	14
a. The Coastal Complex	14
b. The Bay of Islands Assemblage	17
D. Tectonic Interpretation	18
E. Deformation Events During Which Shear Zone Formation May Have Occurred	20
CHAPTER 3: FAULTING AT MID-OCEAN RIDGES	26
A. Slow Spreading Centers	26

B. Fast Spreading Centers	31
C. Moderate Spreading Centers	34
D. Effects of Transform Faults on Mid-Ocean Ridge Structures .	36
E. Summary	38
CHAPTER 4: STRUCTURE	42
A. Introduction	42
B. Field and Microscopic Observations	42
1. Country Rock	42
2. Shear Zone Boundaries and Dimensions	43
3. Foliation	66
4. Lineation	72
C. Microstructural Variations Across Shear Zone Boundaries . .	73
1. Undeformed Country Rock	73
2. Microstructures Developed Adjacent to Shear Zone Boundaries	74
3. Microstructures Developed Within the Shear Zone Boundaries	79
4. Post-Kinematic Veins	84
5. Cataclastic Zones	84
D. Sense of Shear	87
1. Structures From Which Sense of Shear may be Deduced . .	87
2. Results	102
E. Shear Zone Orientations	102
CHAPTER 5: METAMORPHISM	125
A. Analytical Technique	125
B. Shear Zone Mineral Assemblage	125
C. Interpretation	133

CHAPTER 6: CONCLUSIONS AND DISCUSSION	140
REFERENCES CITED	148

LIST OF FIGURES

Figure Number		Page
1.1	Location of the Bay of Islands Ophiolite Complex	4
2.1	Geologic map of western Newfoundland	8
2.2	Early Paleozoic evolution of western Newfoundland	21
3.1	Topography of fast, medium, and slow spreading centers .	27
3.2	Pre-obduction geometry of the Bay of Islands massifs . .	40
4.1	Undeformed diabase dike cutting mylonitized gabbro . . .	44
4.2	Simplified geologic map of the southern half of North Arm Mountain	45
4.3	Location maps	47
4.4	Large-scale maps of each study area	52
4.5	Shear zone boundary	64
4.6	Narrow splays swing into main mylonite	65
4.7	Pod of less deformed material surrounded by mylonite . .	68
4.8	Asymmetric intrafolial fold	68
4.9	Kink in a mylonite	69
4.10	Crenulation of mylonitic foliation	70
4.11	Cataclastic zone	70
4.12	Undeformed country rock	75
4.13	Fine grained, recrystallized plagioclase cutting host grain	77
4.14	Typical view adjacent to shear zone boundary	77
4.15	Amphibole rimming clinopyroxene	78
4.16	Amphibole poikilitically enclosing plagioclase	80
4.17	Fine grained amphibole bridging a fracture in a large amphibole grain	81
4.18	Recrystallizing amphibole	81
4.19	Zone of fine grained amphibole and plagioclase	83

Figure Number		Page
4.20	Adjacent fine and coarse grained zones	83
4.21	Post-kinematic vein cutting mylonitic foliation	85
4.22	Cataclastic zones	86
4.23	Summary sketch of sense of shear indicators	89
4.24	Asymmetric augen with recrystallized tails	91
4.25	Amphibole grains displaced across narrow fractures	93
4.26	Amphibole and plagioclase grains displaced across narrow fractures	94
4.27	Plagioclase and amphibole grains displaced across narrow fractures in opposite sense in the same sample	95
4.28	C- and s-surface orientations	96
4.29	Asymmetric intrafolial fold formation	98
4.30	Structure formed by rotation of a planar structure across mylonitic foliation	99
4.31	Curvature of foliation in pod of material "trapped" in shear zone	99
4.32	Unusual asymmetric grain	101
4.33	Unfolding models 1, 2, and 3	108
4.34	Stereographic projections of lineation, foliation, and slip direction orientations	111
5.1	Plot of amphibole compositions	127
5.2	Plot of plagioclase compositions	131
5.3	Plot of pyroxene compositions	132
5.4	Peristerite solvus	135
5.5	SiO ₂ vs. wt. % Al ₂ O ₃	136
5.6	Calcic-amphibole compositional gap	138
6.1	Hypothetical cross section of the oceanic crust	145

LIST OF TABLES

Table Number		Page
4.1	Summary of sense of shear criteria and reliability within each sample	103
4.2	Amount and sense of rotation of each shear zone for models 1, 2, and 3	110
4.3	Fault types and orientations resulting from unfolding after models 1, 2, and 3	124

CHAPTER 1. INTRODUCTION

A. Purpose

Studies of the ocean floor in the vicinity of mid-ocean ridges have revealed the presence of inward and outward facing normal faults which are oriented sub-parallel to the trend of ridge axes. The maximum throw on these faults ranges from tens of meters on fast spreading ridges (Francheteau and Ballard, 1983; Lonsdale, 1977a; CLIPPER-TON, 1983) up to approximately 350 meters on slow spreading ridges (Macdonald and Luyendyk, 1977). The nature, geometry, and behavior with time of these faults at depth is not well known due to obvious limitations in studying deeper levels of the in situ oceanic crust.

Ophiolites are useful as study areas of deep level oceanic crust. The North Arm Mountain Massif, one of four massifs of the Bay of Islands Ophiolite Complex of western Newfoundland, is a well-preserved, complete ophiolitic section. In his detailed mapping of the southern half of North Arm Mountain, Casey (1980) identified a number of ductile shear zones within the plutonic portion of the complex. This study of several of the shear zones was undertaken to determine if these shear zones may be preserved deep-level expressions of surface-level, axis-bounding, normal faults, and to characterize their properties if they are examples of such faults.

B. Previous Work

Ewing and Heezen (1956) and Heezen (1960) were among the first to recognize that mid-ocean ridge crests were rifts and therefore extensional features, and that earthquake activity along the ridges was

related to faulting in these rifts. Subsequent seismic work across the mid-ocean ridge system has provided a more detailed picture of its structure. For faults with significant surface displacements, inward-facing normal faults bounding the central graben or rift are present in all ridges, while the density of outward-facing normal faults outboard of the inner rift valleys increases with increasing spreading rate (Macdonald and Luyendyk, 1977; Lonsdale, 1977a,b; Crane, 1978). The orientation and characteristics of the normal faults with depth have not been clarified due to problems inherent to marine geology. Direct observation is not possible, and resolution with geophysical tools is not great enough to address this question. Dredge hauls from non-transform domains have brought up mylonites, tectonic breccias, and cataclasites derived from the plutonic section of the oceanic crust (Helmstaedt and Allen, 1977; Bonatti et al., 1975) which have been interpreted as having formed along fault-related, lower crustal shear zones; these may be deep-level extensions of the axis-parallel normal faults on the sea floor. Again, direct observation is lacking.

Well-preserved ophiolites, as pieces of oceanic crust thrust upon continental margins, are useful areas in which to study deep-level oceanic crustal structures. A number of shear zones have been mapped throughout the plutonic section of the North Arm Massif by Casey (1980), who suggested that these may be the elusive normal fault extensions (J. Casey, pers. comm.).

Two previous studies have offered interpretations of shear zones observed in the Bay of Islands Ophiolite Complex. The work of Girardeau and Mevel (1982) was carried out in the lowest portion of the cumulate gabbros (non-tectonized layered gabbros) on the Blow-me-Down

Massif. They identified two sets of shear zones within this section. The first generation of shear zones is subparallel to the gabbroic layering, while the second set crosscuts the first at an angle of approximately 60° . Girardeau and Mevel (1982) are uncertain as to the cause of these shear zones, and suggest magma chamber floor subsidence, lithospheric necking, or lithospheric response to asthenospheric flow as possibilities.

Rosencrantz (1982), in his paper on oceanic crustal formation, suggests that ductile shear zones in the uppermost gabbroic section may be extensions of shallow level normal faults.

This study has investigated shear zones across the entire gabbroic section in order to get a more comprehensive and integrated view of this type of deformation in the crust.

C. Location and Physiography

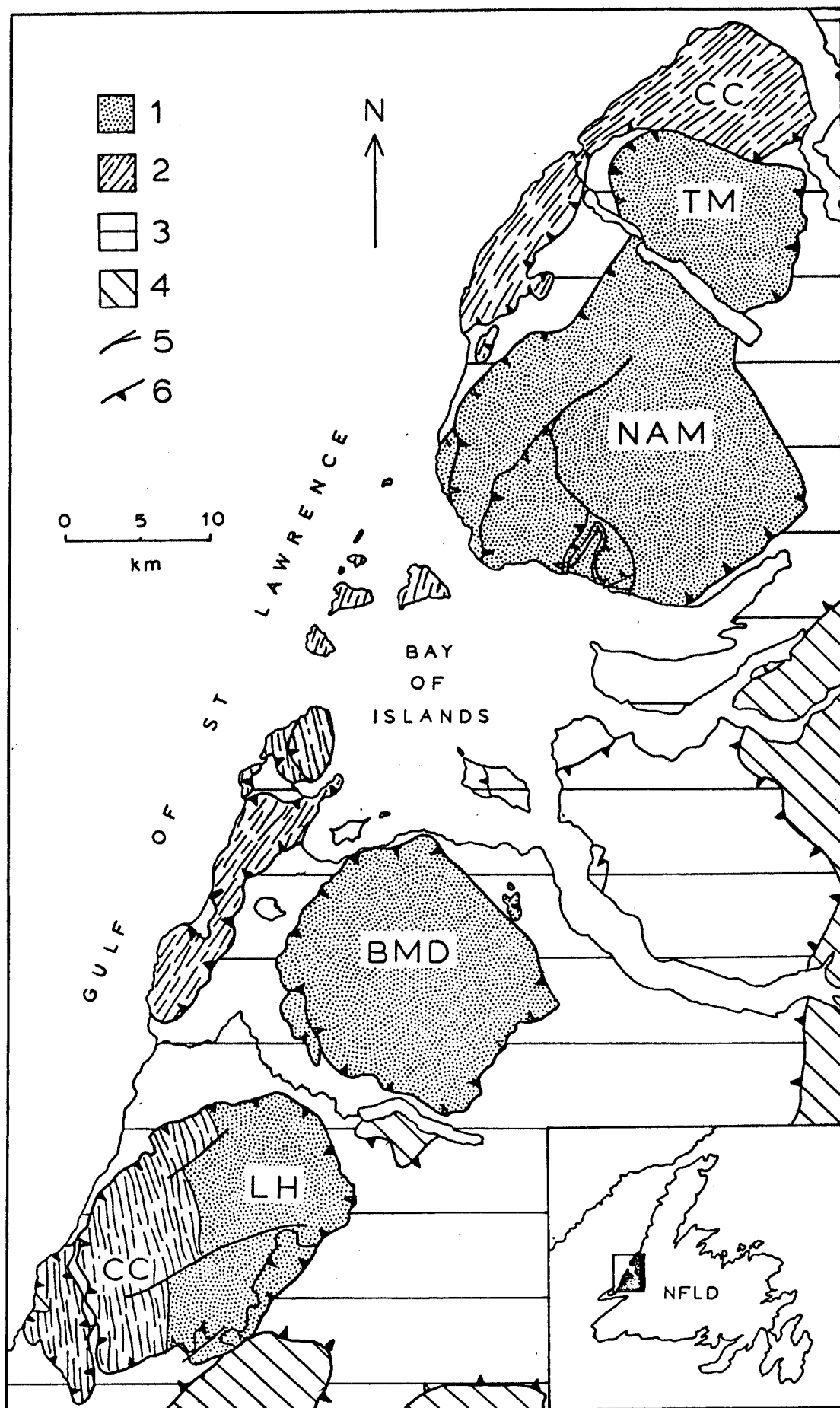
The North Arm Mountain Massif is one of four massifs which make up the Bay of Islands Ophiolite Complex of western Newfoundland (Fig. 1.1). The Bay of Islands Complex is a NNE trending belt of ophiolitic rocks which is bounded to the east by the Humber Valley, and to the west by the Gulf of St. Lawrence. North Arm Mountain is bounded to the south by the Bay of Islands and to the north by the Trout River Ponds.

North Arm Mountain forms a rolling upland plateau which is cut by steep-sided valleys and bounded on all sides by spectacular cliffs. To the south and southwest the cliffs drop into the sea, while in all other directions the base of the cliff merges with lowlands underlain by sedimentary portions of the Humber Arm Allochthon. The hilltops of

Figure 1.1.

The Bay of Islands Ophiolites. TM = Table Mountain, NAM = North Arm Mountain, BMD = Blow-me-Down, LH = Lewis Hills, CC = Coastal Complex.

- (1) Bay of Islands Assemblage
- (2) Coastal Complex
- (3) Allochthonous rocks of the Humber Arm Supergroup
- (4) Autochthon
- (5) High angle fault
- (6) Thrust fault



the uplands are generally bare rock and rubble, while the lower areas are covered with bogs and low, tangled spruce thickets referred to as "tuckamore" by the locals. The streams which dissect the plateau have cut sizeable V-shaped valleys.

North Arm Mountain is not accessible by road, so camp was set up with the help of a helicopter. Food, supplies, and mail were delivered by helicopter every two weeks, and camp moves were made during these visits every two to four weeks. Transportation, once settled on the mountain, was solely by foot which, considering the topography and vegetation, could be challenging. The shear zones which I studied were anywhere from one hundred meters to 1.5 kilometers from base camp.

D. Field Methods

The six shear zones studied were located with the help of aerial photographs at the scale of 1:15,000. These photographs are available from the Canadian Federal Government, through the Department of Mines and Technical Surveys in Ottawa. Close-up maps of each study area were prepared by setting up series of small cairns and measuring direction and distance between cairns and to all points of interest in the study area. By measuring each location relative to two other reference points, accurate large-scale reconstructions of the study areas were possible. Location maps of the study areas were prepared by enlarging sections of 1:50,000 topographic maps of the area.

CHAPTER 2. THE EARLY PALEOZOIC GEOLOGY OF WESTERN NEWFOUNDLAND

A. Introduction

The geology of Western Newfoundland has resulted from the opening of an ocean during late Precambrian to early Cambrian, and its subsequent destruction (Wilson, 1966). A generalized view of the present day geology of Western Newfoundland is given in Figure 2.1. The main features of this area are: (a) the Precambrian basement exposed along the eastern portion of the Great Northern Peninsula, (b) the autochthonous sequence of mainly shelf carbonates which unconformably overlies it, (c) continental rise-derived clastics which have been thrust over the shelf sequence, and (d) the ophiolite complexes which comprise the uppermost slices of the allochthons.

To the east, the Humber Zone is bounded by the Cabot Fault. Work in other areas of the Northern Appalachians indicates right lateral movement on this strike-slip fault (Bradley, 1982), although the amount of displacement across it is uncertain. The relationship of the rocks of the Humber Zone to the rocks of the Fleur de Lys Zone to the east has, in most locations, been obscured by movement on the Cabot Fault. However, there is one locality east of the Port-au-Port Peninsula where polyphase-deformed metasediments of the Fleur de Lys Group and the Precambrian crystalline basement which they overlies are thrust over rocks of the Humber Zone. This thrust contact may represent the "original" tectonically assembled configuration of the Humber and Fleur de Lys Zones (Dewey et al., 1983).

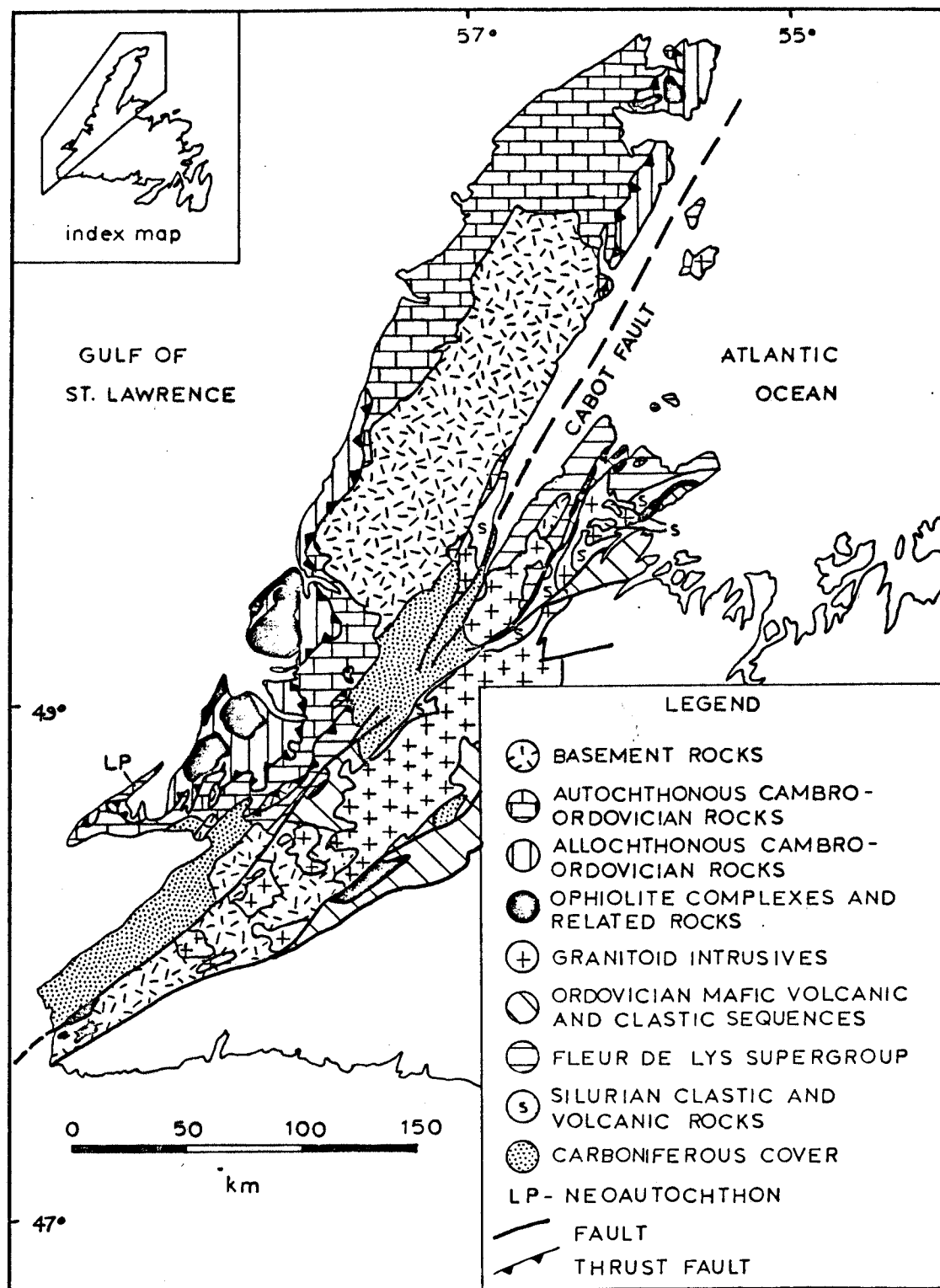


Figure 2.1

Simplified geologic map of Western Newfoundland, after Dewey, Kennedy, and Kidd (1983).

B. Basement and Autochthon

The Western Platform, or Humber Zone, of Newfoundland is underlain by Precambrian crystalline basement consisting mainly of quartzo-feldspathic gneisses. A Rb-Sr whole rock age of $1106 \pm 90^*$ Ma and a K/Ar biotite age of $851 \pm 20^*$ Ma have been measured by Pringle et al. (1971), indicating Grenville affinities. The Precambrian basement outcrops along the length of the NNE-trending Long Range and Indian Head Range Mountains.

During late Precambrian and early Cambrian, rifting of the Grenville basement occurred. NNE trending diabase dike swarms occur in southern Labrador, Belle Isle, and the Long Range Mountains (Strong and Williams, 1972). $^{40}\text{Ar}/^{39}\text{Ar}$ work on whole rock samples collected from several of the Long Range dikes give an age of $615 \pm 10^*$ Ma (Stukas and Reynolds, 1974). The dikes have been observed to feed volcanics (flood basalts (Bird and Dewey, 1970; Strong and Williams, 1972)) which generally directly overlie Precambrian basement. The volcanics are usually conformably overlain by arkoses, but in some cases they are interfingering with the lowest arkosic units (Williams and Stevens, 1969; Strong and Williams, 1972). The tholeiitic nature of the dikes and volcanics, and the fact that the volcanics are flood basalts led Bird and Dewey (1970) and Strong and Williams (1972) to suggest that they formed during the early stages of continental rifting.

The sedimentary rocks which unconformably overly the crystalline basement are immature reddish sandstones and arkoses with pebble conglomerates locally developed along the contact with the basement

* All dates reported have been recalculated according to the decay constants of Steiger and Jäger (1977).

(Schuchert and Dunbar, 1934; Williams and Stevens, 1969). On Belle Isle these clastics are intruded by and interlayered with basaltic lavas, as described previously (Williams and Stevens, 1969).

The clastics grade upward into a sequence of interbedded sandy limestones, shales, limey shales, Archaeocyathid reefs, siltstones, and silty dolostones. Cross-bedding, mud cracks and ripple marks are common primary structures (Lilly, 1967). The thickness and relative proportions of these lithologies varies considerably along the length of the Humber Zone (Brückner, 1966), but in all instances a shallow water depositional environment is most likely.

The entire sequence of clastics and shallow water carbonates and associated lithologies forms a southeastward thickening wedge. A section 150 meters thick is exposed in southern Labrador. The thickness increases to 304 meters in the Highlands of St. John, and to 914 meters in the Bonne Bay area (Lilly, 1967).

The St. George Group conformably overlies the Cambrian section. It consists of a thick sequence of interbedded shallow water limestones and dolostones which was deposited throughout the early Ordovician (Schuchert and Dunbar, 1934), indicating continued gradual subsidence of the continental margin and development of a stable continental shelf. Unlike the older section, these shelf carbonates are exposed and easily identified along the entire length of the Humber Zone. This section thickens to the east; it is 304 meters thick in the west, and over 1219 meters thick in the east (Lilly, 1967).

The contact of the St. George Group with the overlying Table Head Formation is conformable in some locations and disconformable in others. In areas where it is disconformable the uppermost portion of

the St. George Group has been eroded, resulting in karst features (Bird and Dewey, 1970).

Studies of the fauna in the lowest portion of the Table Head have shown that deposition of its base has been diachronous, with progressively younger fauna present to the west (Stevens, 1970). At the type section at Table Point (a westerly exposure of this formation) conodont studies suggest that the base of the Table Head was deposited at or just after the Arenig-Llanvirn boundary (Whittington and Kindle, 1963; Fahraeus, 1970).

The base of the Table Head Formation consists of shallow water, rubbly limestones and limestone conglomerates which grade upwards into a section of interbedded limestones and shales. The top of the section is made up entirely of black shale (Whittington and Kindle, 1963; Schuchert and Dunbar, 1934).

The conglomerates within the Table Head Formation consist of limestone blocks within a middle Ordovician shale matrix. The clasts are derived from limestones of differing ages within the Table Head. The thickness of conglomerates deposited within a limited time-span (152 meters in one graptolite zone at Cape Cormorant) suggests areas of high relief, such as fault scarps, as source areas (Stevens, 1970).

The diachronous nature of the St. George-Table Head contact and the inferred faulting within the Table Head have been interpreted as resulting from the passage of the east-facing margin over the fore-arc bulge associated with an east-dipping subduction zone to the east of that margin (Dewey et al., 1983; Nelson and Casey, 1979; Casey, 1980).

During the Llanvirnian easterly derived-flysch sedimentation began. The basal graywackes, which conformably overly the Table Head,

are fine-grained, distal facies. These grade upwards into coarse-grained, proximal graywackes. Clasts of continental rise sediments and ophiolite detritus are common in the wackes (Stevens, 1970). This sequence indicates the approach of the assembled Humber Arm Allochthons from the east. 786-1219 meters of autochthonous flysch are exposed on the Port-au-Port Peninsula. On the western Port-au-Port the flysch is conformable with the late middle Ordovician neoautochthonous Long Point Formation, which unconformably overlies the Humber Arm Allochthon in the same area (Stevens, 1970; Bergstrom et al., 1974).

C. The Allochthonous Terrain

The Hare Bay and Humber Allochthons are made up of packages of thrust slices. The lowest slices are made up of continental rise prism material, while the upper slices are ophiolites.

1. The Sedimentary Allochthon

There are two groups of rocks which comprise the sedimentary portions of the Humber Allochthon. These are the Cow Head Group (Kindle and Whittington, 1959) and the Curling Group (Stevens, 1970).

The Cow Head Group consists mainly of a very coarse breccia of limestone clasts in a shale matrix. The Cow Head Group has been interpreted as a shelf-edge deposit which resulted from periodic collapse of an oversteepened carbonate bank edge (Stevens, 1970).

The clastics of the Curling Group were deposited in deeper water to the east of the carbonate bank (Rodgers and Neale, 1963), identified by Stevens (1970) and Bird and Dewey (1970) as the continental rise. The base of this sequence consists of thick-bedded, greenish, quartz-

rich, pebbly wackes and siltstones which are interbedded with green and red shales. A Grenville source area for the wackes is suggested by the presence of mafic volcanic clasts which are similar to observed lower Cambrian basal volcanics (Williams and Stevens, 1969) and by the presence of blue quartz pebbles characteristic of Grenville basement gneisses (Stevens, 1970).

The rocks grade upwards into a section of mainly brown, gray and black shales interbedded with siltstones, quartzites, wackes, and minor oolitic limestones. Conglomerate lenses near the top of this sequence contain clasts of plutonics, limestone, siltstone, shale, and vein quartz in a matrix of well-rounded quartz sand (Brückner, 1966; Stevens, 1970).

Continuing upwards in the section a zone of interbedded, thin, platy limestones and black shale is encountered. Local limestone breccias are mainly intraformational, with some clasts derived from other portions of the section.

A complex transition zone characterized by interbedded hard and soft greenish shales with lesser amounts of limestone, dolostone, siltstone, quartzite, graywacke, and chert is overlain by easterly derived, interbedded graywackes and shales. Commencement of deposition of flysch during late Arenig marks the first influx of material from the east (Stevens, 1970). The base of the flysch unit is fine to medium grained and thin to thick bedded. Moving up section the grain size and bedding thickness increase, and massive beds up to 61 meters thick occur locally. Ophiolite detritus (chromite and serpentinite) is present in the graywackes, indicating that the ophiolite nappe was exposed by the time of flysch deposition (Stevens, 1970).

2. The Neoautochthon

On the Port-au-Port Peninsula autochthonous, easterly derived flysch of Arenig-Llanvirnian age is below a thrust contact with rocks of the Humber Arm Allochthon and is conformably overlain by neoautochthonous sediments of shallow water origin which unconformably overlie the allochthon (Stevens, 1970). The age of the base of the neoautochthonous section in this area is late Llandeilian to earliest Caradocian (Bergstrom et al., 1974), which marks the youngest age of final emplacement of the ophiolite.

3. The Ophiolitic Allochthon

The Humber Arm and Hare Bay Allochthons are structurally overlain by a sequence of thrust-bounded slices of igneous and metamorphic rocks. In the Bay of Islands area these include the Bay of Islands Ophiolite Complex, which is made up of four large massifs. From north to south these are the Table Mountain, North Arm Mountain, Blow-me-Down Mountain, and Lewis Hills Massifs. To the west of the ophiolite massifs lies a narrow belt of variably deformed and metamorphosed rocks known as the Coastal Complex (Williams, 1973).

a. The Coastal Complex

Three rock assemblages make up this complex: the Skinner Cove, The Old Man Cove, and the Little Port. The Skinner Cove Assemblage (Williams, 1973; Strong, 1974) consists of alkalic pillow lavas interbedded with minor shales and limestones and conformably overlain by flysch (Kidd and Idleman, 1982). Although the Skinner Cove is consid-

ered to be a portion of the Coastal Complex, its origin is believed to be very different from that of the Old Man Cove and the Little Port (Casey, 1985). The chemistry of these volcanics led Strong (1974) to suggest that they formed off-axis of the ridge at which the Bay of Islands Ophiolite Complex formed. This is supported by field evidence. The Skinner Cove outcrops as thrust-bounded slivers and as blocks in sedimentary melange, occurrences which are associated with the basal thrust of the Coastal Complex and the Bay of Islands Assemblage (Kidd and Idleman, 1982). These exposures suggest that the volcanics and sediments have been overridden by the higher level, ophiolitic slices of the allochthon.

The Old Man Cove Assemblage consists of poly-deformed greenschists and minor marbles with a steeply east-dipping foliation which trends NNE, parallel to the trend of the Coastal Complex. The Old Man Cove Assemblage outcrops locally in a narrow band east of the Skinner Cove coastal outcrops and west of the Little Port Assemblage.

The Little Port Assemblage, which makes up the bulk of the Coastal Complex, consists of a complex assemblage of foliated to massive amphibolitized gabbros, mafic to silicic volcanics, undeformed to deformed mafic dikes and megadikes, and foliated to massive trondhjemites and quartz diorites (Williams, 1973; Karson and Dewey, 1978). The contact between Little Port Assemblage and the Old Man Cove Assemblage, where exposed, appears to be transitional (Karson, 1977), suggesting that these assemblages may be cogenetic (Karson, 1977; Karson and Dewey, 1978). This differs from Williams (1975) interpretation, in which each assemblage is considered to have been derived from a very different setting, and to be in thrust contact with the assemblages

which bound it. Karson and Dewey (1978) have interpreted the Little Port Assemblage and the Old Man Cove Assemblage as remnants of an oceanic fracture zone. The rocks in these assemblages are deformed versions of those found in well-preserved ophiolite suites. A U/Pb zircon date from a Little Port trondhjemite gives an age of 508 ± 5 (Mattinson, 1975), which is very close to the ages determined for the Bay of Islands Ophiolite Complex. Detailed mapping in the Lewis Hills Massif by Karson (1977) has shown that the Lewis Hills Massif is in igneous contact with the Coastal Complex. In their scenario, Karson (1977) and Karson and Dewey (1978) propose that the Coastal Complex consists of oceanic crust which deformed along a right lateral transform fault. As this crust passed the opposing ridge segment, oceanic crust formed at that ridge welded onto the deformed older crust. This package of crust then passed into the fracture zone domain. Karson (1977) and Karson and Dewey (1978) also suggest that obduction of the ophiolite complexes of Western Newfoundland was initiated on this transform fault/fracture zone, a convenient pre-existing zone of weakness. However, recent geochronologic work on the Coastal Complex (B. Idleman, pers. comm.) indicates that although ages determined from igneous rocks within the Complex are very close to ages determined from the massifs, work on deformed Coastal Complex amphibolites has yielded ages comparable to the age of obduction found from the amphiboles of the metamorphic aureole (Dallmeyer and Williams, 1975). This suggests that some portion of the deformation in the Coastal Complex may be obduction, rather than transform, related.

b. The Bay of Islands Assemblage

The Bay of Islands Assemblage (Williams, 1973, 1975) includes the four Bay of Islands ophiolite massifs and their associated basal metamorphic aureoles. On Blow-me-Down and North Arm Mountains complete ophiolitic sections are preserved. The units in the pseudo-stratigraphy are, from base to top, residual mantle ultramafics (mainly harzburgite, with lesser dunite, and orthopyroxenite), magmatically derived ultramafics (dunite and wehrlite with subordinate clinopyroxenite), layered gabbros, isotropic gabbros (with minor trondhjemite and quartz diorite), sheeted diabase dikes, and pillow lavas (Casey, 1980).

Several lines of evidence suggest that the Bay of Islands Ophiolite Complex formed on the NE side of a NW-SE trending ridge axis (present day orientations). The dikes in the sheeted dike complex on the southern half of North Arm Mountain trend approximately NW, indicating that the paleo-ridge axis trended NW relative to the present orientation of this part of the Complex. One way chilling statistics on North Arm Mountain show that the paleo-ridge axis lay to the southwest of the massif (Rosencrantz, 1980). The growth direction of dendritic olivine crystals which grew perpendicular to compositional layering within the gabbros indicates formation on the NE wall of the paleo-magma chamber (Casey, 1980). The sense of large scale curvature of the compositional layering itself also suggests that the Bay of Islands massifs formed on the NE side of a NW-SE trending ridge (Casey and Karson, 1981).

Geochronologic work on the Bay of Islands ophiolites has yielded a U/Pb zircon age of 504 ± 10 Ma (Mattinson, 1976) from a trondhjemite,

and ages of 508 ± 6 Ma and 501 ± 13 Ma from Sm/Nd isochrons of a pyroxene gabbro (Jacobsen and Wasserburg, 1979). These dates fall close to the Cambro-Ordovician boundary.

A thin (<300 meters) metamorphic aureole is present at the base of the ophiolite section. The metamorphic grade decreases rapidly as distance from the base of the ophiolitic section increases (from pyroxene amphibolite down to virtually unmetamorphosed sediments (Casey, 1980)). The aureole is interpreted as the initial obduction-related detachment zone (Williams and Smyth, 1973; Malpas, 1979). Its age may reflect the youngest age of obduction (Casey and Dewey, 1984).

On North Arm Mountain a group of parallochthonous sedimentary rocks unconformably overlie the rocks of the ophiolite suite (Casey and Kidd, 1981). The basal portion of the section is made up of sedimentary breccias containing largely ophiolitic-derived clasts. These breccias are overlain by mainly red and maroon shales with less abundant pale gray, black, and green shales, and pebbly mudstones of gray, green, black, and red. Large blocks of ophiolite-derived lithologies are occasionally present in the shales. Within the shales of this unit Llanvirnian age fossils have been found. The uppermost unit in this section consists of coarse grained, reddish arenites (Casey and Kidd, 1981).

D. Tectonic Interpretation

The first event recorded in the geology of Western Newfoundland is the rifting of Precambrian continental crust in latest Precambrian or earliest Cambrian. Late Precambrian to early Cambrian sediments are immature arkoses and sandstones, interfingered with volcanics. Deeper water facies deposited during the same time period consist of pebbly

wackes and siltstones.

Rift-related sedimentation was followed by development of a carbonate bank along the east-facing North American margin, starting in mid-early Cambrian. A stable system existed from early Cambrian until early Ordovician. During this time shelf, slope, and rise sedimentation continued, and the oceanic crust and upper mantle now exposed in the Bay of Islands Ophiolite Complex was formed farther from the edge of the continent (see section 3, this chapter).

The first sedimentological evidence of change in this system is the influx of easterly derived flysch onto continental rise sediments during late Arenig. Ophiolite detritus within the flysch indicates that uplift of oceanic lithosphere outboard of the continental margin sequence must have commenced by this time, presumably because of subduction and accretion beneath the obducted lithosphere. The collision of an island arc which formed over an east dipping subduction zone with the passive margin of North America accounts for the basic present arrangement of the early Paleozoic geology of western and central Newfoundland.

The passage of the carbonate shelf over the fore-arc bulge is recorded in the diachronous disconformity (at the Arenig-Llanvirn boundary in the western Humber Zone) between the St. George Group and the Table Head Formation. Further evidence for the passage of the shelf over the bulge and down into the subduction zone includes probable fault-related conglomerates in the Table Head and the relatively abrupt change from shallow to deep water sedimentation recorded in the Table Head section (shallow water limestones to graptolite-bearing shales).

The youngest age of the last movement of the Humber Arm Allochthon is late Llandeilian to earliest Caradocian, the age of the base of the neoautochthon at Long Point.

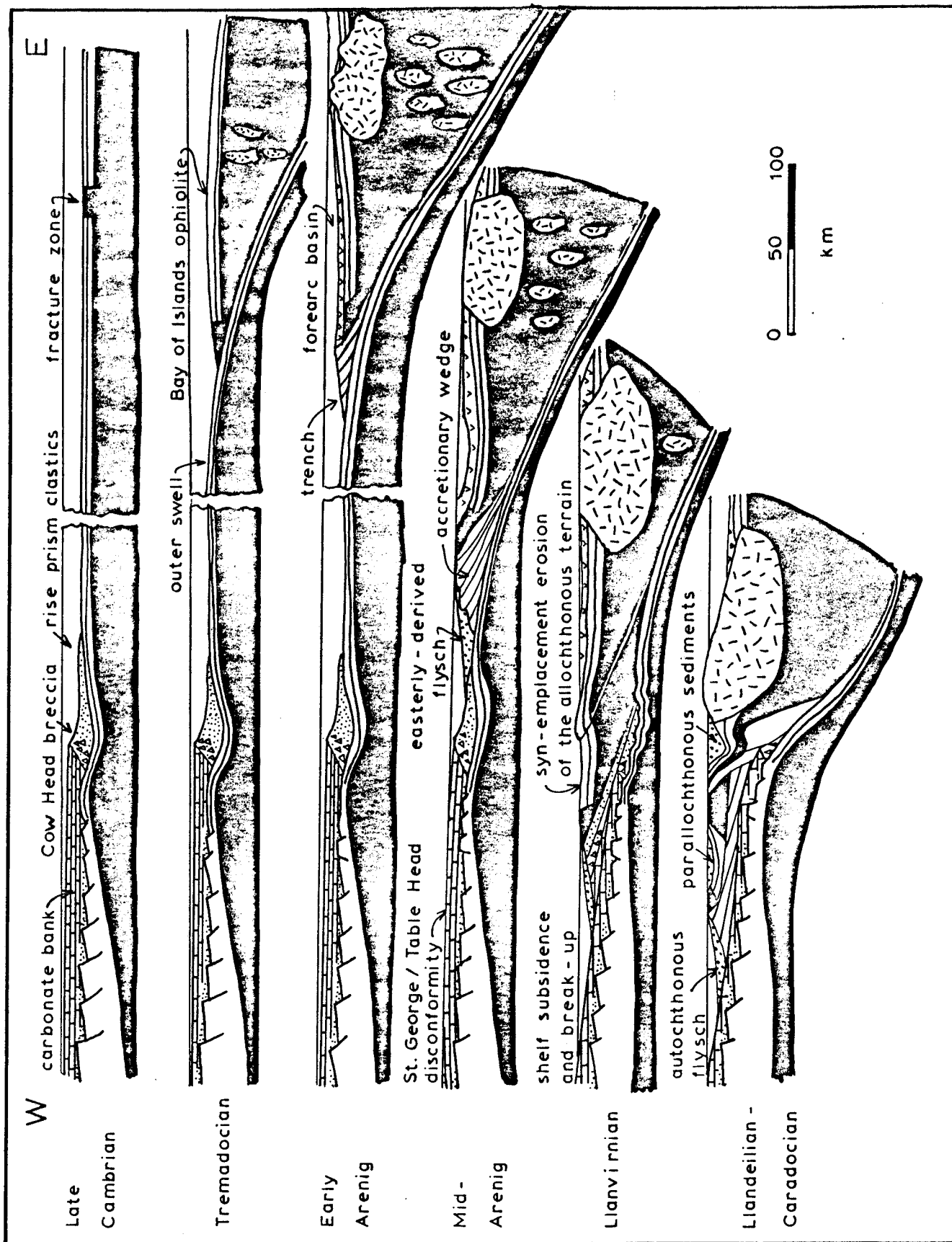
The assembly of the allochthon began well to the east of the North American margin. After thrusting initiated, progressively younger thrusts cut through progressively further west. In other words, the allochthon grew by addition of new thrust slices at its base. This resulted in a bottom to top stacked sequence of thrust slices which reflects the original west to east configuration of the system. The least travelled slices are at the base, while the farthest travelled slices are those which are highest in the package (Stevens, 1970). Paleogeographic work supports this method of allochthon assemblage (see previous sections). In addition, large ophiolite-derived blocks are found in the tectonic melanges (phacoidally cleaved zones of chaotic structure which are present along main slice contacts) throughout the section, indicating that the ophiolites were proximal throughout the assembly history of the allochthon (Williams, 1975). A diagrammatic representation of the development of the Humber Zone is given in Figure 2.2.

E. Deformation Events During Which Shear Zone Formation May Have Occurred

From the time of formation of the oceanic crust which is preserved in the Bay of Islands Ophiolite Complex (about Tremadocian) until late Carboniferous there have been several phases of deformation which have affected the rocks of western Newfoundland, and during which shear zone formation might have occurred. These are briefly outlined below.

Figure 2.2

Diagrammatic representation of the early Paleozoic evolution of Western Newfoundland. After Casey (1980).



(1) Deformation of the newly formed oceanic crust. Oceanic crust formed at a mid-ocean ridge axis undergoes a considerable amount of deformation as it moves away from the ridge axis (see Chapter 3). In present day ridge axes the most frequently occurring structures are inward and outward facing, axis-parallel normal faults with displacements ranging up to about 300 meters. These faults may grade into ductile shear zones at depth.

(2) Obduction and emplacement related structures. Structures in the Bay of Islands Ophiolite Complex which have been interpreted as obduction and emplacement-related include the metamorphic aureole, thrusts and folded thrusts, tear faults, and steeply dipping faults on which the sense of displacement is uncertain (Casey, 1980; Rosencrantz, 1980). The metamorphic aureole is a narrow, ductile feature that formed during the initial emplacement of hot oceanic lithosphere over cold volcanics and sediments. Thrust faults with brittle structural expressions cut the aureole. These faults have been folded and cut by subsequent thrusts, NNW-trending strike slip faults, and N- and NE-trending faults whose displacement is mainly dip slip (Rosencrantz, 1980).

The basal thrust of the Bay of Islands complex is folded (Casey and Kidd, 1981). Gravity data suggests that final emplacement must have occurred along a sub-horizontal thrust which truncates the folded basal thrust and the folds within the Bay of Islands massifs. The "final" emplacement-related thrust is also folded (B. Idleman, pers. comm.). This folding may have occurred during the final stages of emplacement, or may be due to later folding events.

(3) Acadian deformation. Late Devonian Acadian deformation is

not well documented in the Bay of Islands area. One of the few occurrences of Silurian and early Devonian rocks in this area is present on the Port-au-Port Peninsula, where they are steeply northwest dipping to overturned (Rodgers and Neale, 1963). To the east, more internal to the Taconic and Acadian orogenic zones, Acadian deformation is characterized by steeply dipping N to NE trending cleavage and tight to open folding, e.g. at Sop's Arm, White Bay (Lock, 1969). It is possible that all older rocks in the vicinity of the Bay of Islands are affected by this folding, but that it is not easily recognized in the previously deformed Cambro-Ordovician rocks, and may not be the general case.

(4) Carboniferous strike-slip faulting. Strike-slip faulting and related pull-apart basin formation occurred throughout the Carboniferous in the Northern Appalachians (Bradley, 1982). In Newfoundland the area which was most affected by this deformation lies in a narrow belt about the Cabot Fault to the north and the Long Range Fault to the south. It apparently does not greatly affect rocks to the west of this lineament.

From this summary it can be seen that most of the deformation in western Newfoundland has been characterized by folding and brittle faulting. Ductile shear zone formation would be expected, on this evidence, in only two instances: (1) within actively accreting oceanic crust at the spreading ridge crest, and (2) early during obduction of ophiolites (broadly at the same time as the formation of the Bay of Islands aureole). Structures evolving within the oceanic crust would be expected to be mainly paleo-spreading ridge parallel, as is observed in present day ocean floor studies, and to show original normal-fault offset. Obduction-related features which originally trended close to

parallel to the metamorphic aureole would be expected to indicate original thrust sense of offset, while those that formed at high angles to the aureole may show original strike-slip offsets.

CHAPTER 3. FAULTING AT MID-OCEAN RIDGES

Most of the faulting which affects oceanic crust occurs as the new crust, formed along the axis of the mid-ocean ridge, moves away from the ridge axis, out of the axial valley or graben, and into the rift mountains or down the flanks of the rise. The density of faulting, and the orientation and amount of offset across individual faults, varies with spreading rate and proximity to transform faults. Much of what is known about oceanic crustal faulting is based on submersible studies of the sea floor. Seismic studies provide the only information about processes occurring at depth. This chapter discusses mid-ocean ridge morphologies of slow (<5 cm/yr full rate), medium (5-9 cm/yr full rate), and fast (9-18 cm/yr full rate) spreading centers (Fig. 3.1), with emphasis on fault orientations, and sense and amount of offset across faults.

A. Slow Spreading Centers

The Mid-Atlantic Ridge is a typical example of a slow spreading center. It has a well developed rift valley which ranges in depth from 1.5-3.0 kilometers. The faulting and rough topography which are generated in the rift valley are preserved to a great extent in the older ocean basin (Macdonald, 1977). Another feature of the Mid-Atlantic Ridge typical of slow-spreading centers is the relatively close spacing of the transform faults which offset the ridge. In the FAMOUS area transform faults occur every 35-45 kilometers (Ramberg, et al., 1977).

The FAMOUS area of the Mid-Atlantic Ridge between 35°50'N and 37°20'N was the site of an intensive multidisciplinary study between 1972 and 1975. Detailed work on the section of the ridge near 37°N

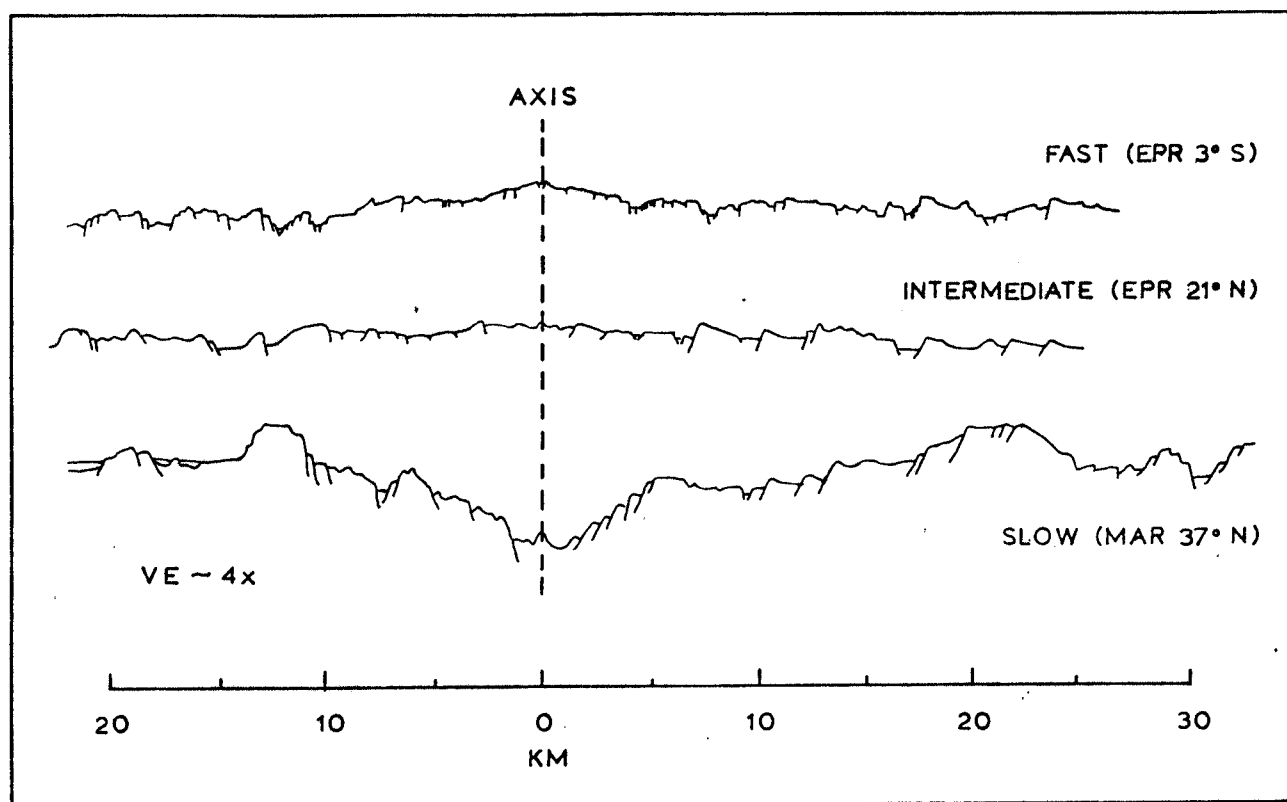


Figure 3.1

A comparison of topography at fast, medium, and slow spreading ridges.
After Macdonald, 1982.

(rift valley 2) will be used as an example of a slow spreading center. Rift valley 2 is approximately 40 kilometers long and is bounded to the north and south by left-lateral slipping transform faults. It is somewhat unusual in that spreading is presently 17° oblique. Magnetic and tectonic features suggest that this non-orthogonal arrangement is steady state in this area (Macdonald, 1977; Luyendyk and Macdonald, 1977). Spreading across rift valley 2 is asymmetric. The half spreading rate on the east portion of the rift is approximately 1.34 cm/yr, while that of the west portion is approximately .70 cm/yr. The difference in spreading rates is reflected in the structures which have developed on either side of the rift (Macdonald, 1977).

Four physiographic provinces have been identified in rift valley 2. They are the inner valley floor, the inner valley walls, the terraces and the outer valley walls (Macdonald et al., 1975; Fig. 3.1). Rift mountains are developed beyond the outer valley walls.

The floor of the inner valley ranges from 1-4 kilometers in width. Along the length of the inner valley there are a series of elongate (length:width = 4:1) volcanic highs which rise up to 150 meters off the inner valley floor. The long axes of the highs trend approximately 017° , parallel to the trend of the rift valley. The volcanics which make up the central highs are covered with the least sediment, are the freshest, least fractured, and most highly magnetized features of the valley floor. This suggests that the actual plate boundary lies within the inner valley and runs through or close to the central volcanic highs, and that the zone of extrusion may be up to 1 kilometer wide. Numerous smaller volcanic constructive features (haystacks and cone-lets) are common on the valley floor. The volcanic highs are separated

along strike by lows which may be either collapse structures or grabens (Luyendyk and Macdonald, 1977).

There is very little faulting within 400-500 meters on either side of the volcanic axis. Outside this zone faulting and fissuring are ubiquitous. These features are steeply dipping, and a study by Macdonald and Luyendyk (1977) has shown that their trend is remarkably parallel to the trend of the median valley (017°). The average trend of the several hundred faults and fissures which were mapped was $017^{\circ} \pm 6^{\circ}$. (The error reported here is the standard deviation. It does not take into account possible error on each measurement, and is therefore a minimum estimate of error.)

The inner valley is bounded on both sides by the 017° trending inner valley walls which are situated 2.2 kilometers to the east and 1.0 kilometers to the west of the volcanic axis. Close examination has shown that these walls are comprised of a series of steep, inward-facing normal fault scarps. The west wall, on bathymetric profiles, appears to be a single massive block fault with a throw of up to 600 meters, but it is actually made up of several narrow fault-bounded slivers. The east wall is made up of several fault blocks 500-1500 meters wide separated by inward-facing normal faults which dip an average of 50° and have throws of 150-350 meters (Macdonald and Luyendyk, 1977). The fault blocks on both sides of the valley tend to tilt away from the valley. The average tilt of tilted blocks is $6^{\circ} \pm 2^{\circ}$, while the average tilt of all blocks is $2^{\circ} \pm 2^{\circ}$ (Macdonald and Luyendyk, 1977). It is likely that listric normal faulting accounts for the tilting of these blocks. Weidner and Aki (1973) have shown from seismic data that the large inner wall faults may extend down to

3 \pm 2 kilometers in the crust, at which depths the dips on normal faults observed on the surface are often observed to flatten in continental and continental margin seismic reflection profiles (Shelton, 1984).

Beyond the inner valley walls of rift valley 2 lie the terraces. These are areas where the topography, like that of the inner valley walls, is controlled by block faulting, but which are overall relatively flat compared to the inner rift. Terraces are not present along all ridge segments of slow spreading centers (Crane and Ballard, 1981), which suggests that they are not steady state features. Fault spacing on the terraces is greater than in the inner rift, and some outward-facing faults are present, forming grabens. Macdonald and Luyendyk (1977) have suggested that these faults are antithetic faults which form in response to gaps opening due to the flattening of the inward-facing faults with depth.

On the edges of many of the terrace blocks there exist topographic highs which range in width from 100-800 meters, and in height from 40-200 meters. Some are equidimensional, while others are elongate. They are morphologically quite similar to volcanic features seen in the inner valley. It may be that faulting occurs on either side of the volcanic highs of the inner valley, and that the highs themselves are carried up over the inner valley walls relatively intact (Macdonald and Luyendyk, 1977; Ballard and van Andel, 1977).

The rift mountains lie beyond the terraces. They are separated from the terraces by the outer valley walls, which are situated 14 kilometers to the east and 8 kilometers to the west of the inner valley walls. The outer walls rise approximately 800 meters above the ter-

ances. As with the inner valley walls, the outer walls are comprised of inward-facing normal faults.

In the rift mountains the topography is rugged and, as in the median valley, it is dominated by block faulting. Throws on the faults range up to 300 meters. Outward-facing faults are more common in the rift mountains than in the other domains, and they contribute to the topography of the mountains (Macdonald and Luyendyk, 1977).

There are several mechanisms by which the rift valley/rift mountain transition may take place. One possible mechanism involves faulting in a reverse sense on relict normal faults. This is not in keeping with focal mechanism results from mid-ocean ridges (Sykes, 1967; Weidner and Aki, 1973), suggesting that it is not a major mechanism. A second mechanism calls for tilting of fault-bounded blocks away from the rift valley as they reach the outer wall and cross into the rift mountain domain. A third mechanism calls for the development of outward facing normal faults beyond the outer walls of the rift valley (Macdonald, 1982). Macdonald (1982) favors interaction of all three mechanisms to account for observed changes between the rift valley and mountains. Tilting of blocks away from the ridge axis, possibly a result of observed normal faults becoming listric with depth, and subsequent antithetic outward-facing faulting are likely to be the dominant mechanisms.

B. Fast Spreading Centers

The morphology of fast spreading ridges differs significantly from that of slow spreading ridges (Fig. 3.1). The section of the East Pacific Rise south of 20°N is spreading at rates of up to 16.5 cm/year

(Rea and Blakely, 1975), and there have been several studies of areas on that section of the Rise.

At the crest of the East Pacific Rise there exists a triangular high which is superimposed on the regional rise (Francheteau and Ballard, 1983; Lonsdale, 1977a). It has been suggested that the axial high is a horst (Rosendahl, et al., 1976), but observations made from manned submersibles and photos taken of the sea floor indicate that the axial high is actually a large volcanic constructive feature (CYAMEX, 1981). Lonsdale (1977a) describes the high as a broad and extremely elongate Hawaiian-type shield volcano. The outward-facing slopes of the axial high consist mainly of draped pillow lavas which are cut by axis-parallel fissures (Francheteau and Ballard, 1983; Lonsdale, 1977a). Macdonald and Fox (1983), in a very detailed Seabeam study of the East Pacific Rise between 8°N and 18°N , have observed six small offsets of the neovolcanic zone across overlapping spreading centers over a 1200 kilometer length of this fast spreading portion of the rise.

The axial high near 13°N is approximately 3 kilometers wide and 250-200 meters high (Francheteau and Ballard, 1983; CLIPPERTON, 1983). Near $3^{\circ}25'\text{S}$ the high is approximately 2 kilometers wide, and it rises approximately 100-150 meters above the flanks of the rise (Lonsdale, 1977a). At the summit of the axial high there is a graben; at both locations it is less than 500 meters wide and 35-40 meters deep. The summit graben is bounded by an en echelon set of inward-facing normal faults which trend sub-parallel to the rise axis. Displacements across the faults are on the order of 10 meters (Francheteau and Ballard, 1983; Lonsdale, 1977a; CLIPPERTON, 1983). The displacement across the

faults observed at 3°25'S gradually decreases along strike, until the faults terminate in fissures 1-2 meters wide (Lonsdale, 1977a).

The summit graben is the site of the youngest volcanics, mainly flows, which pooled and froze, forming elongate fossil lava lakes (Francheteau and Ballard, 1983; Lonsdale, 1977a; CLIPPERTON, 1983). Fissuring has not been directly observed on the floor of the axial rift at 3°25'S, although narrow (10-20 meters), steep-sided, axis-parallel, volcanic constructions are present along the floor of the graben at that location. These edifices may indicate the location of buried eruptive fissures (Lonsdale, 1977a). Fissures striking parallel to the rise trend and varying in width from 10's of centimeters to 4 meters have been observed within the axial graben near 13°N (CLIPPERTON, 1983).

From 1-10 kilometers to the west and 1-15 kilometers to the east of the rise axis at 3°25'S is the marginal horst and graben zone (Lonsdale, 1977a). This zone is characterized by the presence of closely spaced inward and outward-facing normal faults which bound the horsts and grabens. The throw on these faults is generally < 100 meters, and their trend is sub-parallel that of the rise axis (Lonsdale, 1977a).

Beyond the marginal horst and graben terrain lie the rise flanks. Here the throws across the normal faults are frequently 100-300 meters. Both inward and outward-facing normal faults persist. The grabens which these faults bound are often 200-300 meters deep, and they and their associated horsts form the foundation of the rolling abyssal hill terrain typical of flank areas of fast-spreading centers. Burial by 5-10 meters of sediment by the time the crust is 500,000 years old

(approximately 37 kilometers from the rise axis at $1/2$ rate of 7.5 centimeters/year) tends to obliterate fine scale structures in these hills (Lonsdale, 1977a).

C. Moderate Spreading Centers

The East Pacific Rise at 21°N and the Galapagos Rift at 86°W are two examples of spreading centers which are spreading at a moderate rate. In many ways their morphology is also "moderate" - somewhere in between that of the characteristic slow-spreading center rift and the fast-spreading center rise (Fig. 3.1).

The Galapagos Rift at 86°W is opening at a rate of 6.6 cm/year (Klitgord and Mudie, 1974). The rift valley is situated in the middle of a broad (25-30 kilometer) regional high. It is 200-260 meters deep, and 3-4 kilometers wide (Crane, 1978). Crane (1978) has identified four physiographic provinces within the axial valley. From the central portion of the valley outwards these are the central high, the inner floor, the marginal highs and lows, and the inner walls (terminology after Macdonald et al., 1975).

The central high is a volcanic ridge which rises 20-60 meters above the adjacent inner floor (van Andel and Ballard, 1979). It varies in width from 0.2-1.3 kilometers (Crane, 1978). The morphology of this volcanic high is midway between the discrete volcanos seen on the inner floor of the slow-spreading Mid-Atlantic Ridge and the single continuous volcano characteristic of fast-spreading centers. The high at $86^{\circ}10'\text{W}$ is topped by four elongate domes which vary in length from 1.1-3.7 kilometers, and which are up to 0.6 kilometers wide (Crane, 1978). The domes are aligned along a portion of the rift which is

approximately 12 kilometers long. Lonsdale (1977b) reports the presence of a system of rift-parallel fissures at the crest of the central high.

The inner valley floor flanks the central high and varies in width from 0.2-1.4 kilometers (Crane, 1978). It is covered by smooth pahoehoe lava flows (Lonsdale, 1977b) which are cut by a system of axis-sub-parallel fissures which average 0.8 kilometers in length (Crane, 1978).

The inner valleys of the Galapagos Rift at 86°W and the East Pacific Rise at 21°N are the sites of active hydrothermal vents (Ballard et al., 1981; Crane and Ballard, 1981). The vents in both locations are present along the axis of most recent volcanic flows. At 21°N on the Rise exit temperatures of as high as 350°C were measured. This high temperature discharge indicates a nearby heat source which is likely to be a shallow level magma chamber.

To the north and south the terrain of marginal highs and lows rises from the inner valley floor. The boundary of the marginal highs on the north side of the rift with the inner floor is marked by the presence of several inward-facing normal faults. These faults dip $50-60^{\circ}$, and the displacement across each of them is approximately 40 meters. Marginal highs on the south side of the inner rift are separated from it in some sections by a system of outward-facing normal faults (throws from 5-55 meters) and in others by sets of fissures (Crane, 1978).

The marginal highs and lows alternate along strike. The axis-sub-parallel lineaments they define (Allmendinger and Riis, 1979) is further accentuated by fissuring and inward and outward-facing normal faulting (Crane, 1978). Crane (1978) noted that highs on one side of

the rift valley face lows on the opposite side of the valley. The cause of this anti-symmetry is unclear.

The inner walls are the next physiographic feature encountered moving away from the rift axis. On the Galapagos Rift near $86^{\circ}10'W$ the southern boundary of the marginal high and low terrain is a 3 kilometer wide zone of normal faulting. Most of the faults have offsets between 25 and 50 meters, and few have throws exceeding 100 meters (Lonsdale, 1977b). East of $86^{\circ}09'W$ the southern wall is actually a 200 meter wide horst bounded by an inward-facing normal fault to the north and outward-facing normal faults to the south. West of $86^{\circ}09'W$ the edge of the marginal high and low terrain is marked by a fault-bounded 160 meter deep valley (Crane, 1978; van Andel and Ballard, 1979). The northern wall is less complex. It is comprised of a set of inward-facing normal faults, in some places with offsets exceeding 100 meters, and with a combined offset of 200-260 meters. The major fault scarps of the Galapagos Rift often extend for several kilometers laterally (Crane, 1978; Lonsdale, 1977b).

Beyond the inner valley walls lie the abyssal hills. Lonsdale (1977b) has noted tilting of 1.0-1.5 kilometer wide crustal blocks away from the axis across inward-facing faults. The amount of tilting observed ranges up to 15° .

D. Effects of Transform Faults on Mid-Ocean Ridge Structures

The effects of transform faults on mid-ocean ridge structures have been studied at several ridge/transform fault intersections, including the intersection of the Tamayo Transform with the East Pacific Rise (Tamayo Tectonic Team, 1984), the intersection of the Oceanographer

Transform with the Mid-Atlantic Ridge (OTTER, 1984), and the intersection of the Kane Fracture Zone with the Mid-Atlantic Ridge (Karson and Dick, 1983). At each of these locations similar systematic changes occur along the ridge axis as the intersection is approached. In each case the floor of the inner rift valley deepens towards the transform. Deepening ranges between 700 meters in the Tamayo area, and 1400 meters in the Oceanographer area. Within several kilometers of each of the ridge transform intersections, the orientation of ridge parallel structures (faults, fissures, and dikes) on the transform (as opposed to fracture zone) side of the ridge begins to change, swinging away from parallelism with the ridge. At the ridge/transform intersection these structures form a 60° angle with the transform (and 30° with the ridge axis). Observations of slickenside striae orientation on some of the fault scarps, and of the displacements across them, indicate that at least some of the motion across these faults has been dip-slip (Karson and Dick, 1983). This observation does not exclude a strike-slip component of displacement across the faults. The most satisfactory explanation for the dip-slip component of displacement involves the "sealing" of the transform by the freezing of hot, rising asthenosphere on the ridge side of the transform against the old, cold lithosphere across the transform. As the lithospheric plates on either side of the fault continue to move past one another this mantle weld rotates and deforms, deforming shallower levels of the crust with it (Fox and Gallo, 1984). The initial orientation of extensional structures in this domain would be approximately the orientation of the observed scarps. Continued deformation in this domain would necessitate strike-slip movement on these features, but at the ridge-transform interface

they may be carried up and out of the rift valley before this occurs.

At the Kane Fracture Zone ridge-transform intersection, structures on the fracture zone side of the ridge remain axis-parallel (Karson and Dick, 1983). At the west end of the Clipperton fracture zone on the East Pacific Rise, structures on both the transform and the fracture zone side of the ridge curve towards the transform fault (P. Fox, personal communication). This apparent difference may be due to differences in behavior of the crust at fast and slow spreading centers, or it may be a result of lack of sufficient observations of the bathymetry at the Tamayo and Oceanographer examples of the fracture zone side of the ridge transform intersection.

E. Summary

Normal faulting is widespread along the mid-ocean ridge system. Inward-facing, axis-parallel normal faults predominate, and form the inner valley walls of slow spreading ridges and the summit graben of fast spreading rises. The throws on these axial valley bounding faults range up to approximately 150 meters on slow spreading ridges, but only up to ten meters or so on fast spreading rises. Beyond the inner valley or summit graben, outward-facing normal faults are observed in addition to more common inward-facing normal faults. Outward-facing normal faults are more common on fast spreading rises, where a horst and graben terrain lies outboard of the summit graben. Throws on faults in the horst and graben terrain are generally <100 meters. On the rise flanks, up to 15 kilometers away from the spreading center axis, normal faults with throws of typically about 100 meters, to as much as 200 meters, bound horsts and grabens which form the foundation

of the rolling abyssal hills typical of fast-spreading rise flanks. At slow-spreading centers, some outward-facing normal faults are present on the terraces (which are not developed in all sections of slow-spreading ridge axes). Outward-facing faults are somewhat more common in the rift mountains, but still out-numbered by inward-facing faults. Throws on faults in the rift mountains range up to 300 meters.

Normal faults which form on "normal" mid-ocean ridge segments, i.e., sections of the ridge which are far from ridge-transform intersections, trend sub-parallel to the ridge axis. As a ridge-transform intersection is approached, structures on the side of the ridge which abuts the active portion of the transform fault form oblique to the ridge axis. They appear to "swing around" from axis parallel to transform parallel. In the case of slow spreading ridges, most of the structures present on the side of the ridge that abuts the relatively inactive fracture zone are axis parallel, although a small number of axis oblique and perpendicular normal faults may be expected (Karson and Dick, 1983). Structures on both the fracture zone and transform fault sides of the ridge transform intersection swing towards the transform faults at fast spreading ridges (P. Fox, personal communication). The pre-obduction geometry of the Bay of Islands ophiolites proposed by Casey et al. (1983) calls for formation of the ophiolites near the fracture zone side of a ridge-transform intersection at a moderately fast spreading ridge (Fig. 3.2). In this setting, most of the fault or shear zone structures which formed within five kilometers of the ridge-transform intersection would be axis-oblique (Tamayo Tectonic Team, 1984), while most of those forming farther from the intersection would be axis-parallel. In either case, structures would

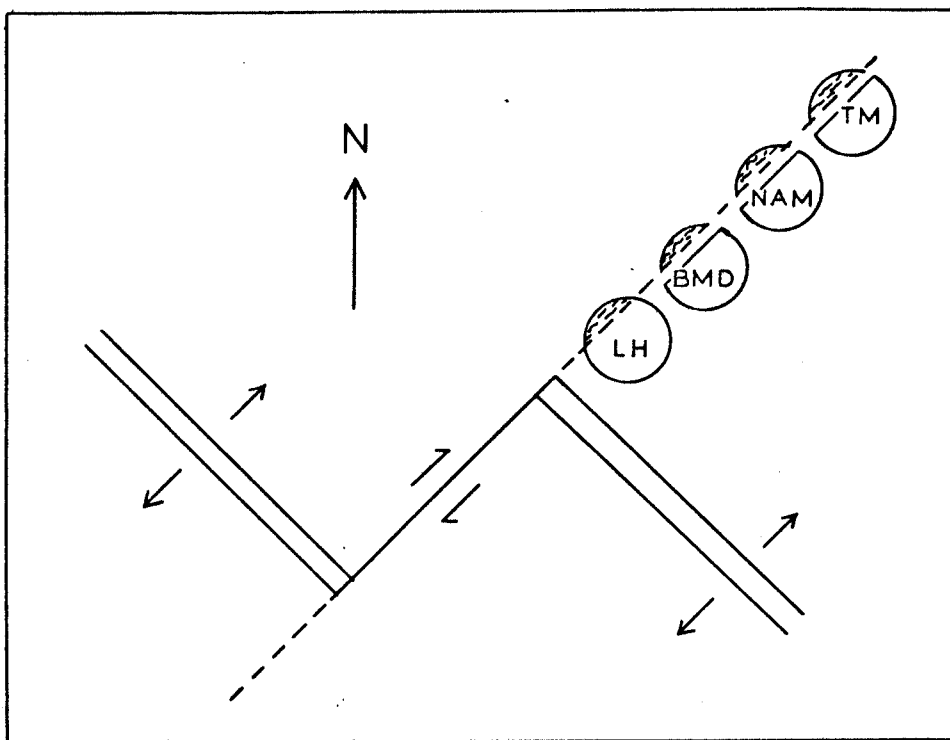


Figure 3.2

Cartoon of the pre-obduction geometry of the Bay of Islands ophiolite massifs. After Casey et al. (1983).

be expected to form parallel to the strike of the dikes, whose trend is affected in the same manner as other structures near ridge-transform intersections.

CHAPTER 4. STRUCTURE

A. Introduction

This chapter is divided into two main sections. In the first section field and microscopic characteristics of the shear zones are described. Because the shear zones are similar in many ways, their structures are discussed together in a general context, and individual exceptions are noted where necessary. In the second section the orientations in which the shear zones formed relative to the paleo-ridge axis and the constraints on the timing of movement on these zones are discussed.

The quality and extent of outcrop varies considerably from shear zone to shear zone. In areas where the shear zone could only be traced for a relatively short distance due to large expanses of low, scrubby spruce thickets and rubble (II, V, VI), a large-scale map of the entire zone was prepared. The amount of outcrop relative to the amount of rubble in each of these zones is shown on the large-scale maps. The three remaining shear zones (I, IV, VII) were traced for much longer distances (i.e. SZ I is over a kilometer long). Small areas with high proportions of outcrop were chosen for large scale mapping in these shear zones. In the case of SZ's I and IV, well over 75% of the length of the zone was traced by looking for strongly foliated boulders in the rubble.

B. Field and Microscopic Observations

1. Country Rock

The six shear zones covered in this study are very fine to fine

grained, white and green chalky weathering, strongly foliated zones within the plutonic portion of the North Arm Mountain Massif. Shear zones I, II, and IV cut layered gabbros. The gabbros are medium to coarse grained and in places have a weakly developed foliation defined by grain shape. The compositional layering in the gabbros is locally very distinct, although in the immediate vicinity of all the shear zones it is indistinct, and several centimeter-thick darker, pyroxene-rich layers and lighter, plagioclase-rich layers are very vague and difficult to discern. Shear zones V, VI, and VII cut isotropic gabbros. These are medium to coarse grained gabbros which are similar to the layered gabbros, but with the layering absent. In addition to cutting gabbro, shear zone VI cuts a diabase dike. There is a pod of dike material, which is undeformed in its center and sheared along its margins, in the center of the zone. The dike could not be traced outside the zone due to lack of outcrop. Shear zone VII is cut by several diabase dikes. The undeformed dikes cut across the foliation of the shear zone and have "baked" the mylonitic rocks which are in contact with them (Fig. 4.1). Details of the mineral assemblages in the gabbro and in the shear zones are discussed in Chapter 5.

2. Shear Zone Boundaries and Dimensions

The dimensions of the shear zones vary greatly. Width of the main portion of the zones ranges from 30 cm (SZ II) to approximately 6 m (SZ's VI, VII), while exposed lengths vary from approximately 1 m to almost a kilometer. Location maps and large scale maps of the shear zones and the study areas within them are given in Figures 4.2, 4.3, and 4.4. These may be referred to for comparison of size and present



Figure 4.1

Undeformed diabase dike cutting mylonitized gabbro of Shear Zone VII.

Figure 4.2

Simplified geologic map of the southern half of the North Arm Mountain Massif, Bay of Islands Ophiolite Complex, after Casey (1980).

- 1 - Basal metamorphic aureole
- 2 - Dominantly harzburgite, dunite, and orthopyroxenite, with subordinate areas of lherzolite
- 3 - Ultramafic rocks of magmatic origin, dominantly dunite, wehrlite, and clinopyroxenite
- 4 - Interlayered gabbroic and ultramafic rocks of magmatic origin
- 5 - Layered gabbroic rocks
- 6 - Isotropic gabbroic rocks with subordinate trondhjemite and quartz diorite
- 7 - Gabbro-diabase transition
- 8 - Diabase dikes
- 9 - Pillow lavas with some diabase dikes
- 10 - Parallochthonous sediments
- 11 - Undifferentiated volcanics and diabase including volcanics of the Skinner Cove Assemblage
- 12 - Clastic rocks of the Humber Arm Supergroup

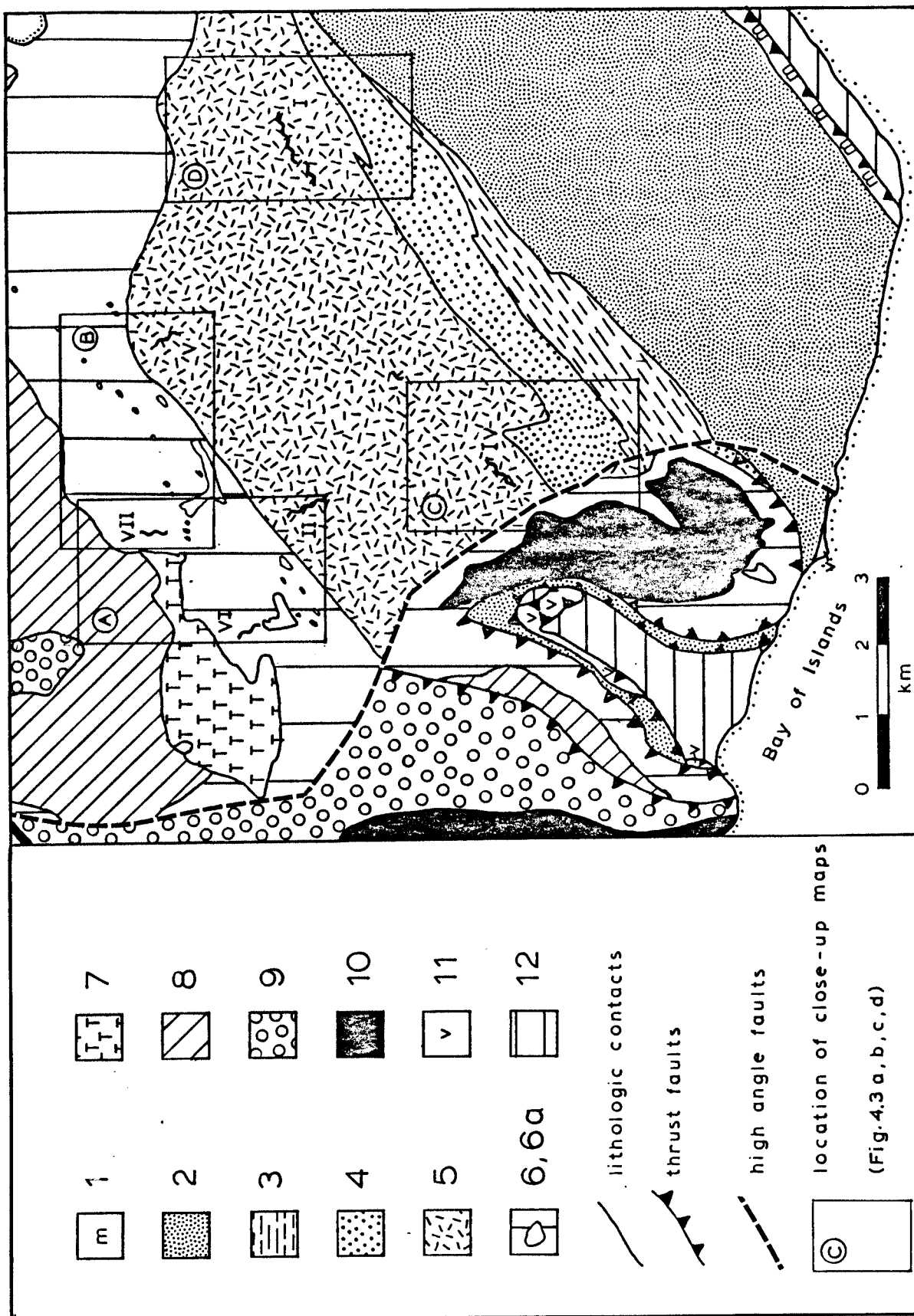
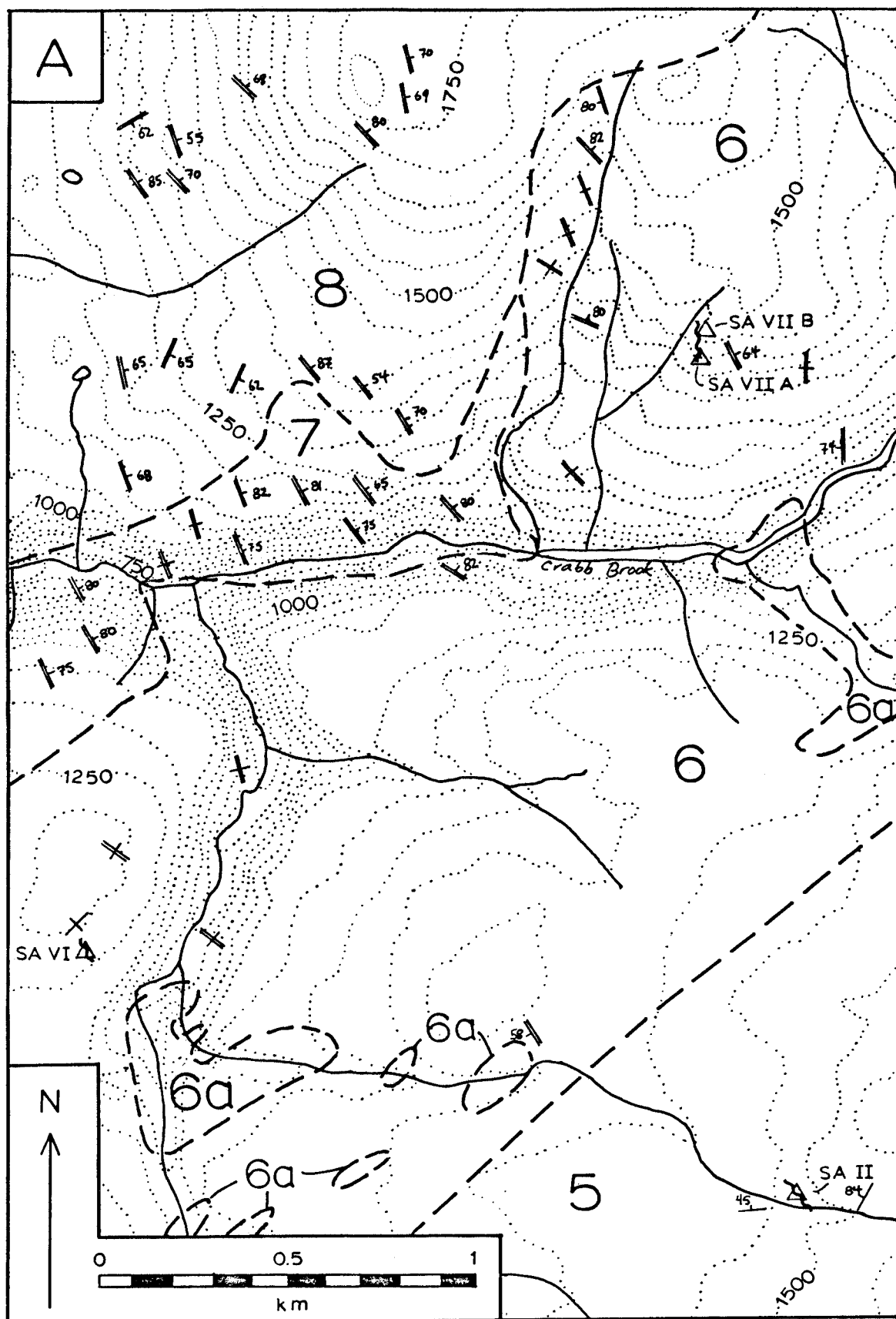
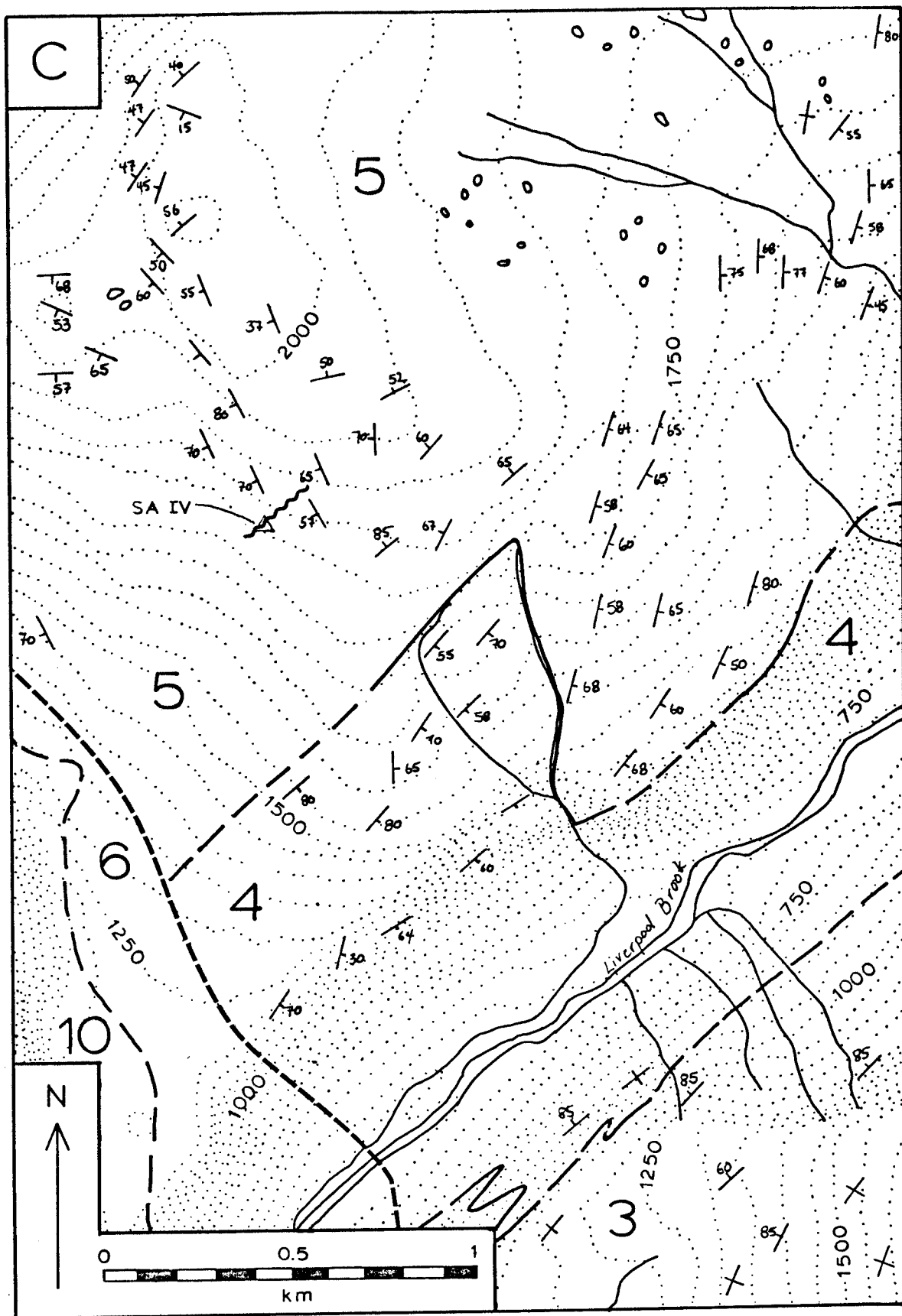


Figure 4.3

Location of shear zones and study areas within each shear zone. A) locations of shear zones II, VI, and VII, B) locations of shear zones V and VII, C) location of shear zone IV, D) location of shear zone I. Map units are the same as those in Figure 4.2, geology after Casey (1980).





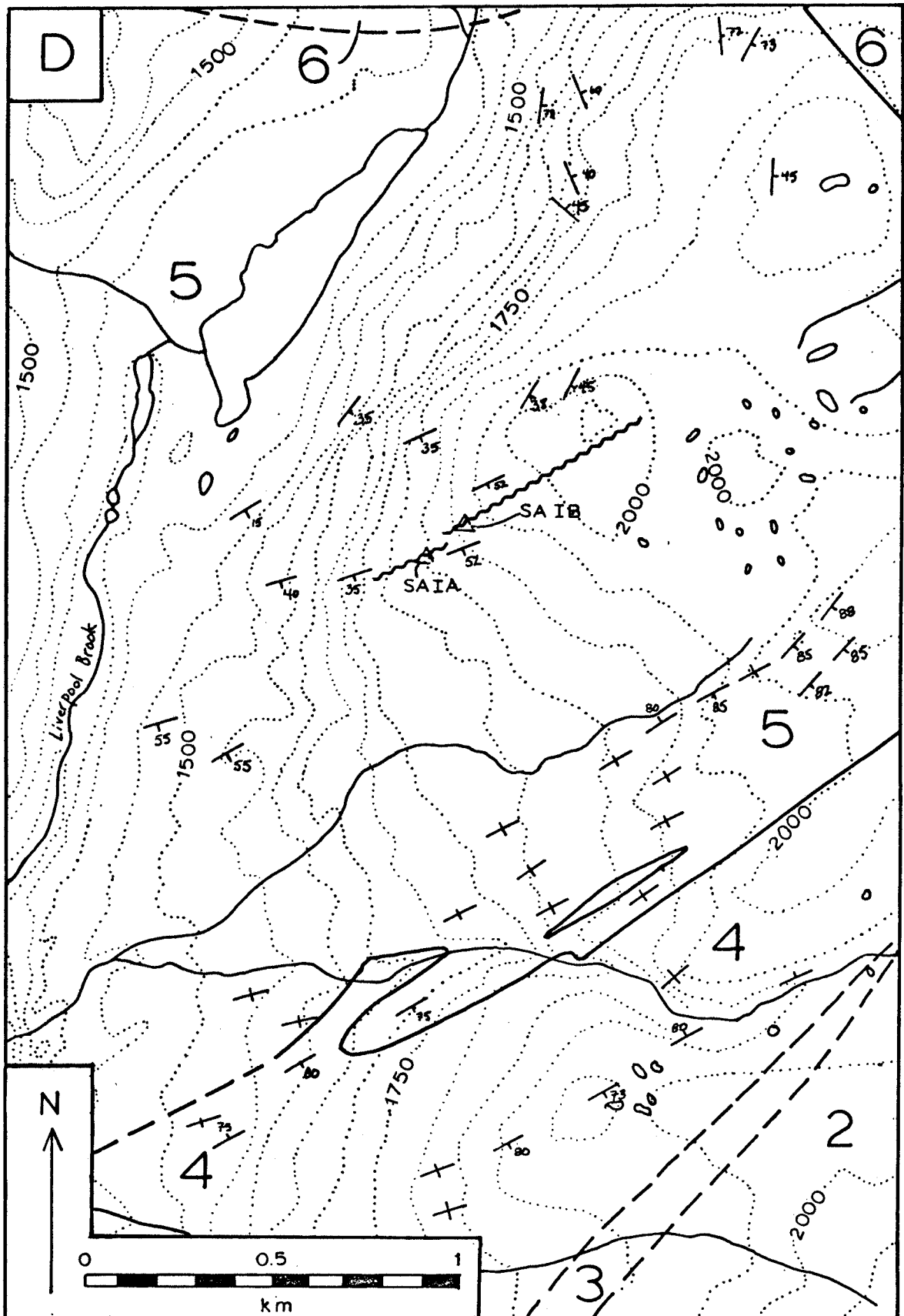
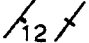
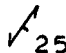
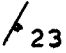




Figure 4.4

Close-up maps of study areas selected within each shear zone. A) extent of shear zone I, B) study area IA, C) study area IB, D) study area II, E) extent of shear zone IV, F) study area IV, G) study area V, H) study area VI, I) study area VIIA, J) study area VIIB.

 mylonitic foliation: inclined, vertical
 crenulation cleavage
 compositional layering
  lineation: plunging, horizontal

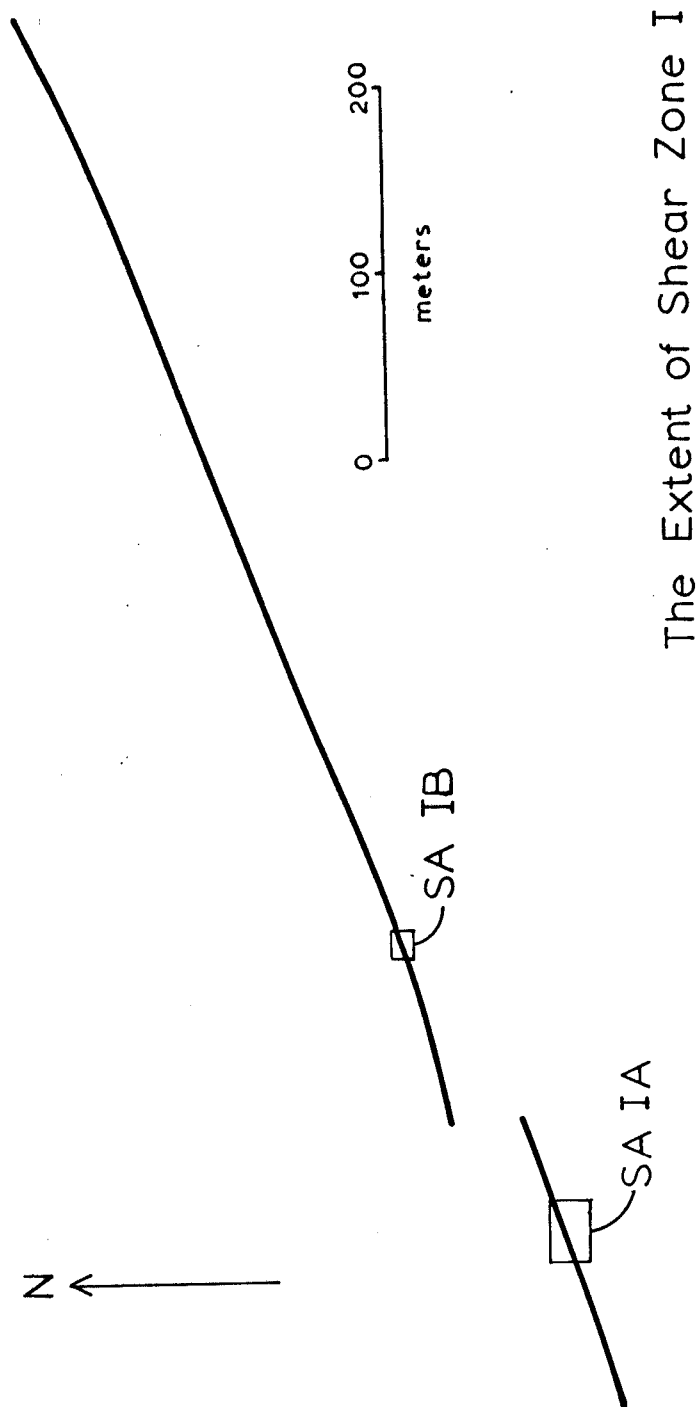


Figure 4.4 A

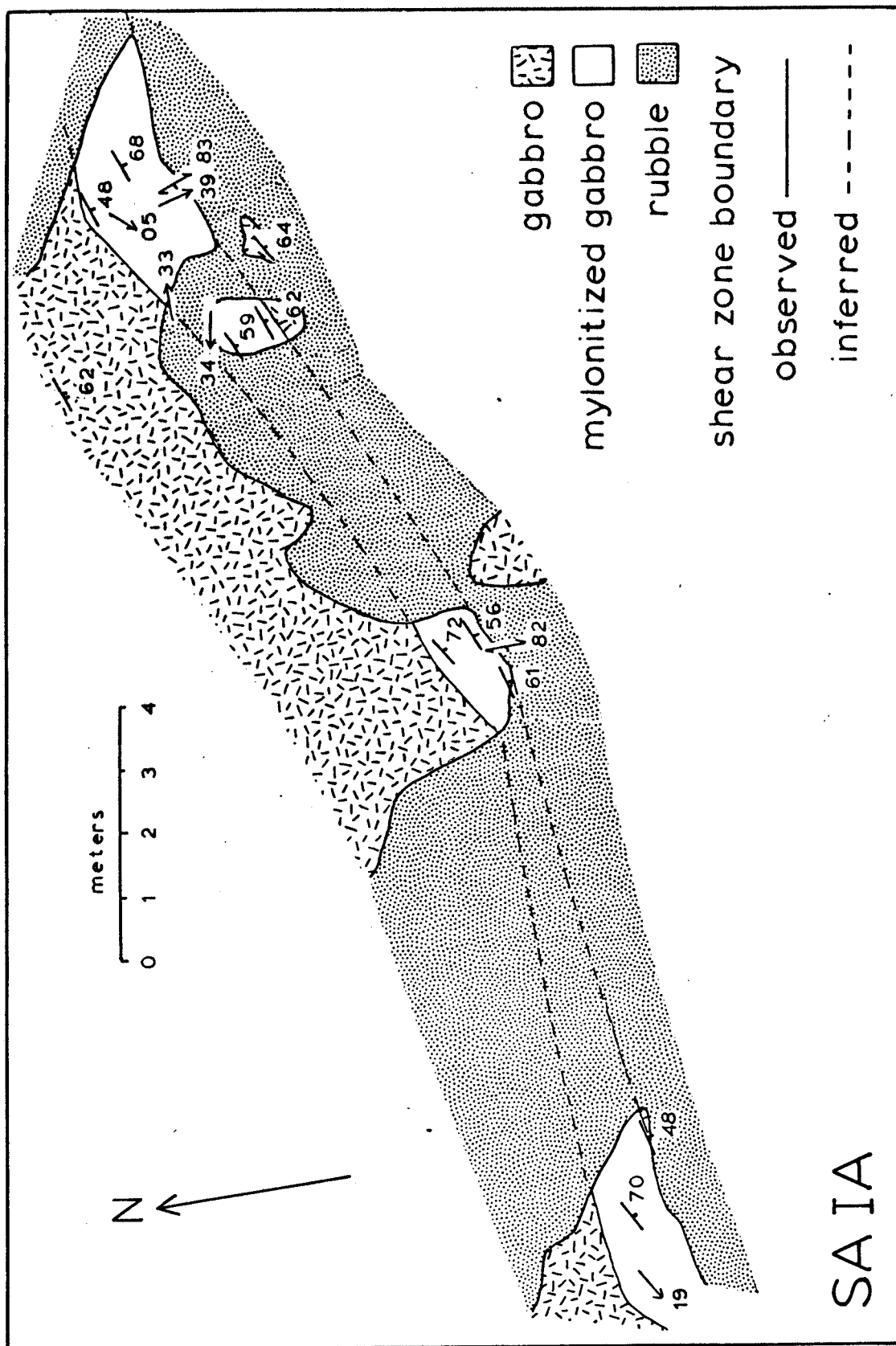


Figure 4.4 B

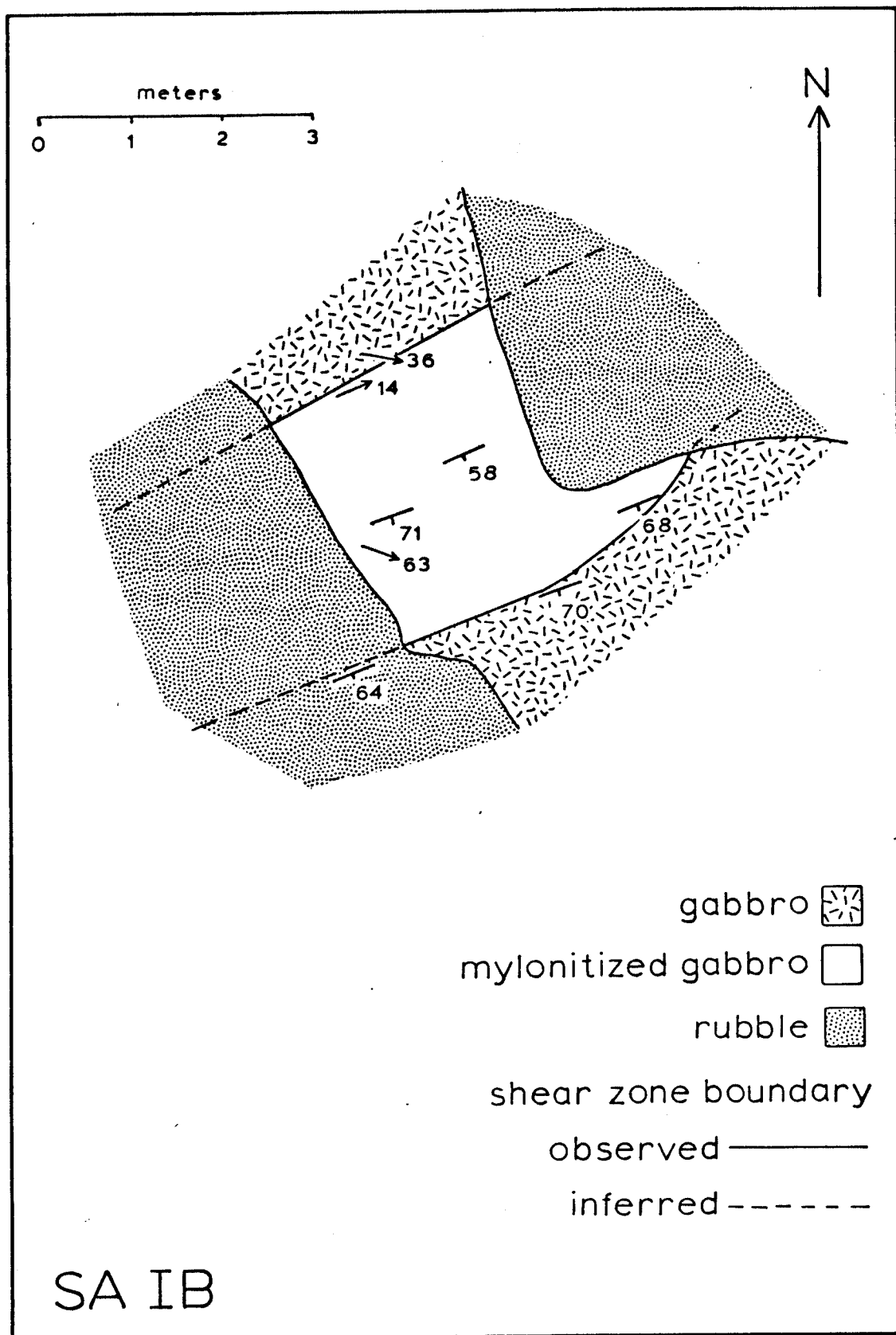


Figure 4.4 C

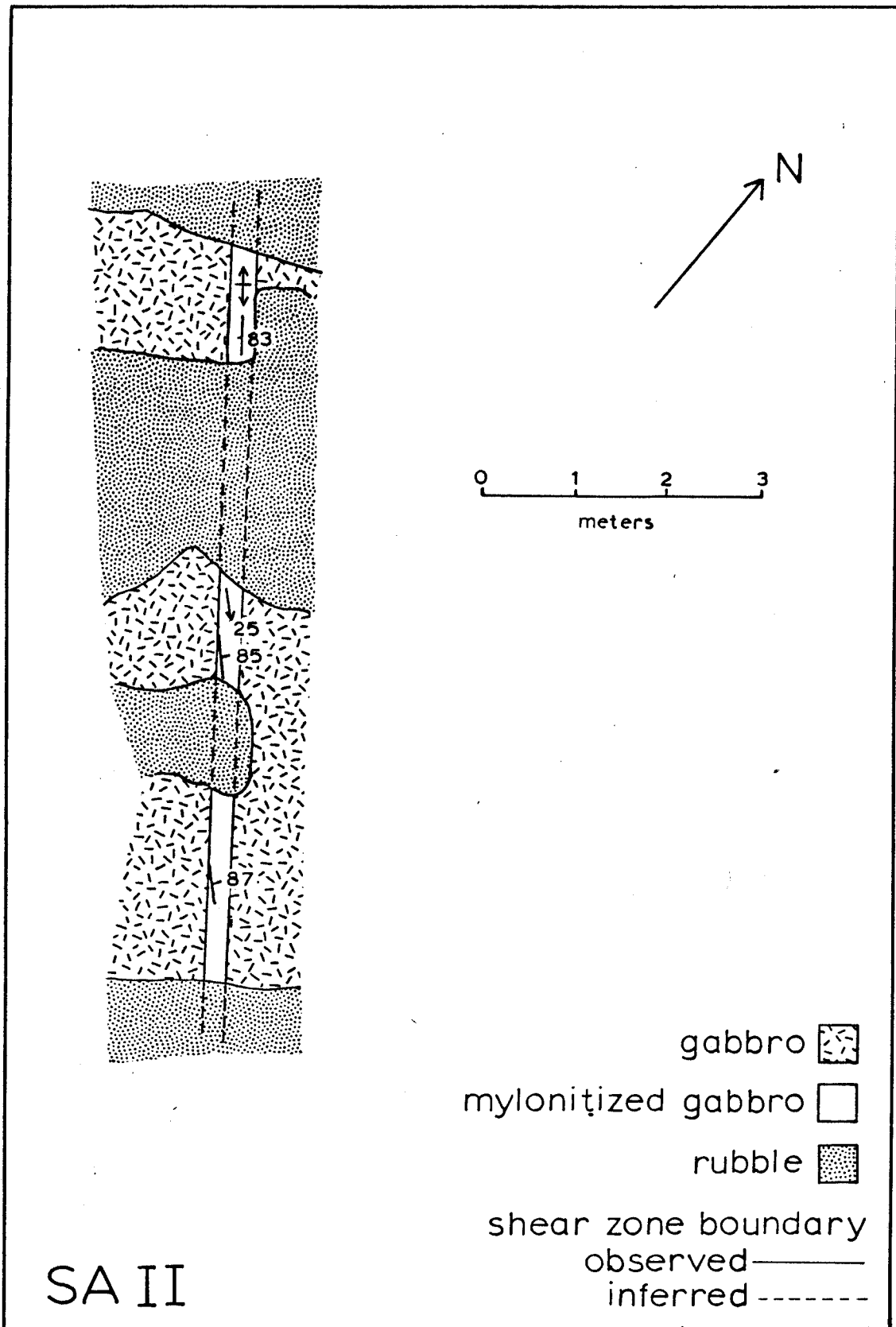


Figure 4.4 D

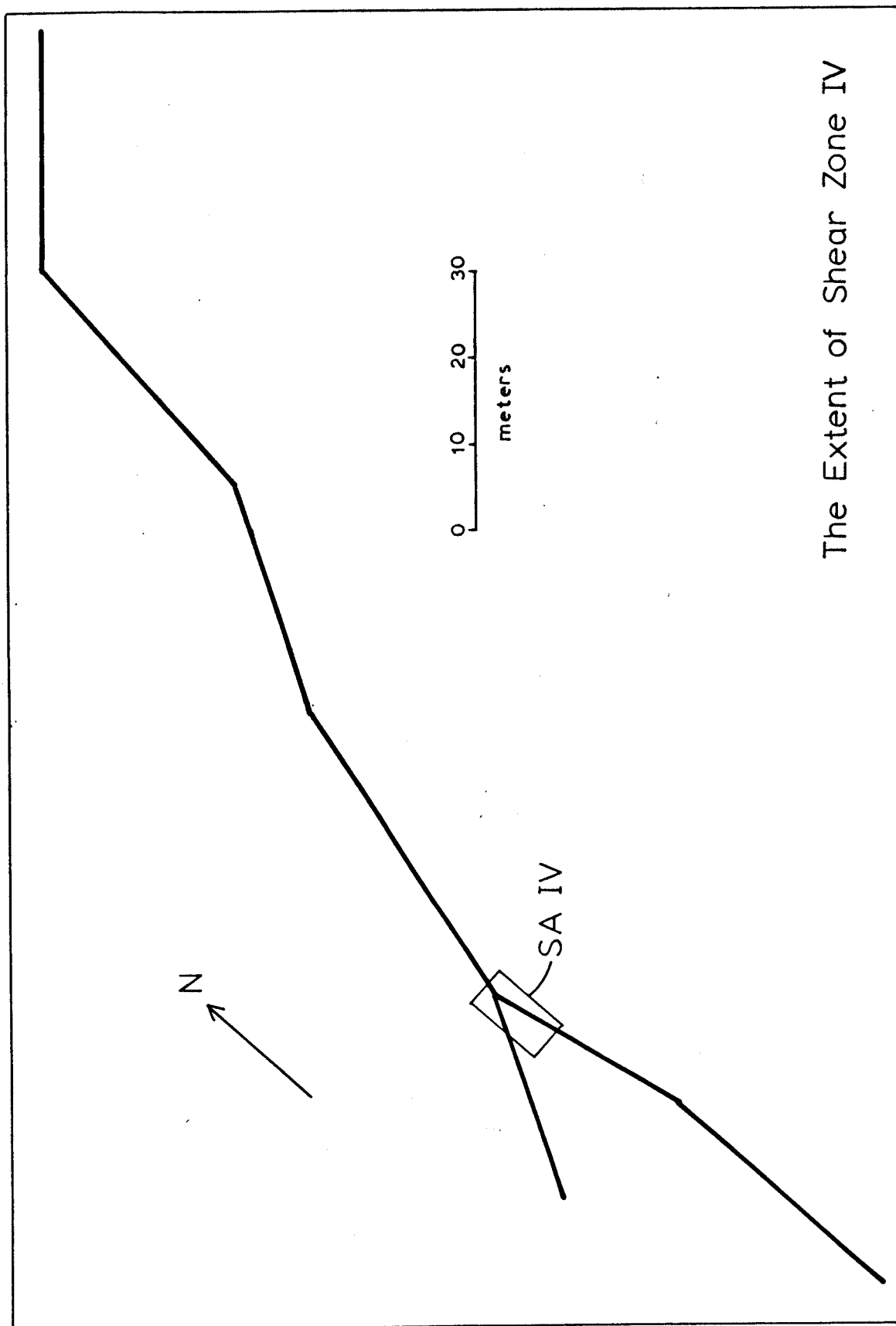


Figure 4.4 E

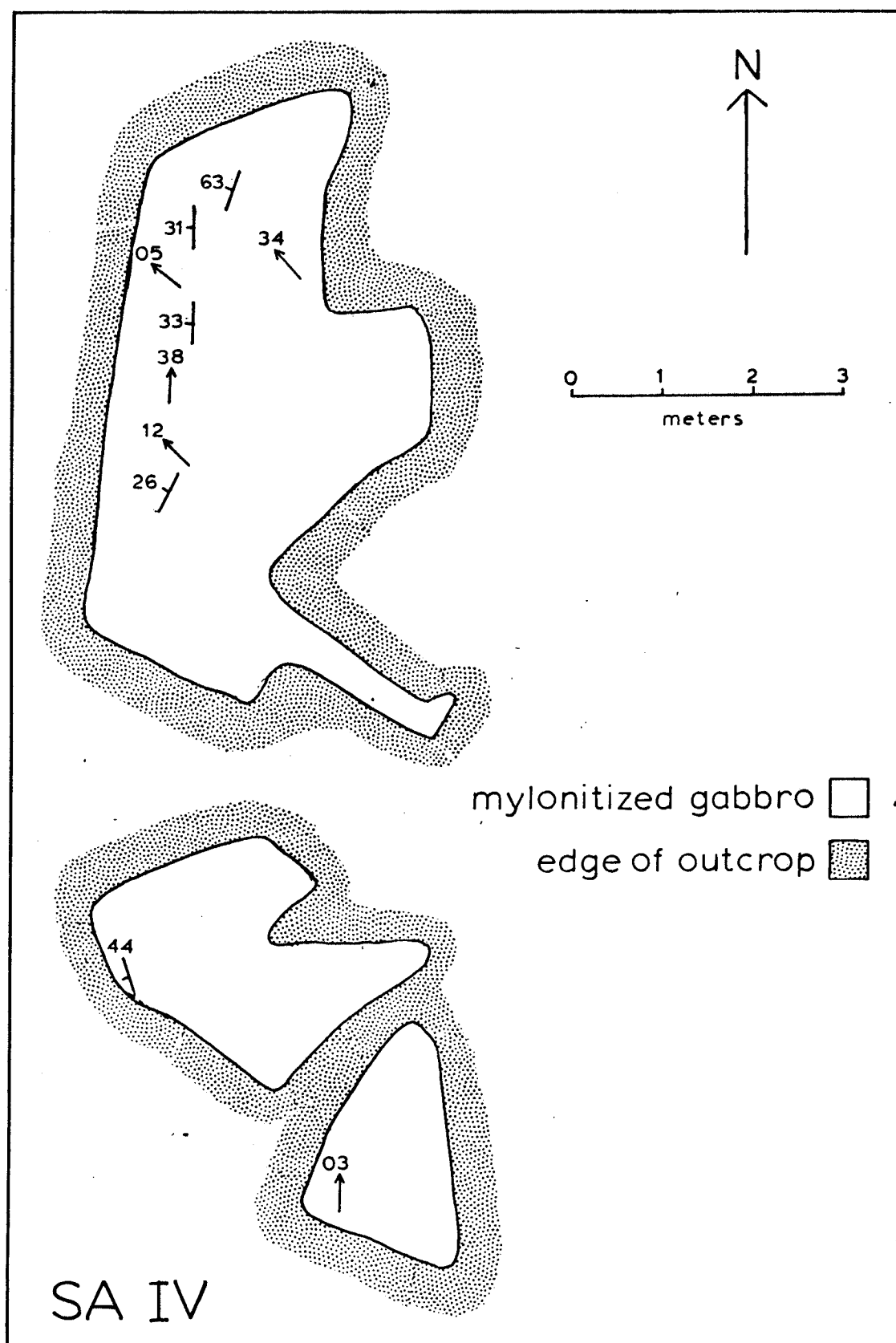


Figure 4.4 F

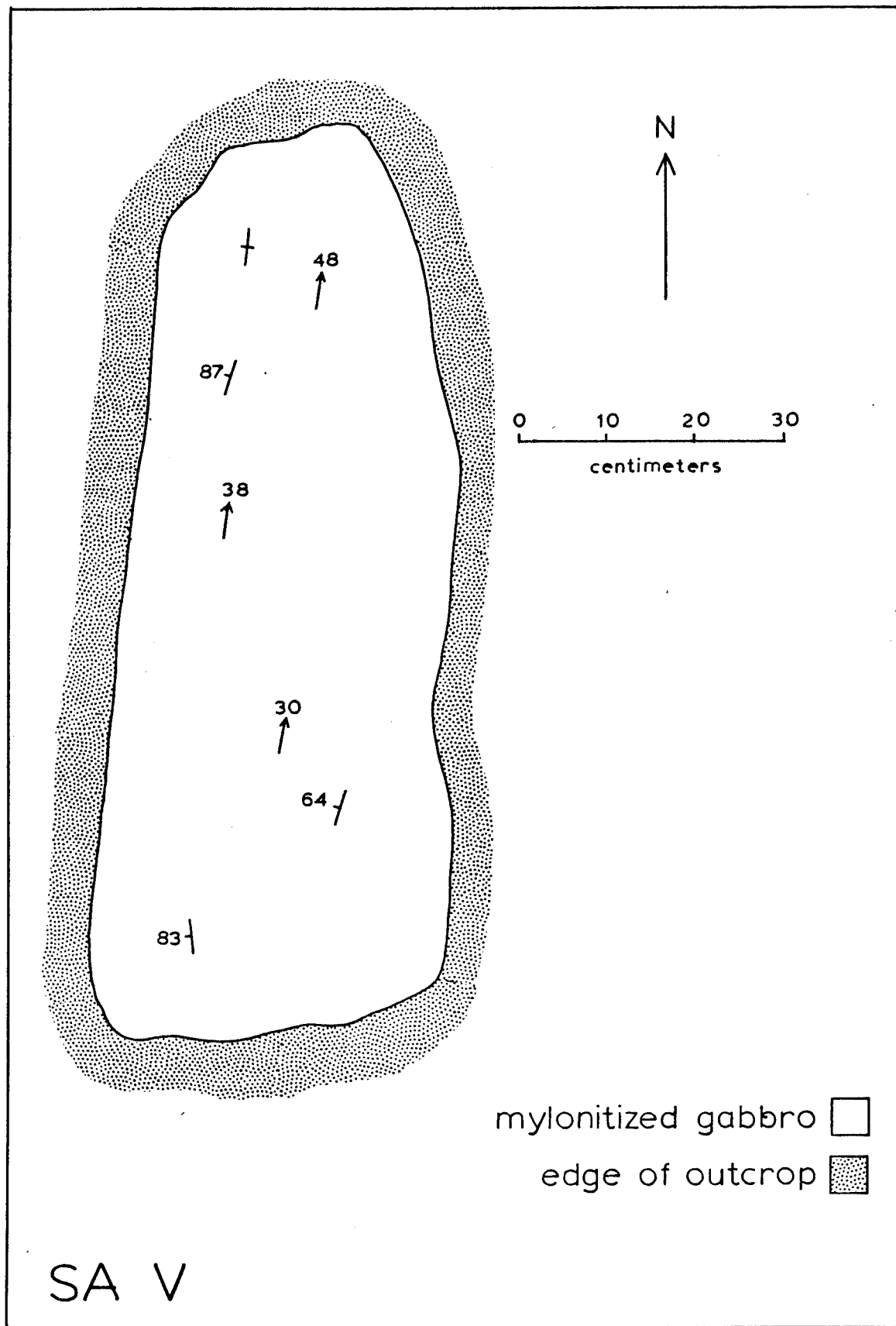


Figure 4.4 G

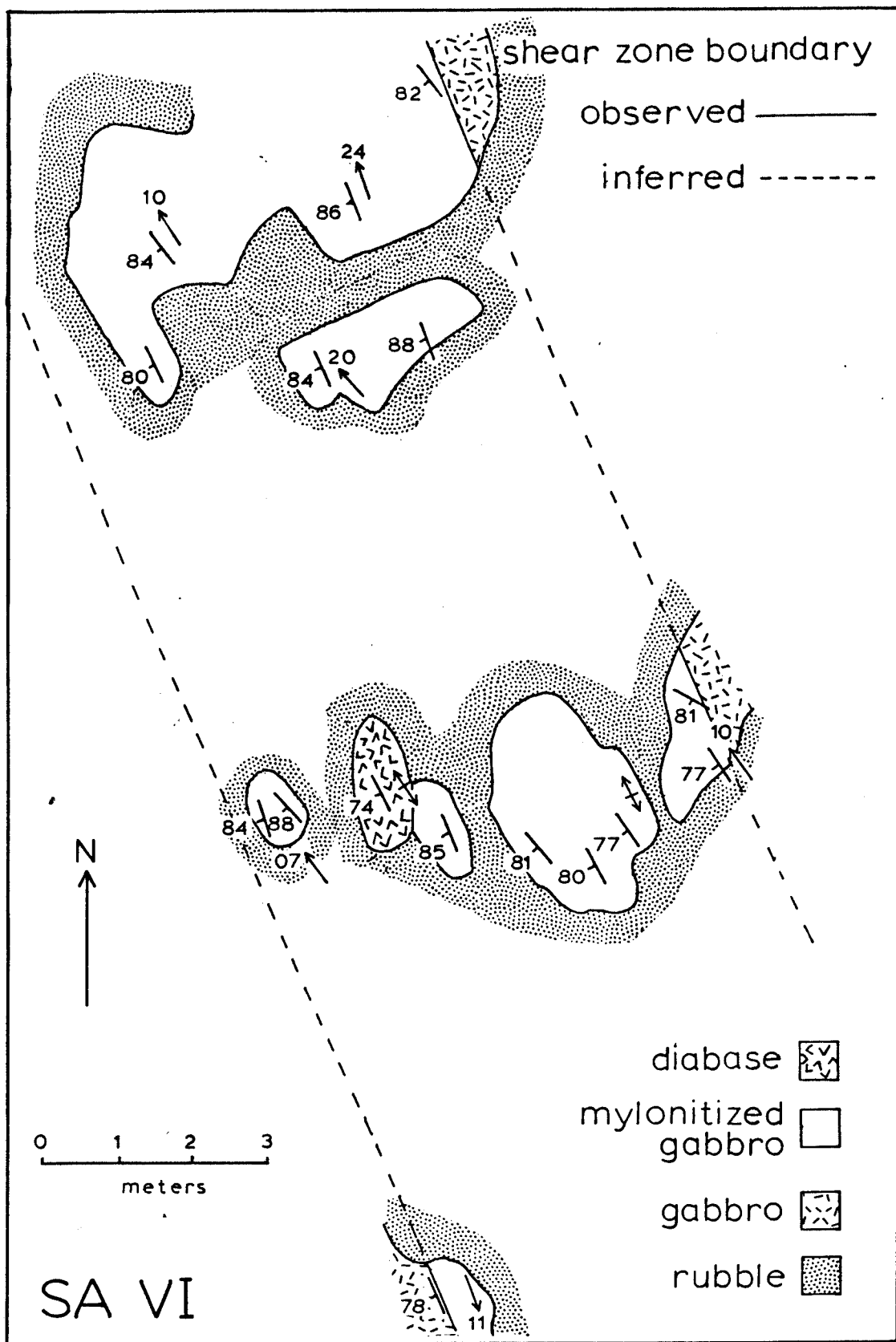


Figure 4.4 H

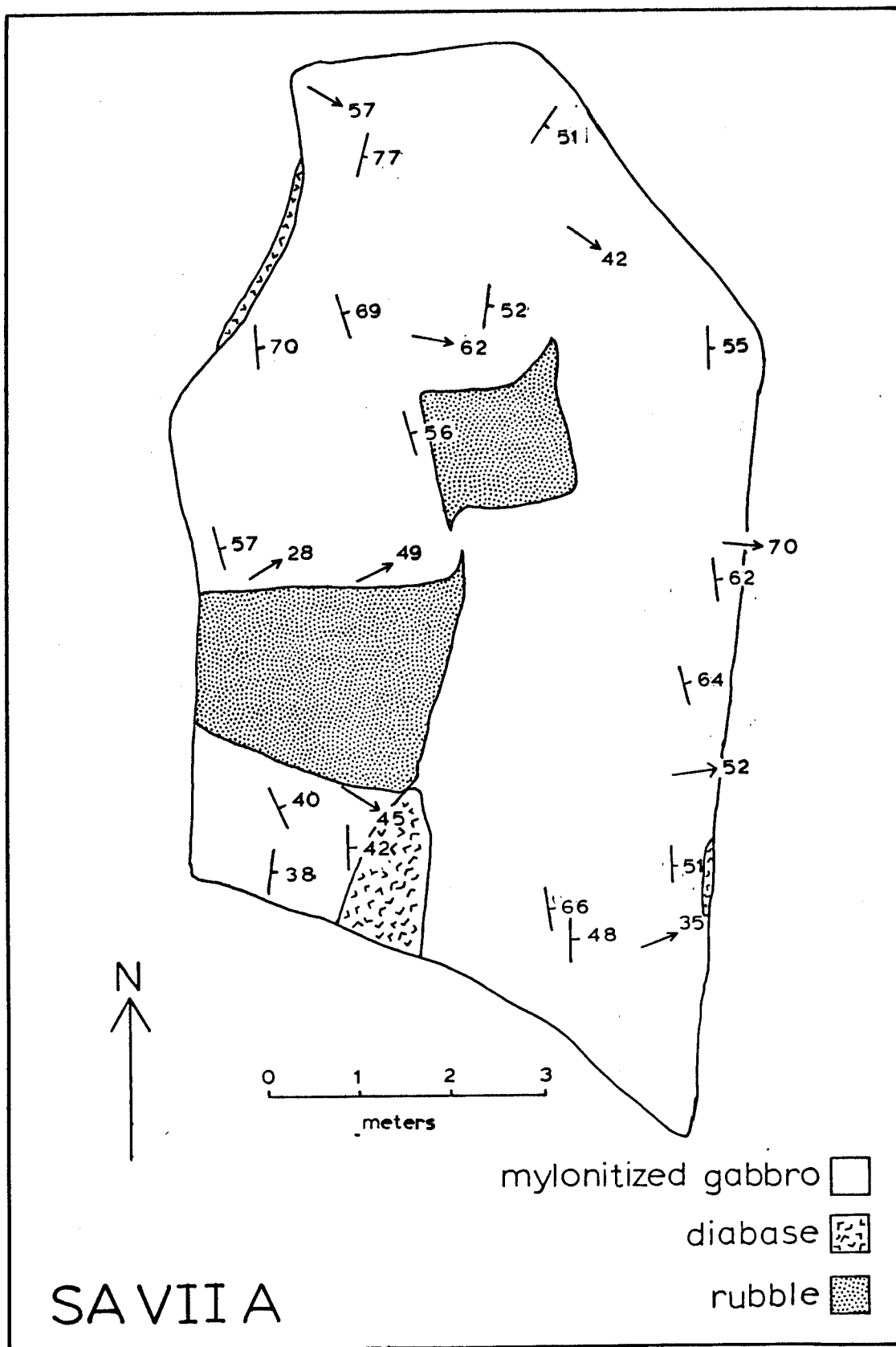


Figure 4.4 I

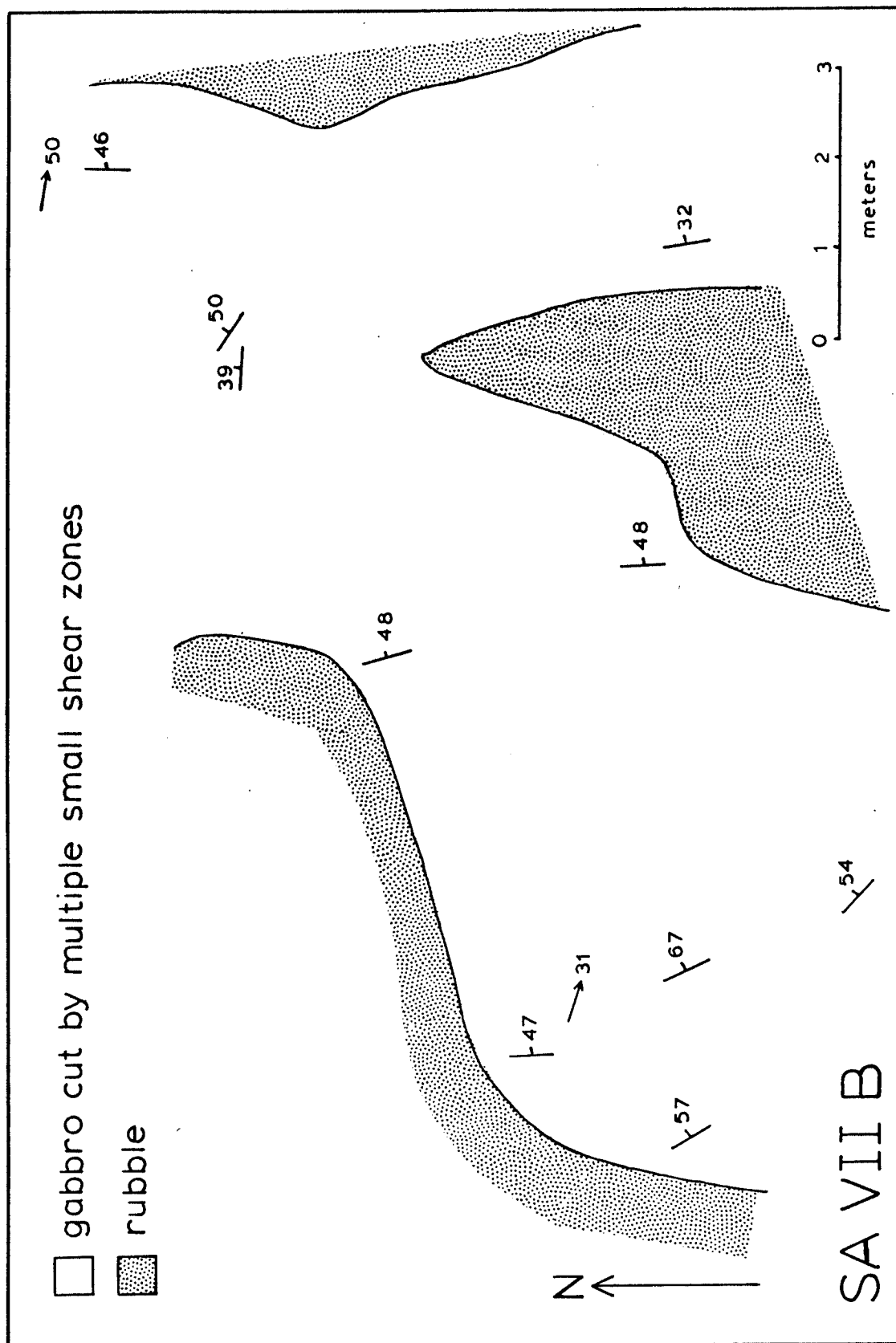


Figure 4.4 J

orientation.

The boundaries of the shear zones seen in outcrop are usually abrupt, with fine grained, strongly foliated, mylonitic material directly in contact with weakly or non-foliated, medium to coarse-grained gabbro (Fig. 4.5) with no visible shear-related deformation. Occasionally the shear zone boundary is not as abrupt, and a faint foliation which swings into the main mylonitic foliation over a few millimeters is developed. Deformation of the country rock which is not visible in outcrop is present on a microscopic scale. The changes in structure and texture from the country rock through the most deformed rocks within the shear zones are discussed in a later section.

The main exception to this description is SZ VII. To the east of the main body of SZ VII there is a 12 meter wide zone of gabbro which is cross-cut every few centimeters by narrow (several millimeters wide) shear zones (see Fig. 4.4, SZ VIIB). The individual "mini-shears" are not represented in the diagram, but all measurements were taken from such deformed areas. Such a zone may also be present to the west of SZ VII, but there is little outcrop to prove this. In several locations (SZ's IV, VII) narrow splays veer out from the main body of the shear zone (Fig. 4.6).

No terminations of the shear zones were observed, again due to paucity of outcrop. Even in the case of long shear zones such as SZ I and SZ IV, much of the length of these zones was traced by looking for blocks of foliated material in rubble. It is likely that most of the shear zones terminate gradually, and that the well-defined zone of deformation becomes a more diffuse zone, with the amount of deformation within any given area gradually decreasing away from the main shear



Figure 4.5

Typical shear zone boundary. Unfoliated gabbro to the left, strongly foliated mylonite to the right. Shear Zone II.



Figure 4.6

Narrow shear zones (chalky white weathering) swing into the mylonitic foliation. Main mylonite is present at the top of the outcrop, approximately parallel to short dimension of the photograph. Shear Zone IV.

zone. The west end of SZ IV is splayed, which may reflect proximity to the shear zone termination. It is also possible, although not observed, that the SW ends of some of the shear zones may have terminated in the paleo-magma chamber at which the rocks of the massif formed (see Casey, 1980). In this case highly strained material within the shear zones would terminate abruptly against undeformed gabbro which would have plated against it.

Shear zone I is offset approximately 10 meters in a sinistral sense across a very narrow fault zone. Outcrop of highly deformed material at the two terminations ends abruptly in rubble, and no outcrop is present between them (Fig. 4.3 and 4.4).

3. Foliation

The foliation in all of the shear zones is very well developed. It is defined by alternating amphibole- and plagioclase-rich layers and a grain-shape preferred orientation. It is very easy to pick out the foliation on weathered surfaces because the plagioclase-rich layers weather chalky white, while the amphibole-rich layers weather green. In addition, plagioclase weathers in relative to amphibole, leading to relief on a weathered surface. In areas where the grain size and layer thickness are very small this difference in weathering characteristics makes the foliation readily apparent. The overall shape of the shear zones is planar to slightly curvilinear (Fig. 4.4). The foliation within the shear zones is composed of subparallel to slightly anastomosing foliae throughout the zones, and is subparallel to the shear zone boundaries. In areas where foliation with slightly different orientations intersects, pods of less deformed material are sometimes

present (Fig. 4.7). Asymmetric intrafolial folds are present in places (Fig. 4.8), but are not common. In SZ II there is a kink in the foliation (Fig. 4.9) which may be related to movement across the fracture seen to the right in the photo. In one location in SZ I the main mylonitic foliation is crenulated (Fig. 4.4 and Fig 4.10), and at the same location a small area of cataclastic material is present (Fig. 4.11).

On the microscopic scale, two planar surfaces are developed. These are the c- and s-surfaces of Berthé et al. (1979) and Lister and Snoke (1984). S-surfaces are foliation planes which form oriented approximately parallel to the flattening plane (XY) of the infinitesimal strain ellipse, and may, in early stages of formation, remain approximately parallel to the XY plane of the finite strain ellipse. However, recrystallization may "periodically reset the 'finite-strain clock'" (Lister and Snoke, 1984) and return s-surface defining elements to parallel with the XY plane of the infinitesimal strain ellipse. The c-planes are active planes of shearing (cisaillement) which may displace the s-planes and which are oriented parallel to the shear zone boundaries (Fig. 4.28).

Lister and Snoke (1984) have defined two types of s-c mylonites in quartz-mica rocks. Type I mylonites are those in which the s-planes are dominant and define the mesoscopic foliation. The s-surfaces in Type I zones are frequently continuous, and they can be traced as they anastomose in and out of the narrow high strain zones which define the c-surfaces. In Type II mylonites the c-surfaces dominate. They form the mesoscopic foliation, and the s-surfaces are often difficult to discern in thin section and hand sample. The shear zones in this study



Figure 4.7

Pod of less deformed material surrounded by mylonite. Rubble, shear zone IV.



Figure 4.8

Asymmetric intrafolial folds. Rubble, shear zone IV.

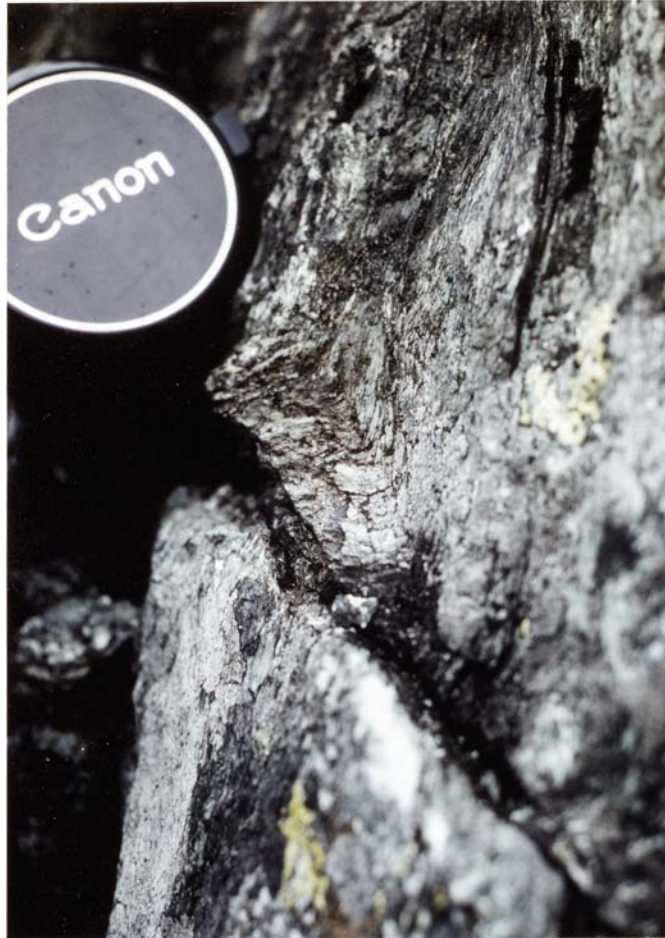


Figure 4.9
Kink in the mylonitic foliation. Shear Zone II.

Figure 4.10

Crenulation of the main mylonitic foliation. Shear zone I.

Figure 4.11

Small zone of cataclastic material. Shear zone I.



Figure 4.10



Figure 4.11

are similar to the Type II mylonites which Lister and Snoke (1984) described in quartz-mica rock. The shear zone boundary-parallel c-surfaces define the main mylonitic foliation.

The density of development of c- and s-surfaces varies from sample to sample. In all samples c-surfaces are visible. S-surfaces in some samples are not visible. In others, the s-surfaces are defined by one or more of the following: a) preferred grain shape orientation of recrystallized plagioclase grains, b) orientation of elongate blades of fine grained amphiboles in areas between c-surfaces, c) the shapes of asymmetric augen in which two sides are parallel to the c-surfaces and two sides are parallel to the s-surfaces.

The angle between s- and c-surfaces, where both are developed, ranges from about 45° in some samples, down to $10-15^{\circ}$ in others. Due to the effects of recrystallization mentioned above, these angular relationships are not very useful in determining finite strain.

4. Lineation

SZ VII is the only shear zone in which a lineation is obvious on outcrop scale. On a weathered surface the lineation is defined by aligned elongate green amphibole rods, surrounded by a chalky pale green to white matrix. The elongate rods lie in the plane of the foliation, and are slightly flattened parallel to the foliation plane. In areas where lineation is not obvious, oriented samples were taken. In some samples careful examination of the weathered surfaces revealed the presence of a lineation similar to that present in SZ VII, although finer grained and harder to distinguish. Other samples were split parallel to the foliation, and the foliation planes were examined

carefully with hand lens and binocular microscope. In some cases a very faint lineation lying within the foliation plane and defined by elongate aggregates of very fine grained amphibole and plagioclase is present. The lineated samples were reoriented (at SUNYA) out of doors, and the orientations of the lineations were measured.

C. Microstructural Variations Across Shear Zone Boundaries

The thin sections from which these microstructural observations were made were cut parallel to the lineation and perpendicular to the main mylonitic foliation in the sample, an orientation generally believed to be parallel to the shearing direction and perpendicular to the shearing plane (see Lister and Snoke, 1984). All samples collected were oriented in the field, allowing reorientation at SUNYA. This orientation information was useful when determining sense of shear from microstructural criteria. The structures characteristic of the undeformed country rock, rocks adjacent to the shear zone boundary, and rocks within the shear zones are discussed. The terminology of White, et al. (1982) is followed.

1. Undeformed Country Rock

The rocks which the shear zones cut are hypidiomorphic granular gabbros, olivine gabbros, and meta-gabbros (amphibolitized). In some cases plagioclase poikilitically encloses clinopyroxene or olivine, while in others hornblende (originally clinopyroxene) poikilitically encloses plagioclase. Most samples have a slight foliation defined by grain-shape. Growth twinning is common in the plagioclase, and widespread but infrequent occurrences of mechanical twinning are

present. Plagioclase grain boundaries are straight and intersect at 120° angles, forming triple junctions. The other phases in the country rock are subhedral and untwinned (Fig. 4.12).

2. Microstructures Developed Adjacent to Shear Zone Boundaries

In outcrop, the country rock just outside the shear zone boundary looks undeformed; however, microscopic observations show that deformation in these rocks is pervasive. Coarser grained areas which are highly fractured are separated by finer grained, ductile zones where recrystallization has occurred. The ductile zones typically comprise less than 20% of the rock outside the shear zone boundaries, while over 80% of the rocks within the shear zone boundaries fall within this category. As the amount of fine grained material increases, the coarser grained material that remains is present in pods or in layers bounded by finer grained material. This contact is in some cases gradational and in others abrupt.

Plagioclase in the coarser-grained areas is extensively fractured and twinned. Twins which have sharply defined, parallel boundaries are present and are probably growth twins. These are also widespread in the country rock. Commonly, however, the twin boundaries are slightly curved and terminate in points, suggesting mechanical twinning. Twin boundaries in some grains are bent, and undulose extinction within plagioclase in the coarse grained zones is ubiquitous.

The fractures that cut the plagioclase grains are frequently lined with fine amphibole shreds. These shreds are usually aligned with their long axes parallel to the fracture, although in some instances the fracture-lining amphibole lies parallel to the main myloni-

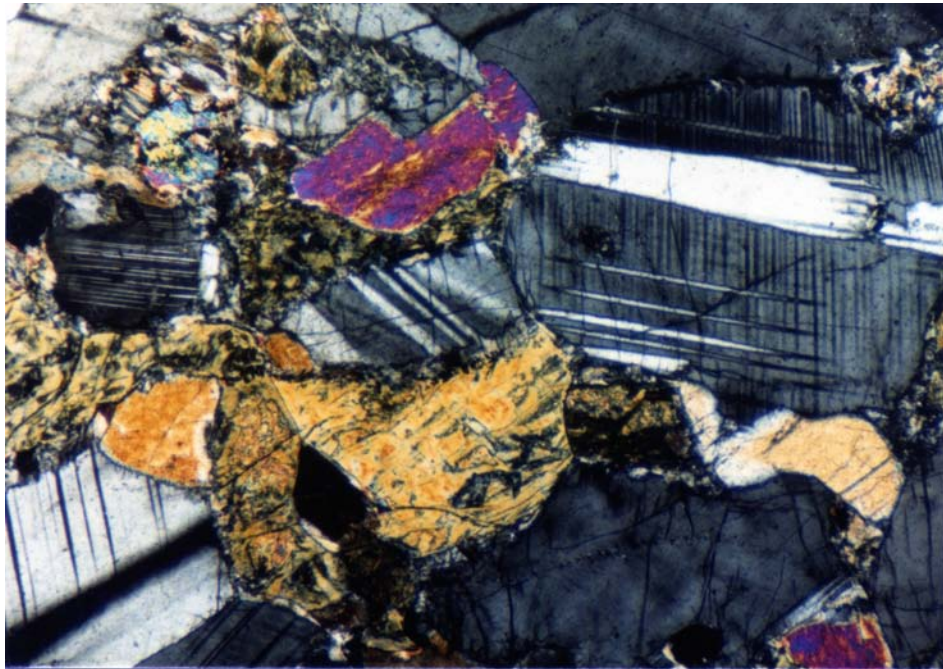


Figure 4.12

Undeformed country rock. Diagonal approximately 3.64 mm.
Note mechanical twinning in plagioclase, upper right.

tic foliation. The grain shapes of the plagioclase porphyroclasts which result from this fracturing range from angular to subrounded, and they are generally between 0.10 and 1.5 mm in diameter.

The porphyroclasts are surrounded by varying amounts of very fine grained, recrystallized plagioclase. The grain boundaries in the recrystallized plagioclase are serrated, and a faint to moderately well developed grain shape preferred orientation is often developed. In a few samples, very narrow bands of recrystallized material cut across remnant large plagioclase grains (Fig. 4.13). The fine grained plagioclase sometimes surrounds small islands of the host grain, making it difficult to distinguish isolated portions of host grains from new grains. Twinning is present in up to 15% of the fine grained plagioclase. As in the coarser grained areas, some of the twins are growth twins, while others are mechanical (criteria discussed above). The twinning in fine grained areas may, in part, have resulted from isolation of very small portions of twinned host grains. Mechanical twinning may have resulted from continued deformation after initial recrystallization. Undulose extinction is common within recrystallized portions of the predominantly coarse grained areas (Fig. 4.13). In some samples, extensive subgrain formation within large plagioclase grains is present. The subgrains are polygonal and strain-free. Figure 4.14 is a typical view of a sample adjacent to a shear zone boundary.

Clinopyroxene, where present, occurs mainly as porphyroclasts, which are covered by dusty alteration products. Fine grained amphibole commonly rims the clinopyroxene (Fig. 4.15) and is present in fractures which cut it. Stringers of fine grained, equant, unaltered clino-

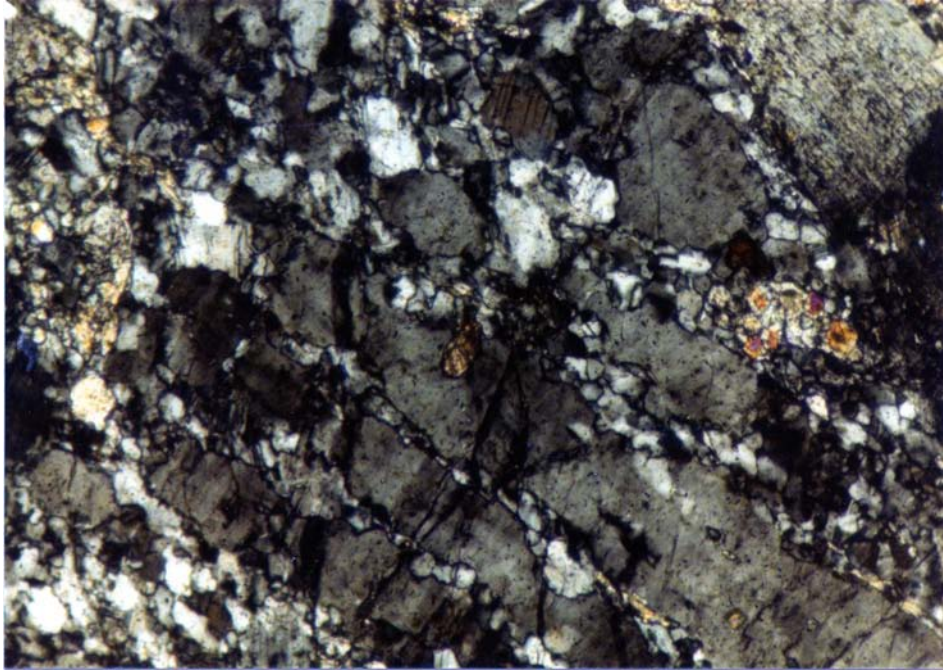


Figure 4.13

Fine grained, recrystallized plagioclase cutting across host grain. Note serrated grain boundaries, undulose extinction and infrequent twinning in the recrystallized grains. Diagonal approximately 1.46 mm. Shear zone I.

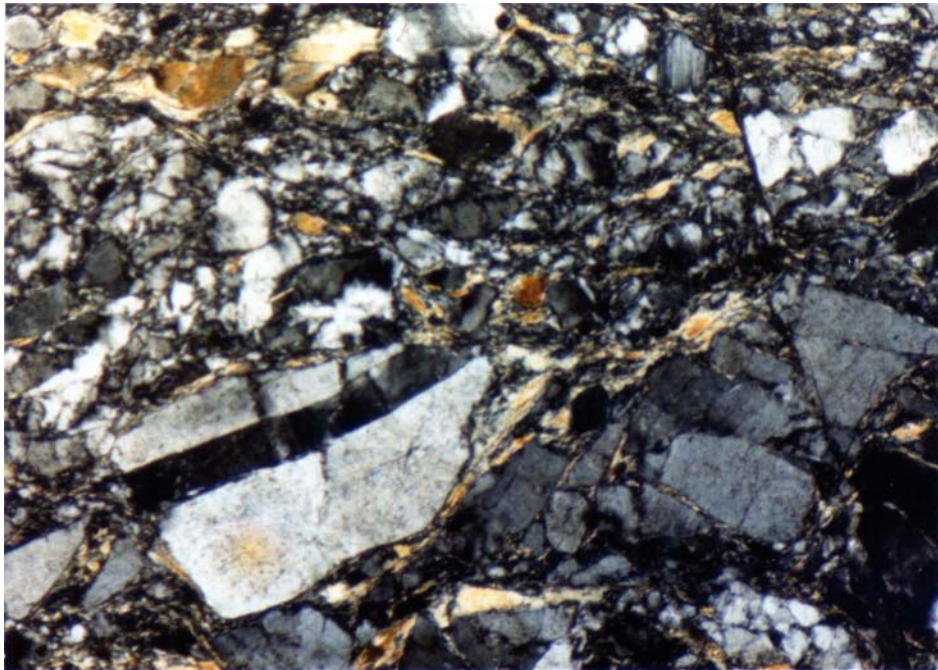


Figure 4.14

Typical view of a sample adjacent to a shear zone boundary. Note twinning, undulose extinction, and amphibole shreds. Diagonal approximately 3.64 mm. Shear zone VI.

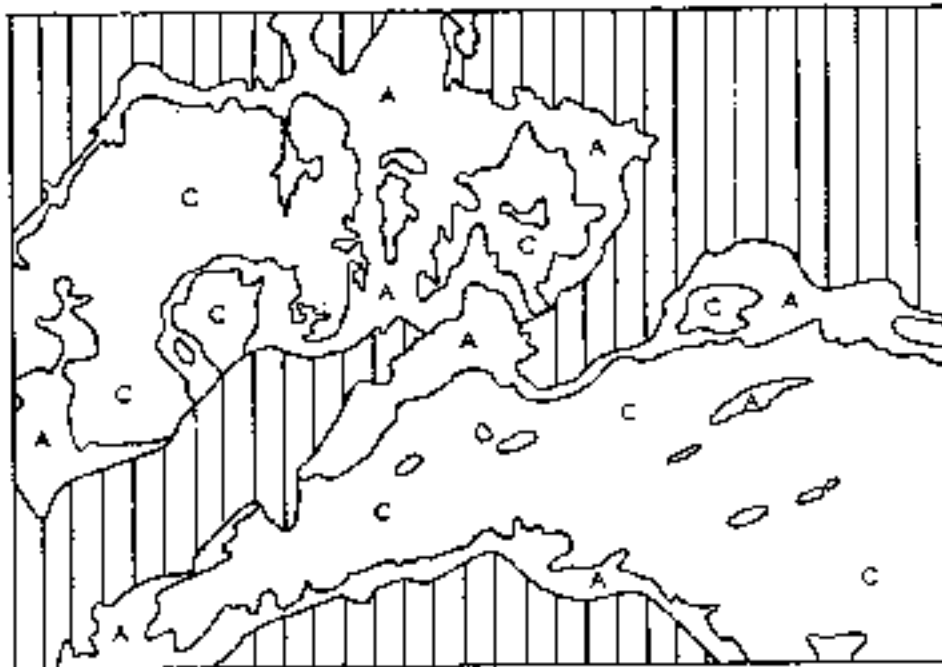
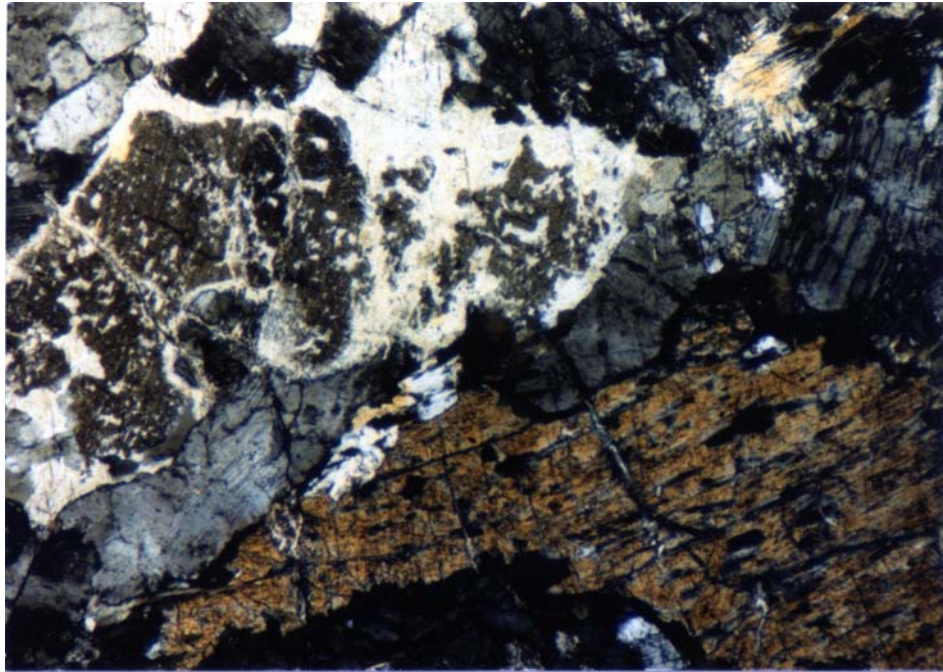


Figure 4.15

Amphibole rimming clinopyroxene. A = amphibole, C = clinopyroxene, vertical lines = other phases. Diagonal approximately 3.64 mm. Shear zone IV.

pyroxene are occasionally present in the fine grained portions of the samples.

In most samples the clinopyroxene has been completely altered to amphibole (the range of amphibole compositions is discussed in Chapter 5). Igneous textures are sometimes preserved in these areas. Figure 4.16 shows several plagioclase grains poikilitically enclosed by amphibole which altered from clinopyroxene. Amphibole which occurs adjacent to shear zone boundaries is also commonly fractured. Fractures are "bridged" by fine grained amphiboles (Fig. 4.17) which appear to join points on opposite sides of the fracture which were originally in contact, and to have grown as the fracture formed. The amphibole grains (or porphyroclasts as fracture density increases) range from .75 - 1.5 mm, and in one case up to 9 mm across. Although this size range is very similar to that of plagioclase porphyroclasts, the ratio of coarser to finer porphyroclasts is higher in the amphiboles, and the ratio of porphyroclasts to recrystallized material is lower. This suggests that once enough strain has accumulated within an amphibole porphyroclast it tends to recrystallize (Fig. 4.18) rather than fracture into smaller porphyroclasts. The presence of narrow zones of fine-grained, recrystallized amphibole blades which cut even the least deformed rocks adjacent to the boundaries of the shear zones indicate the readiness with which amphiboles recrystallize.

3. Microstructures Developed Within the Shear Zone Boundaries

The material within the shear zone boundaries is mainly mylonitic, with less frequently occurring blastomylonite and ultramylonite. Typically less than 20% of the material within a shear zone is coarse

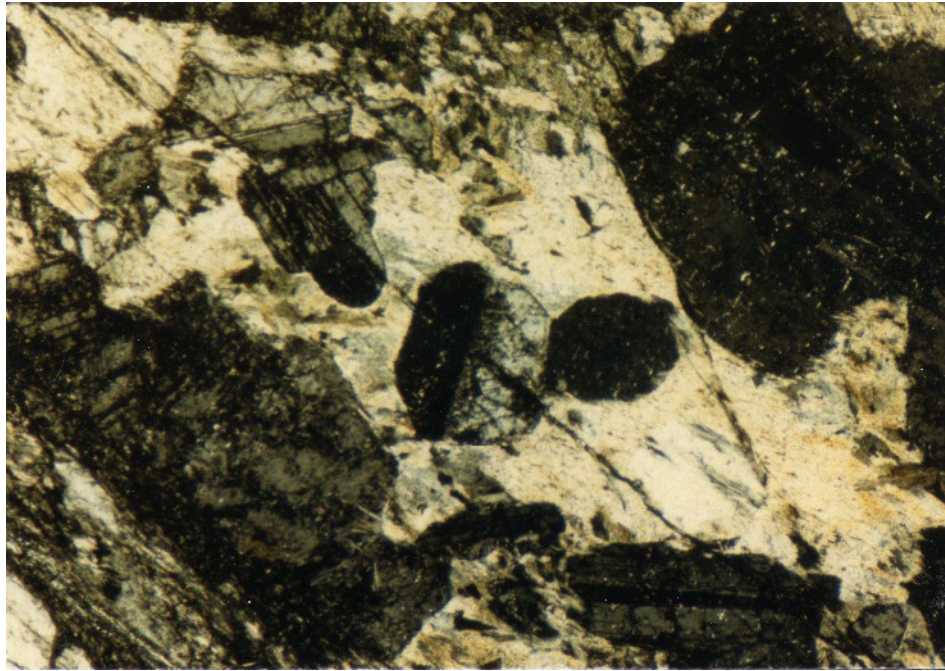


Figure 4.16

Amphibole (pale yellow), altered from clinopyroxene, poikilitically enclosing plagioclase grains. Diagonal approximately 3.64 mm. Shear zone VII.

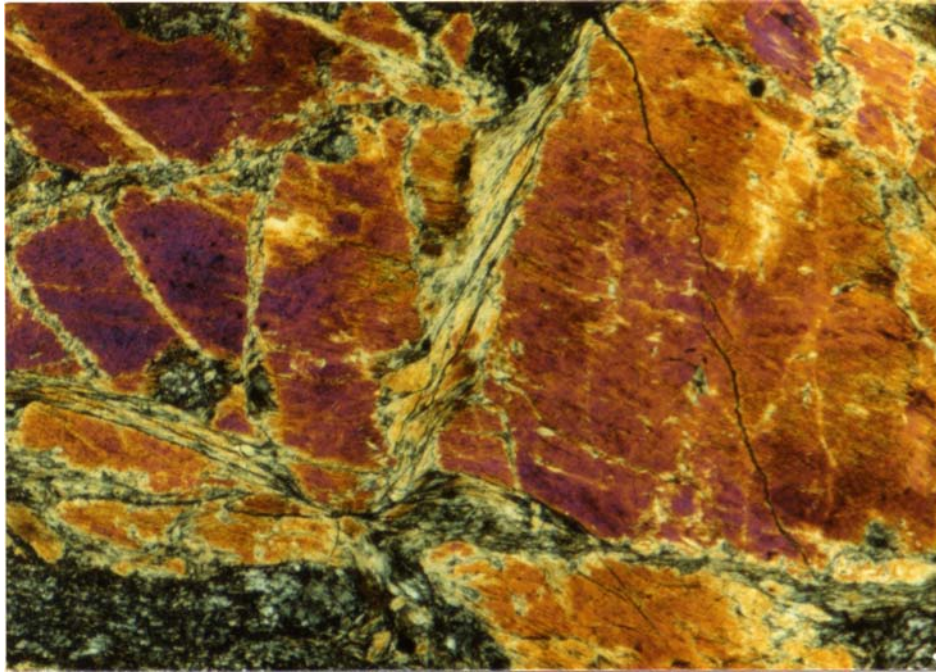


Figure 4.17

Fine grained amphibole “bridging” a fracture in an amphibole porphyroblast. Diagonal approximately 3.64 mm. Shear zone VII.

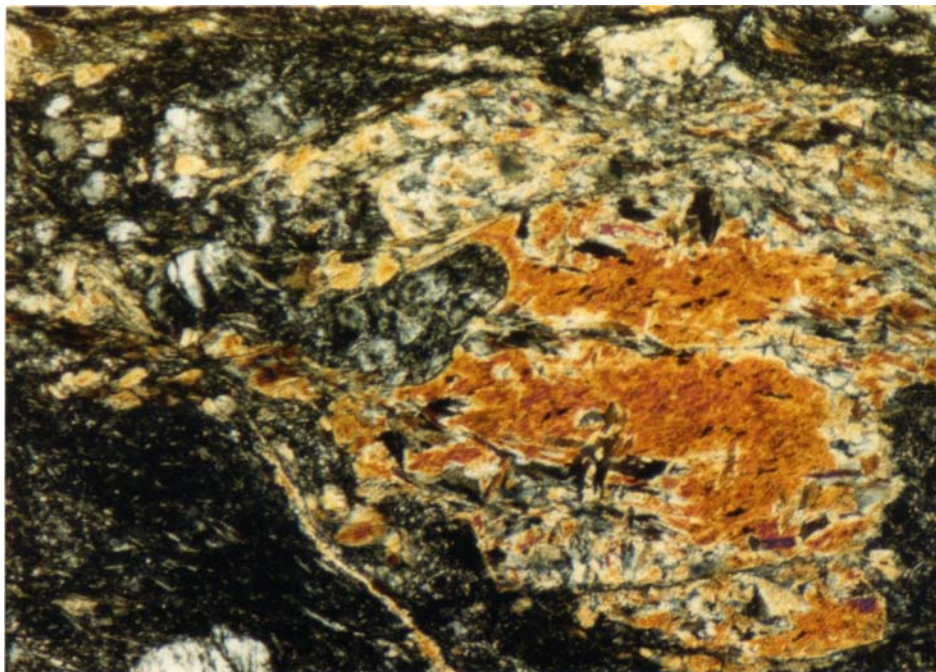


Figure 4.18

Amphibole porphyroblast being replaced by fine grained amphibole blades. Diagonal approximately 3.64 mm. Shear zone VI.

grained and fractured.

The fine grained zones are similar to those described above, except that they are more extensively developed. Plagioclase grains range from $< .01$ mm to $< .05$ mm in diameter. Serrated grain boundaries and undulose extinction are widespread, and twinning is present in up to 10-15% of the fine grained plagioclase. A slight grain shape preferred orientation is often developed in the fine grained plagioclase. In cases where this preferred dimensional orientation is best developed it can be seen that it is slightly oblique to the main mylonitic foliation defined by the orientation of amphibole aggregates and alternating plagioclase and amphibole-rich layers. The plagioclase dimensional orientation is one of the features which defines the s-surfaces in these samples.

Amphibole within the shear zone boundaries is very fine grained (individual blade dimensions are approximately $.01 \times .10$ mm or less) and shows a very well developed grain shape and crystallographic preferred orientation (c axis within or close to the plane of the thin sections cut parallel to lineation and perpendicular to foliation). Amphibole is present as the main constituent of amphibole rich bands, as a fine overgrowth of needles in plagioclase rich zones, and as isolated "shreds" which may be oblique or parallel to the main mylonitic foliation. The fine grained amphibole zones are often slightly wavy (Fig. 4.19).

The porphyroclasts which remain in the mylonitic areas are smaller than those in less deformed areas, ranging up to $.5$ mm in diameter, as opposed to several millimeters. Some areas are almost entirely devoid of porphyroclasts, and individual grains are so small that they are

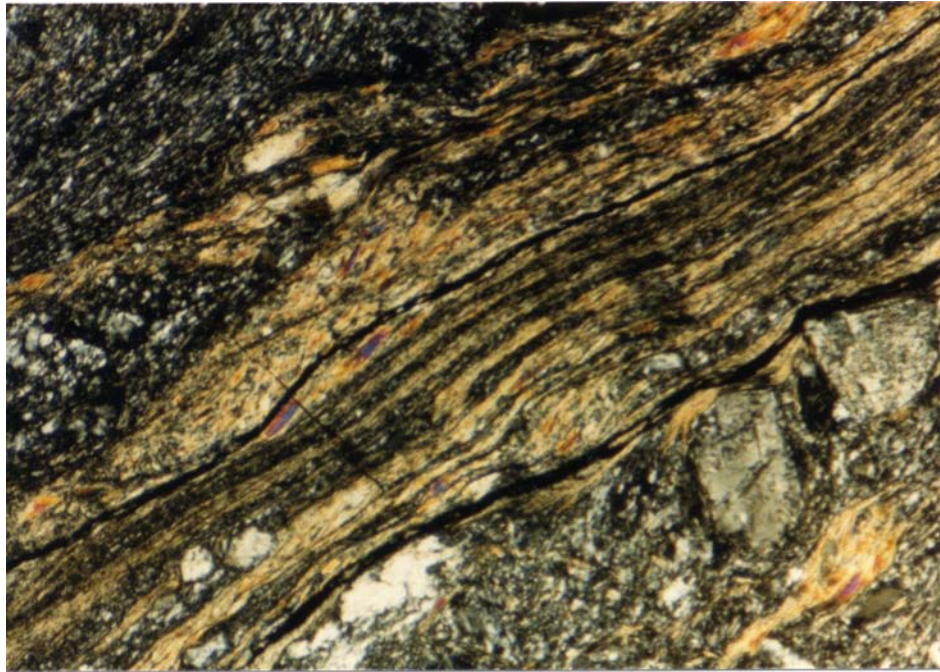


Figure 4.19

Typical fine grained amphibole- and plagioclase-rich zones, with some porphyroclasts. Diagonal approximately 3.64 mm. Shear zone VII.

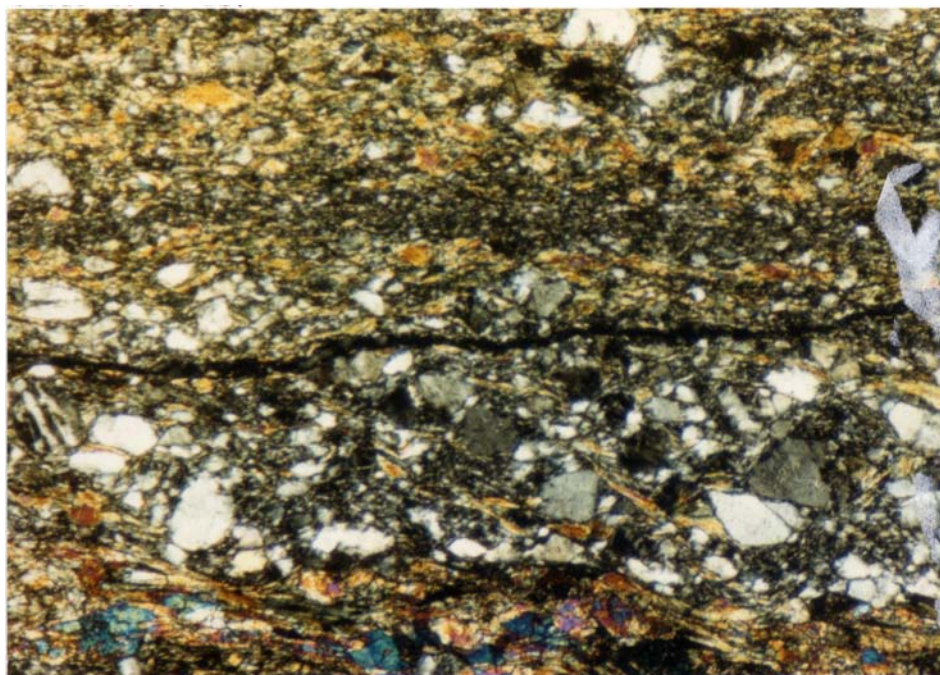


Figure 4.20

Adjacent fine grained and coarse grained zones. Note amphibole shreds oblique to main foliation in coarser grained, plagioclase rich zone just below the center of the photograph. Diagonal approximately 3.64 mm. Shear zone VI.

difficult to pick out, even under the microscope. In others, small porphyroclasts are numerous. Adjacent layers within the mylonite may vary considerably with respect to composition, grain size, and dominant type of deformation (Fig. 4.20).

4. Post-Kinematic Veins

The shear zones are frequently cut by veins which cut across the foliation (Fig. 4.21). The veins are undeformed, and therefore post-date movement across the shear zones. Typical vein minerals include zeolites, chlorite, clinozoisite, smectite, and prehnite, and occasionally calcite and quartz. These minerals are zeolite-greenschist facies phases which are quite different from the low pressure amphibolite facies phases of the mylonites.

5. Cataclastic Zones

In several thin sections and in one outcrop occurrence mentioned above, brittle disruption which cuts across the mylonitic foliation is present. This apparently late-stage brittle deformation in some cases forms mini-faults which cut the mylonitic foliation at a high angle (Fig. 4.22a), and in others forms chaotic zones several millimeters wide that are at a low angle to mylonitic foliation. In these zones, foliated fragments in random orientations are surrounded by a fine grained matrix (Fig. 4.22b). These zones are different from the usual cataclastic zones within the mylonites and protomylonites in that they involve already-foliated material, and therefore post-date initial foliation rather than contributing to initial grain size reduction and

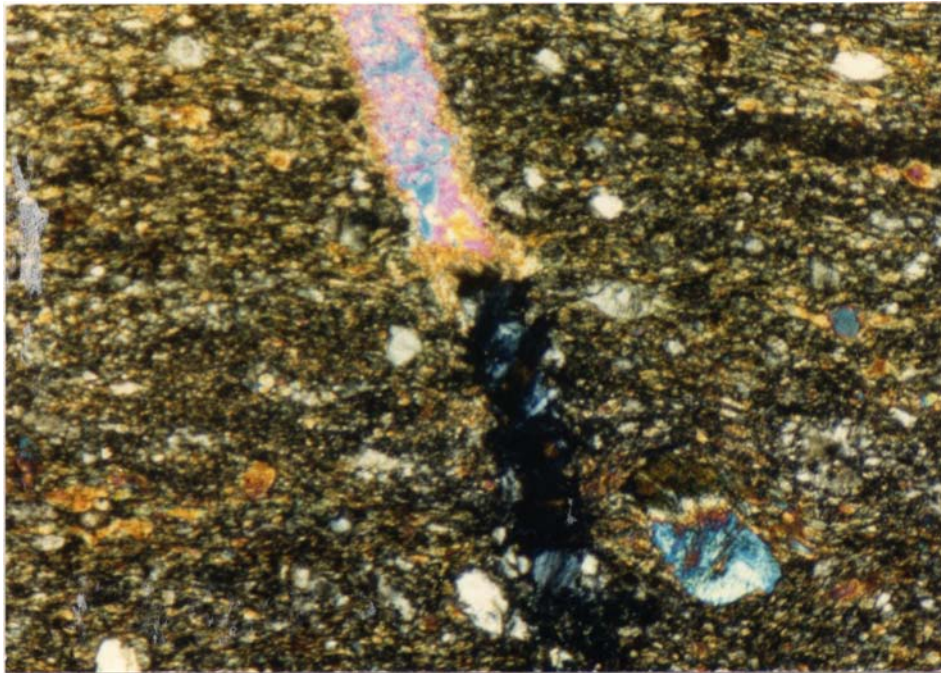


Figure 4.21

Post-kinematic vein. Vein minerals include chlorite (blue and brown anomalous birefringence) and prehnite (second order birefringence). Diagonal approximately 3.64 mm. Shear zone VI.

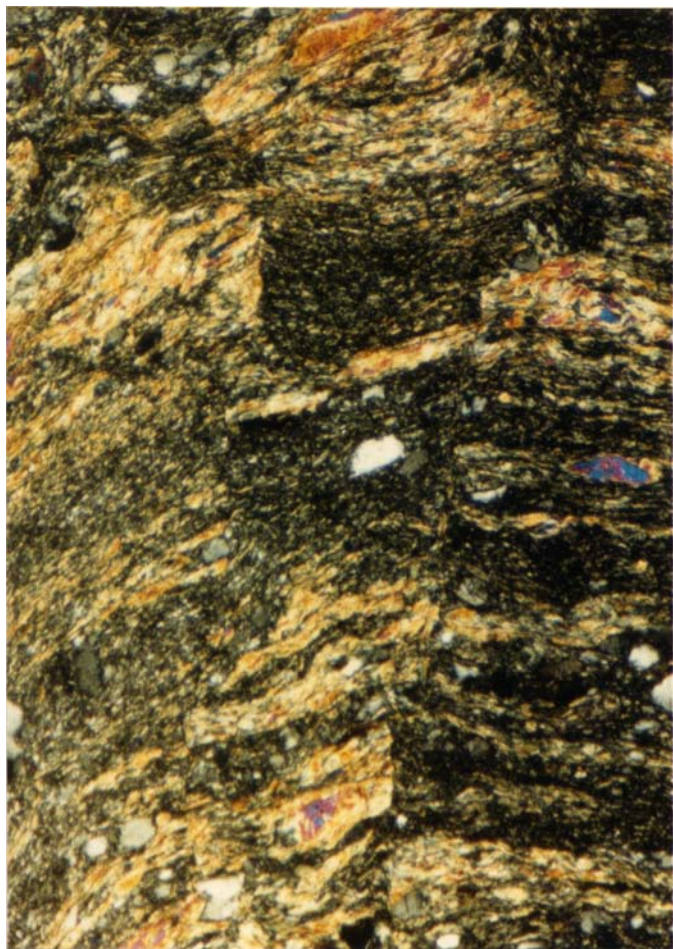


Figure 4.22A

Diagonal approximately 3.64 mm



Figure 4.22B

Diagonal approximately
5.82 mm

Brittle deformation cutting mylonitic foliation. A) high angle “mini-faults”, B) narrow cataclastic zone.

foliation development. A combination of brittle and ductile deformation mechanisms is not apparent in these zones; they have formed solely by brittle processes.

D. Sense of Shear

1. Structures from which Sense of Shear may be Deduced

There many indicators which are useful in determining sense of shear across a shear zone. On outcrop scale, the sense of offset of features such as dikes, lithologic units, or obvious layering or other horizons are ideal sense of shear indicators if one is looking at a section which is parallel to the slip direction. The swing of foliation into ductile shear zones is also useful. Often, however, these most reliable field indicators are not present, and microstructural criteria must be used to determine the sense of shear across a zone.

In the shear zones covered in this study, no displacements of mesoscopic marker horizons are present. Compositional layering in the immediate vicinity of each of the shear zones is not well developed, and displacement of these layers is therefore not readily apparent. In the case of SZ VI, where dike material is caught up in the shear zone, the outcrop does not extend far enough to be able to trace the dike outside the shear zone. The boundaries of the shear zones are generally quite abrupt, without the well developed swing of foliation into the zone described by Ramsay and Graham (1970), and so this criterion is only rarely applicable. In several of the shear zones small splays off the main zone swing into the main zone over the distance of several tens of centimeters (Fig 4.6). It is possible that these narrow, discrete zones have formed in lieu of a more pervasive foliation in the

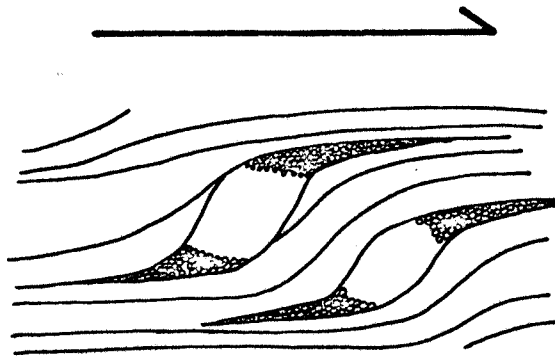
country rock. The sense of offset deduced from the orientation of several of these splays relative to the main shear zones with which they are associated, based on a Ramsay and Graham (1970) model, is consistent with microstructural evidence discussed below, and so will be considered as a useful secondary indication of sense of shear.

On the microstructural scale there are many sense of shear indicators which have proven to be reliable to one degree or another. For a more complete review of these structures the reader is referred to Simpson and Schmid (1983) and Lister and Snoke (1984). The structures which have proven most useful in this study are asymmetric augen, the displacement of grains across narrow fractures, and the orientations of c- and s-surfaces.

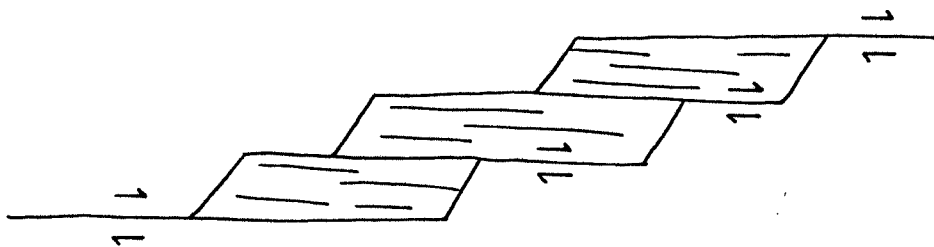
Asymmetric augen or retort shaped grains form where there are coarser grained amphibole or plagioclase porphyroclasts in a finer grained matrix. Tails of finer grained, recrystallized material of the same composition as the host grain form on two opposite corners of the porphyroclast. The tails are foliation parallel, and they point towards the relative sense of motion across the porphyroclast (see Fig. 4.23). The amphiboles often have very well developed tails of recrystallized material (Fig. 4.24a), while plagioclase grains may show a typical asymmetric shape without developing long, fine grained tails (Fig. 4.24b). In areas where there is little variation in grain size, grain shape asymmetry is often not well developed, and among the asymmetric grains which are present there is a great deal of inconsistency as to the sense of shear which they indicate. It seems that interference among many grains of near equal size prevents the formation of well developed tails. It important to note that the tails

Figure 4.23

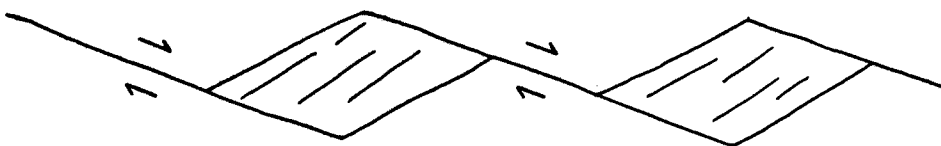
Several microscopic sense of shear indicators. A) asymmetric augen, B) and C) fractured, displaced grains in which sense of offset is the same as the bulk sense of shear, D) fractured, displaced grain in which sense of offset is opposite to the bulk sense of shear. After Simpson and Schmid (1983).



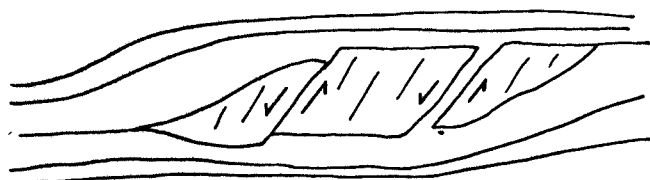
A



B



C



D

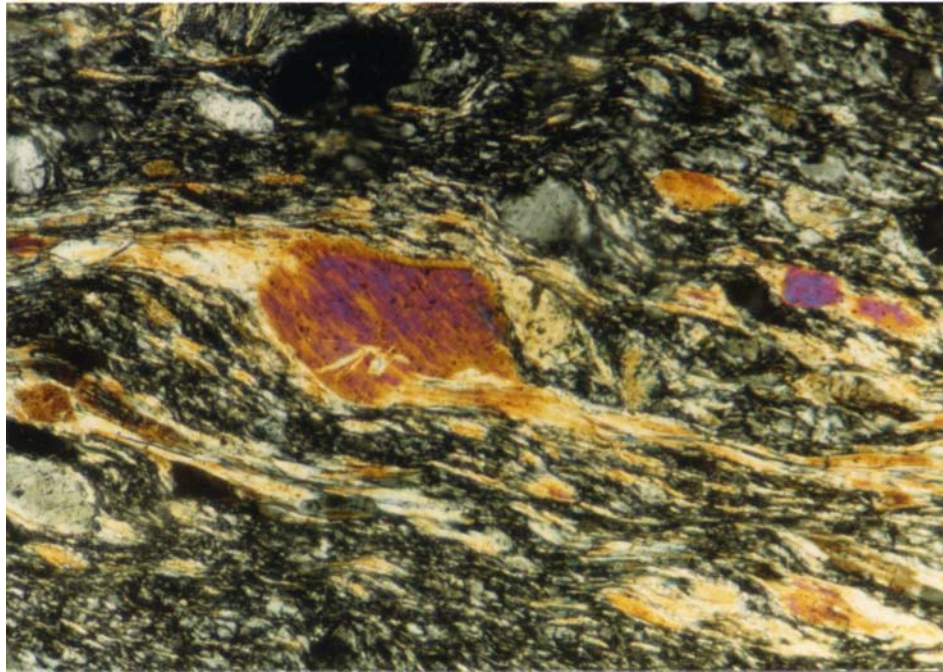


Figure 4.24A

Amphibole augen with asymmetric, recrystallized tails indicating sinistral sense of shear. Diagonal approximately 1.46 mm. Shear zone IV.

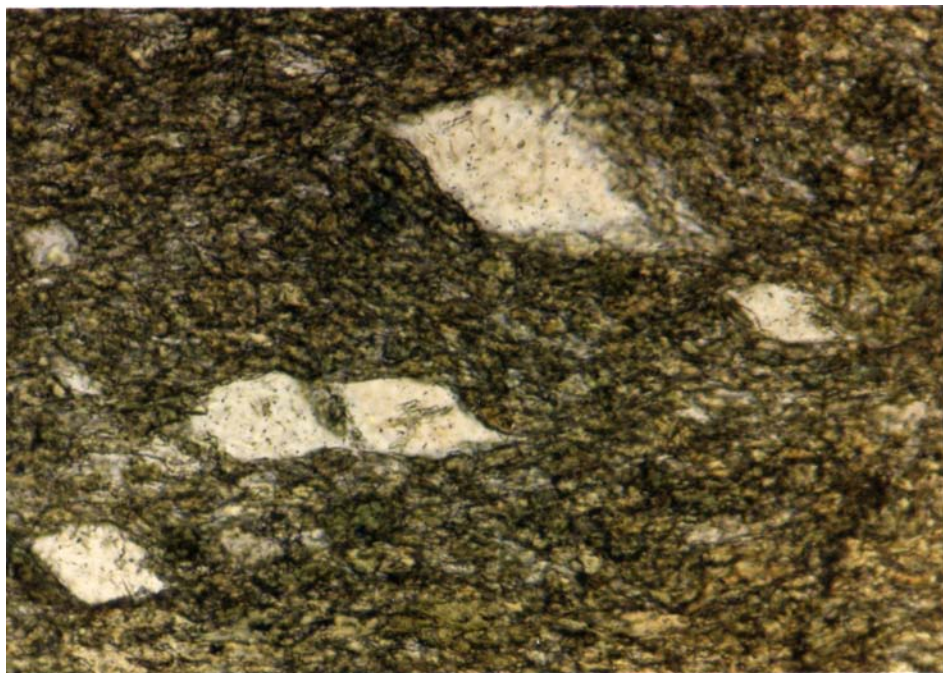


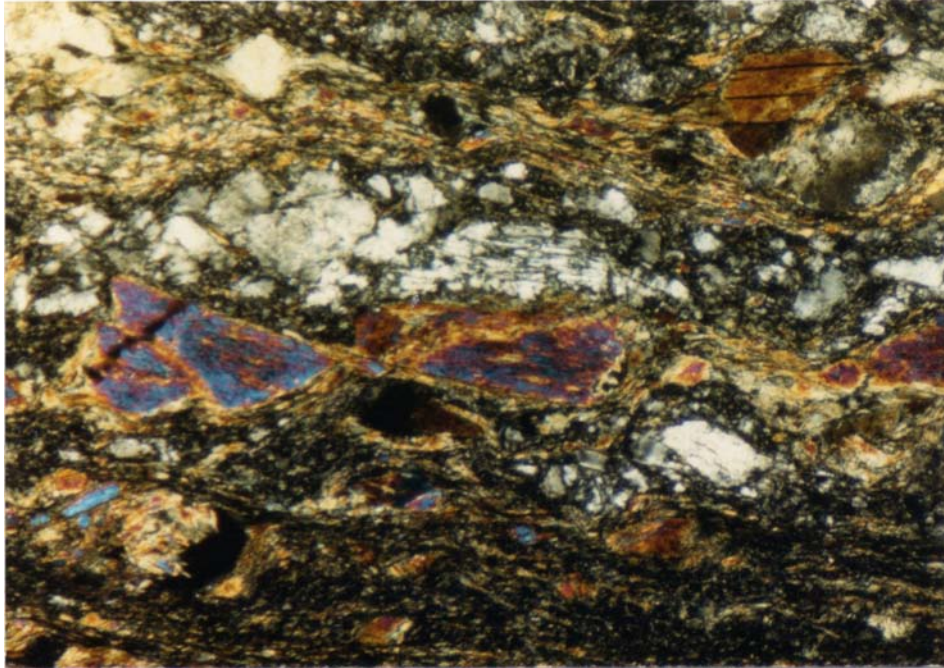
Figure 4.24B

Asymmetric plagioclase porphyroclasts surrounded by fine grained amphibole indicating sinistral sense of shear. Diagonal approximately 1.46 mm. Shear zone I.

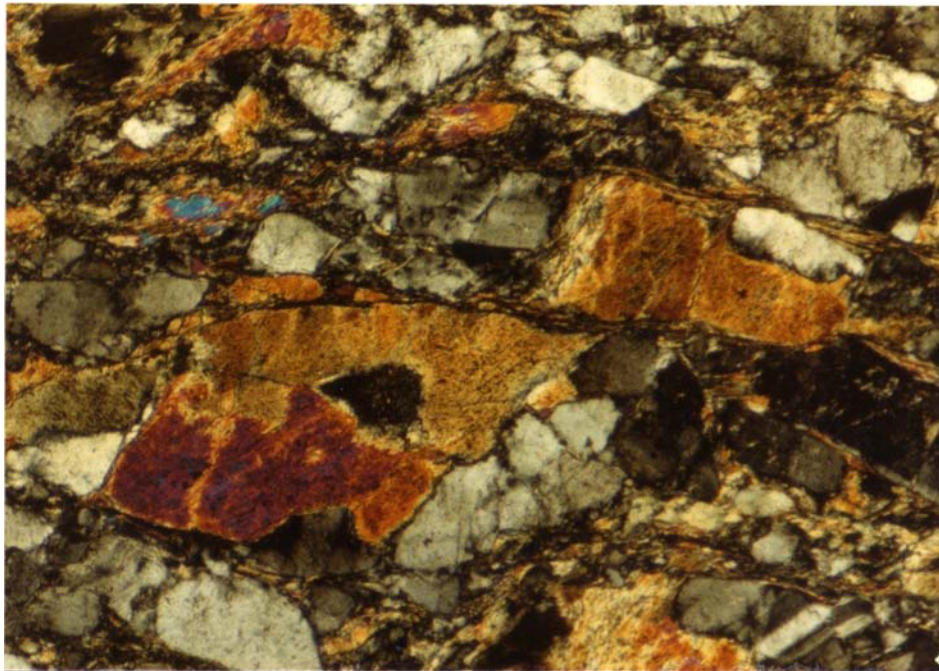
discussed here are not pressure shadows, which may occur in different orientations depending on how they form.

The second commonly occurring feature which may be used to determine sense of shear is the sense of displacement of fractured grains. This criteria must be used with caution because, depending on the initial orientation of the fracture, the offset of the pieces of the grain may be in the same or the opposite sense as that of the overall deformation. Fractures which form at a high angle to the bulk flow plane will tend to have offsets opposite to the overall sense of shear, while the offset across foliation-parallel fractures are consistent with the overall sense of shear (Fig. 4.23, 25, and 26). Both of these cases are pictured in Figure 4.27, from a sample which has undergone a dextral sense of shear. The amphibole at extinction in the upper left hand corner of the photograph shows a dextral offset, while the plagioclase grain in the lower right hand corner of the photograph shows sinistral offset. The mylonitic foliation in this sample is approximately parallel to the long dimension of the photograph. Fractured grains are commonly found in coarser grained samples and portions of samples.

The third criterion which has proven useful in deducing sense of shear is the relative orientation of c- and s-surfaces. These terms are being used in the sense of Berthé et al. (1979) and Lister and Snoke (1984), which is described in an earlier section. The angular relationship between c- and s-planes in a mylonite is related to the bulk shear sense in the way illustrated in Figure 4.28. It is interesting to note that the intersection of c- and s-planes isolates asymmetric pods of material. It may be that the shapes of the asymmetric



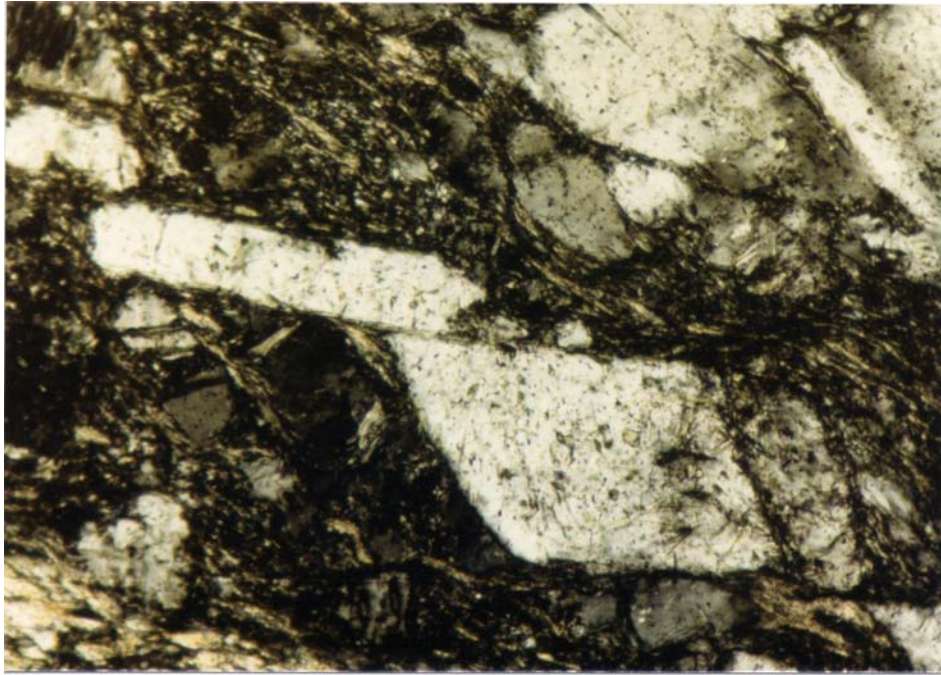
A



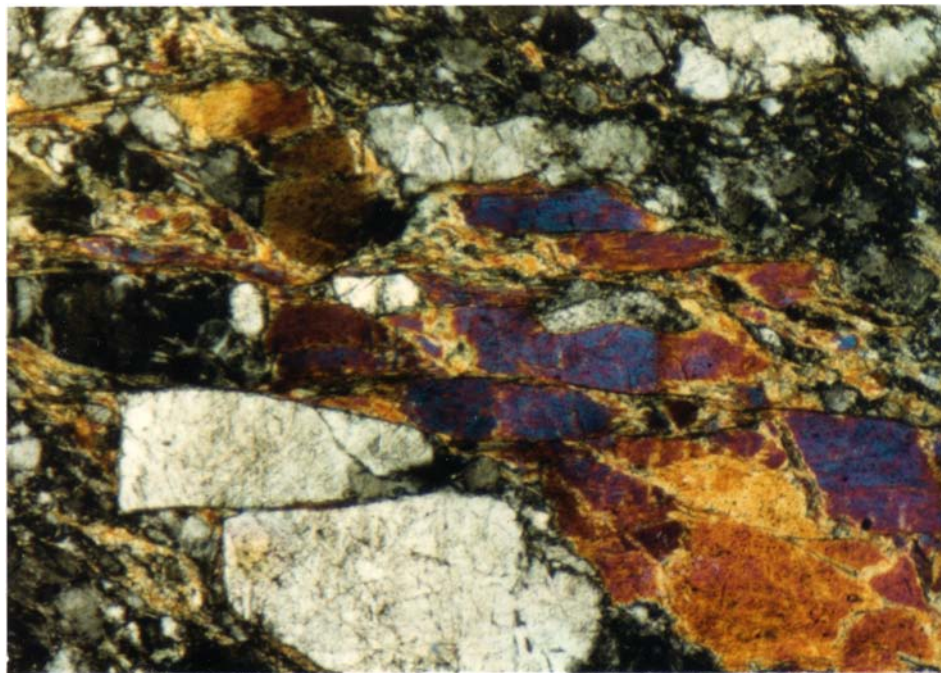
B

Figure 4.25

Two examples of offset amphiboles from the same sample, both indicating dextral sense of shear. Diagonal for both A and B approximately 3.64 mm. Shear zone VI.



A



B

Figure 4.26

Several sinistrally offset grains from one sample. A) offset plagioclase grain, diagonal approximately 1.46 mm. B) offset plagioclase and amphibole grains, diagonal approximately 3.64 mm. Shear zone VI.

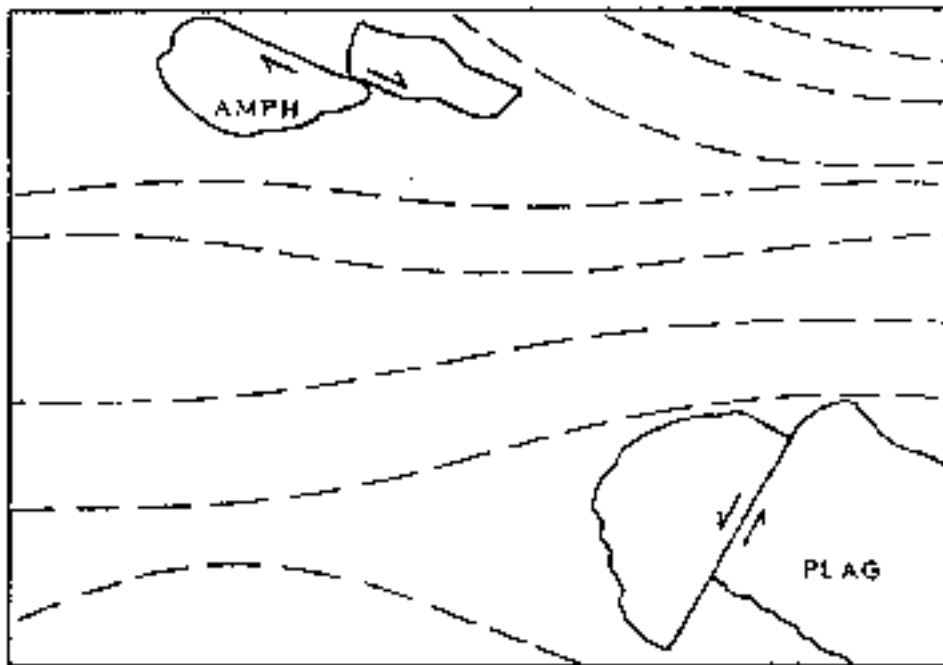
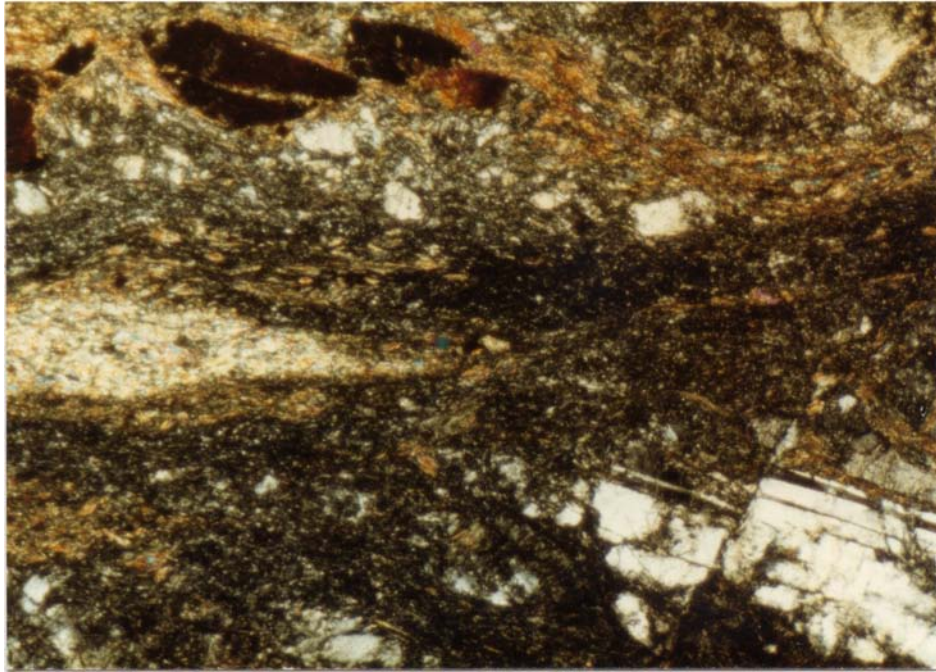


Figure 4.27

Both sinistrally and dextrally displaced broken grains from a dextral shear zone. AMPH = amphibole grain, PLAG = plagioclase grain, dashed lines = foliation. Diagonal approximately 5.82 mm. Shear zone VII.

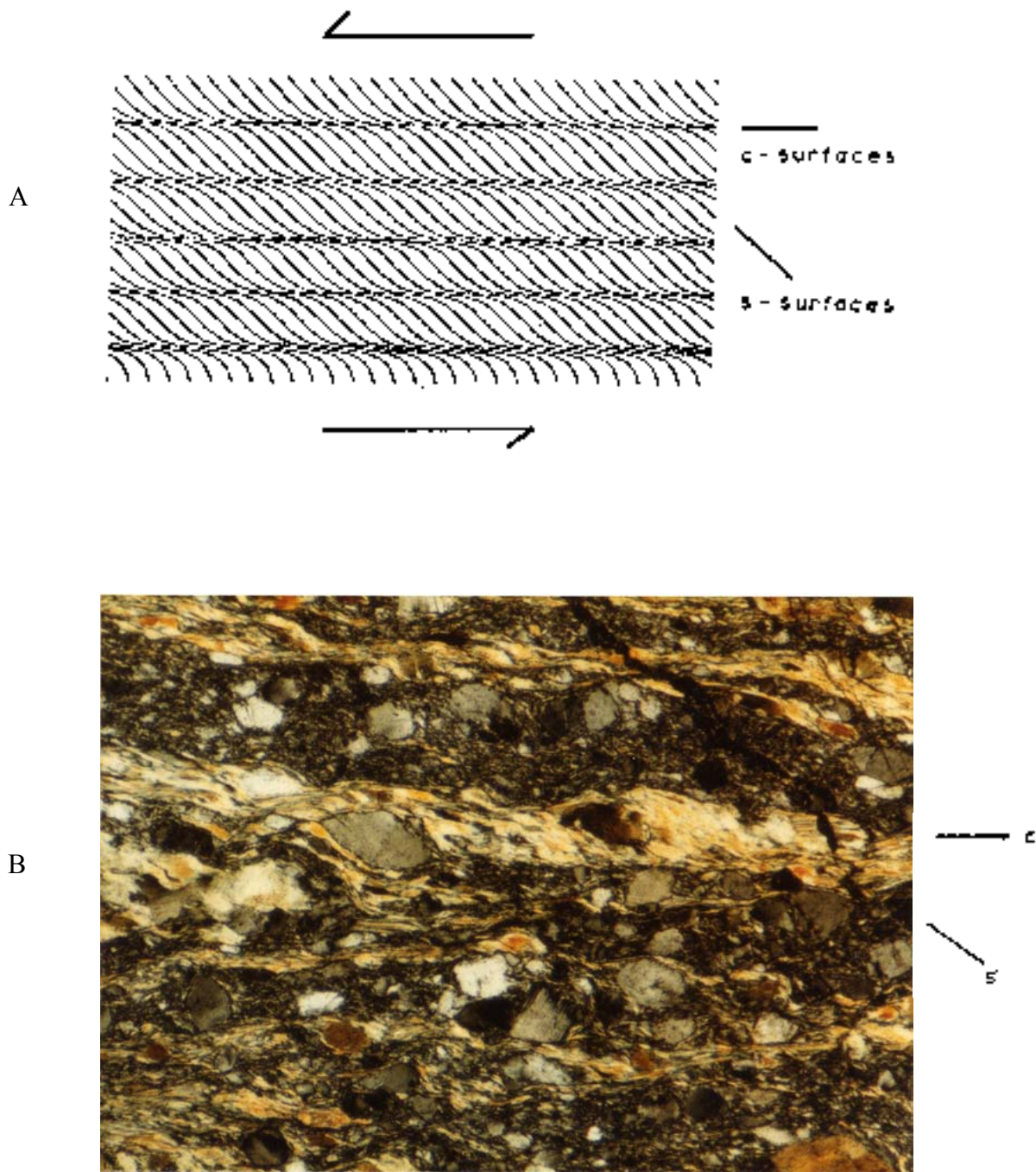


Figure 4.28

A) Relative orientations of c and s surfaces and the sense of shear they indicate. After Lister and Snoke (1984). B) Sample in which c and s surfaces are developed which indicate sinistral sense of shear. Diagonal approximately 3.64 mm. Shear zone IV.

augen described above are controlled, to an extent, by the orientation of c- and s-surfaces (compare Fig. 4.28a and 4.28b).

Several less frequently occurring structures have also been useful as "back-up" or secondary shear-sense indicators. Asymmetric intrafolial folds may indicate sense of shear when they involve folding of portions of the mylonitic foliation by a process like that outlined by Williams (1983). The progressive folding of a disturbed layer within a region of non-coaxial laminar flow in this case results in the formation of asymmetric folds whose sense of asymmetry reflects the overall sense of shear within the zone (Fig. 4.29a). In general, asymmetric folds must be used cautiously because ways of forming them without the apparent shear motion across them can be envisaged. One of these formation processes is outlined in Figure 4.29b. Well developed asymmetric intrafolial folds are only rarely found in outcrop and thin section. Where they are found (Fig. 4.8) they are moderately reliable indicators of bulk sense of shear.

A related structure is described in Lister and Snoke (1984). Figures 18 a, b, and c of their paper are examples of samples where pre-existing planar surfaces have rotated into the shortening field of the finite strain ellipse and have been cut by new shear surfaces forming close to parallel to the bulk flow plane. This process is likely to have formed the structure pictured in Figure 4.30. In this case the pre-existing anisotropy is the mylonitic foliation. It has apparently rotated clockwise, during which folding and cross-cutting by narrow zones of high strain occurred. A dextral sense of shear accounts for this structure; this is consistent with other structures present in this shear zone.

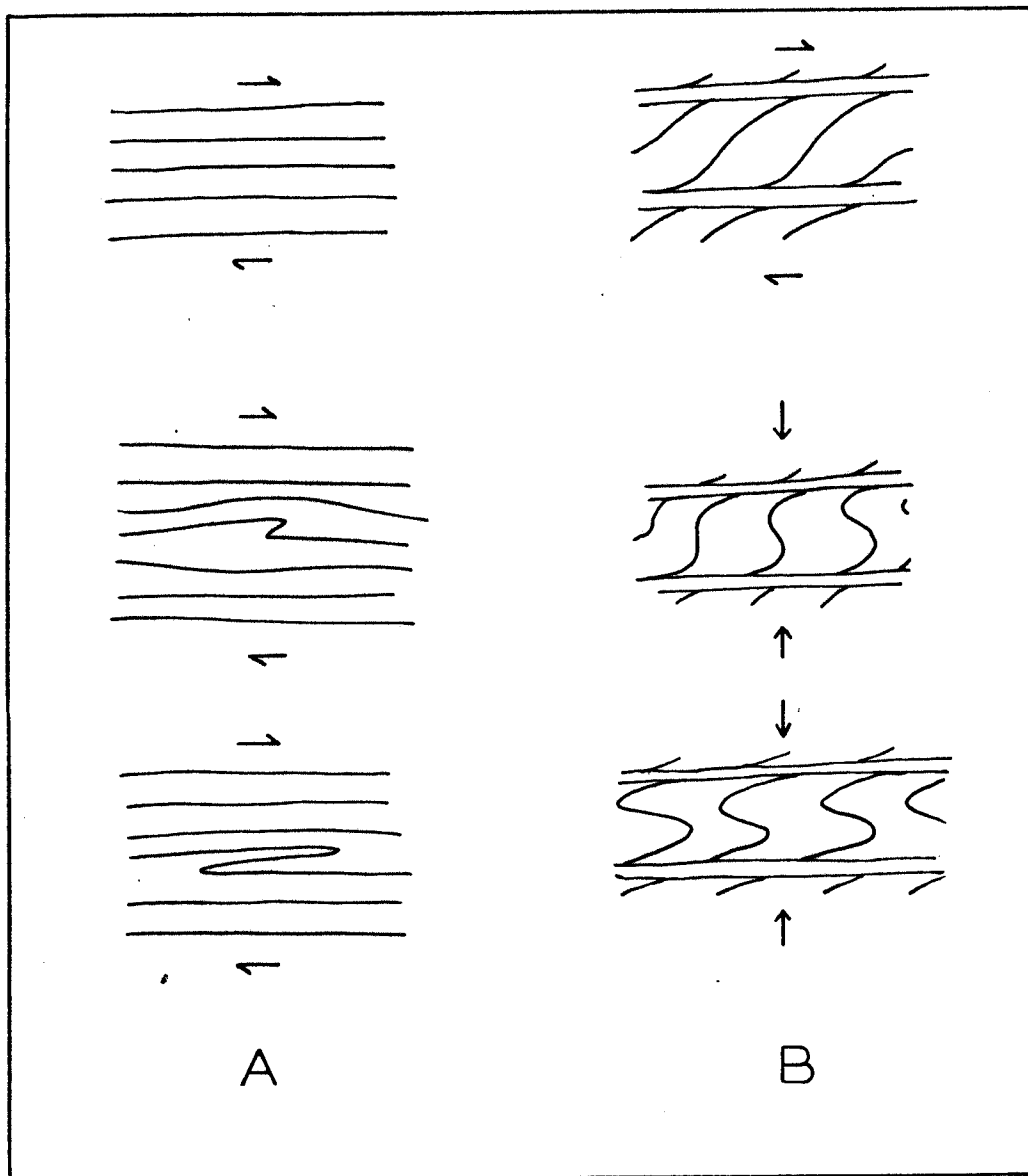


Figure 4.29

A) Asymmetric intrafolial fold formation. Sense of asymmetry reflects bulk sense of shear. After Williams (1983). B) Asymmetric intrafolial fold formation in which asymmetry is opposite and not solely related to bulk sense of shear. In this case dextral sense of shear and s-plane formation are followed by "flattening" perpendicular to the c-planes, leading to folding of the s-planes into asymmetric intrafolial folds.

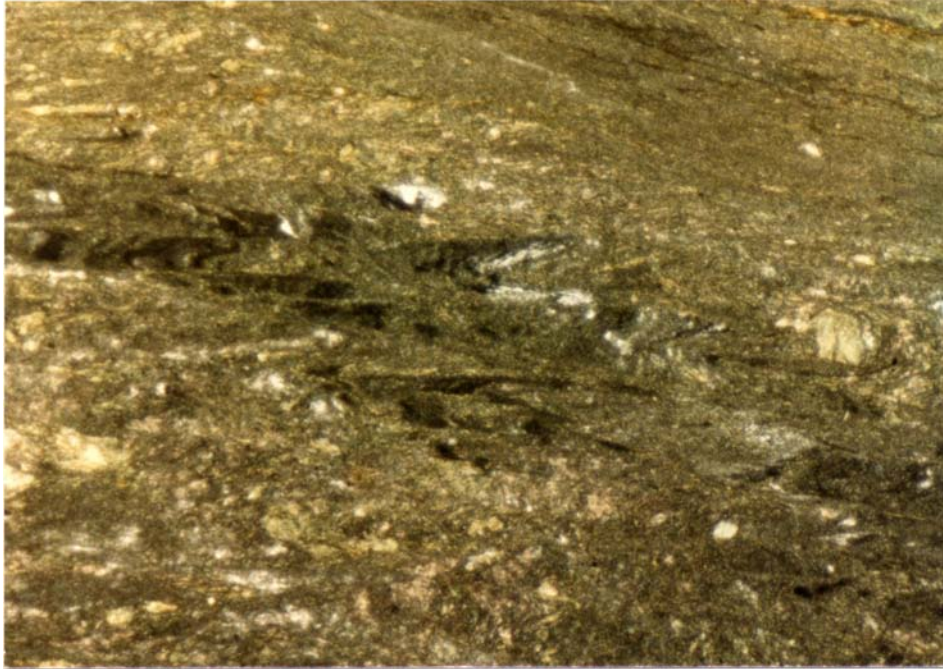


Figure 4.30

Structure formed by rotation of c-surface-parallel feature into shortening field. Diagonal approximately 5.82 mm. Shear zone VI.



Figure 4.31

Curvature of foliation in pod of material (center of slide) suggesting dextral sense of shear. Shear zone IV.

Another infrequently occurring structure from which sense of shear may be deduced is pictured in Figure 4.31. In this sample, a foliated pod of material has been cut by a transecting foliation in a slightly different orientation. Where these foliations intersect, the first foliation curves into the plane of the second foliation. The sense of curvature suggests a right-lateral sense of shear across the zone, which is consistent with the bulk sense of shear determined by the microstructural evidence.

In one case a very unusual asymmetric structure is present which does not readily fall into any of the previously mentioned categories, or those mentioned by previous authors (Fig. 4.32). At first glance it appears to be a rolled amphibole porphyroblast which has grown, as it rolled, over a pre-existing foliation defined, in part, by fine grained, amphibole rich layers, causing the foliation to be bent into a sigmoidal shape as it passes through the large amphibole grain. Given this interpretation, the sense of shear deduced from this structure is dextral. However, several observations suggest that this interpretation is not the best one. The first of these is that where amphibole-rich zones are present in this sample, they tend to be narrow, discrete zones. The fine grained amphiboles present within the large amphibole are spread across the entire grain, whose width is greater than that of the amphibole rich zones on either side of it. No discrete foliation planes pass through the large grain. In addition, amphibole porphyroclasts commonly recrystallize into fine grained amphibole blades, while the growth of large amphiboles is not seen anywhere else. Lastly, there are many reliable sense of shear indicators in this slide which consistently indicate a sinistral sense of shear. A reasonable expla-

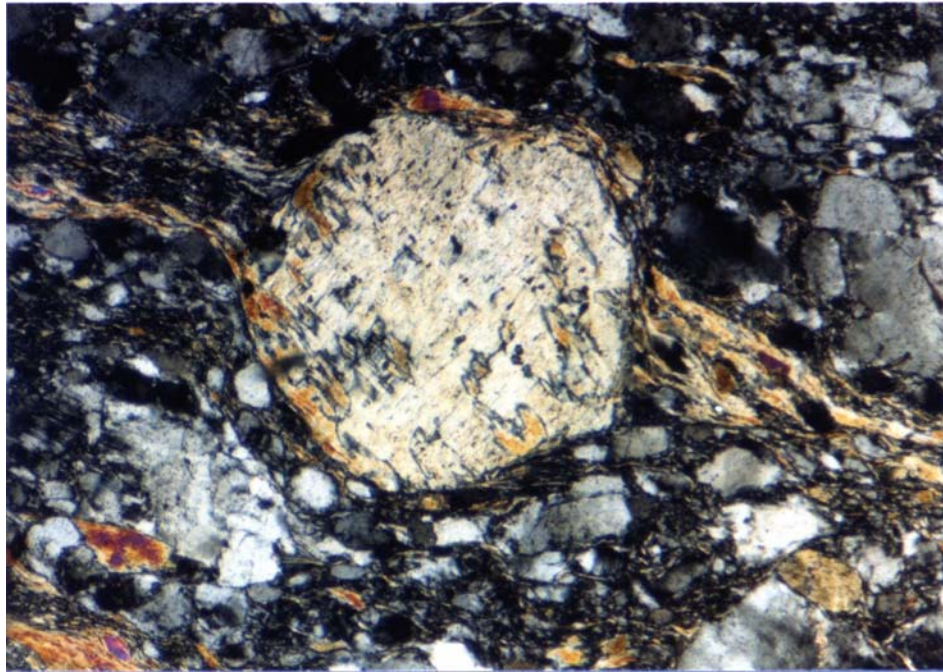


Figure 4.32

Unusual asymmetric porphyroblast. Diagonal approximately 3.64 mm. Shear zone II.

nation which accounts for this structure is that the large amphibole is a grain which was originally oriented in a direction which made it difficult to deform. Amphiboles in thin sections cut parallel to the lineation direction are almost all in a high birefringence orientation (c axis in the plane of the section), yet the large grain is in an unusual low-birefringence orientation. The fine grained amphiboles are not remnant foliation, but new grains which are recrystallizing in the common high birefringence orientation. They are growing in a strong grain shape preferred orientation which appears to approximate the s-plane orientation. The fine grained tails are the recrystallized tails typical of asymmetric augen.

2. Results

The overall sense of shear deduced from microstructural and mesoscopic criteria for each shear zone is indicated on stereographic plot of the present-day orientations of each zone (Fig. 4.34). Criteria used to deduce sense of shear and degree of reliability from individual thin sections and outcrops are summarized in Table 4.1.

E. Shear Zone Orientations

In order to determine the original orientations of the shear zones in this study, the structure of the southeast portion of the North Arm Mountain Massif where they are located must be considered. This section provides a complete, intact, cross-section because it lies on the southeast limb of a syncline with a NE-SW trending, subhorizontal axis (Casey, 1980; Rosencrantz, 1980). The syncline axis is roughly perpendicular to the dikes of the sheeted dike complex, and therefore

Table 4.1

Summary of criteria used to deduce sense of shear, and estimate of reliability of sense of shear determination from each sample. Sense of shear criteria: (1) asymmetric augen; (2) fractured, displaced grains; (3) c- and s-surface orientation; (4) asymmetric intrafolial folds; (5) splay off of the main shear zone; (6) swing of foliation into main zone; (7) inconsistent or no sense of shear indicators.

Table 4.1

Shear Zone	Sample Number	Sense of Shear Criteria	Reliability		
			Poor	Good	Very Good
I	32//L	. 1			X
I	33 A	. 1		X	
I	37 A	. 1			X
I	43 A	. 1			X
I	50//L	. 1	X		
I	51 A	. 7			
I	63 A	. 7			
I	127 A	. 1	X		
I	outcrop	. 4, 6		?	
II	70//L A	. 1, 3			X
II	outcrop	. 6		X	
IV	26//L	. 7			
IV	76//L	. 1, 2			X
IV	78//L	. 1, 2	X		
IV	80//L	. 1, 2, 3		X	
IV	81//L	. 1, 2			X
IV	86//L	. 1, 2, 3			X
IV	outcrop	. 5		X	
V	91//L	. 1, 3		X	
V	139//LA	. 1, 2		X	
VI	92//L	. 1, 2			X
VI	93//L	. 1, 2			X
VI	94//L	. 1, 4	X		
VI	96//L	. 1, 3		X	
VI	97//L	. 1, 2		X	
VI	100 A	. 1		X	
VII	111//L	. 1		X	
VII	114//L	. 7			
VII	118//L	. 1, 2, 3		X	
VII	120//L	. 1, 3			X
VII	121//L	. 1, 2			X
VII	122//L	. 1, 3	X		
VII	133//L	. 1, 3		X	
VII	134//L	. 7			
VII	135//L	. 2	X		
VII	outcrop	. 5		X	

the cross-section is roughly perpendicular to the paleo-ridge axis and parallel to the paleo-spreading direction. Unfolding about the syncline axis to restore the dikes to sub-vertical and large-scale lithologic boundaries to subhorizontal should restore the section and the structures within it to their original orientations relative to one another. However, this process is complicated by the difficulty in determining the orientations of the lithologic boundaries from the map. Casey (1980) estimates that, in general, the gabbro-diabase contact dips between 20 and 30 degrees NW, and that the lithologic contact between the transition zone and the layered gabbros parallels local compositional layering and is therefore close to vertical. In this view of the structure any paleo-horizontal surface should now strike NE and be either subvertical or dip to the northwest. In the lowest portion of the gabbros such surfaces would dip steeply to the NW, while higher up in the section they would be expected to dip NW at a shallower angle.

This is not what is observed in the lowest portion of the gabbros in the vicinity of SA IA and IB. In both these areas compositional layering is proposed to have formed sub-horizontally (Casey, 1980), yet it presently dips to the SE at approximately 58 degrees (Fig. 4.3 C and D). There are several possibilities which may account for this unexpected layer orientation, including paleo-magma chamber floor irregularities, non-vertical (present day) paleo-magma chamber axis orientation, and deviations from a simple monocline as the overall structure of the massif. The first two possibilities may well exist, but are difficult to pick out. It is likely that local variations in the shape of the walls of the paleo-magma chamber occurred over time, affecting

compositional layer orientations. It appears that the paleo-magma chamber axis is presently close to vertical as evidenced by the (now) steep attitudes of compositional layering halfway up the gabbro section (see Casey, 1980, for details).

Since the paleo-magma chamber axis is near vertical the main factor that must be taken into consideration when restoring the section to horizontal is the overall structure of the massif. Three possible fold structures are considered. The first of these (Model 1, Fig. 4.33) is a simple monocline. In this case the SE dipping layering orientations in question may have arisen from paleo-magma chamber variables. In the alternative fold structures pictured in Figure 4.33 (Models 2 and 3) the SE dipping compositional layering is an artifact of the folding of the massif. Each of these models was used to "unfold" the massif about a NE trending, subhorizontal axis (parallel to the strike of large-scale lithologic boundaries) and thereby determine the original orientation of each of the shear zones relative to the paleo-ridge axis (Fig. 4.34). The amount that each shear zone was rotated to return it to horizontal for each model is presented in Table 4.2. It is not possible to determine absolutely which model is closer to the truth.

Table 4.3 summarizes the sense of offset across each shear zone in its "original" orientation, and describes the fault type relative to the paleo-mid-ocean ridge axis as determined by unfolding by models 1, 2, and 3. (The paleo-ridge axis is considered to have lain to the (present-day) southwest - see Chapter 2 for discussion).

Model 2 is the least likely model. Unfolding of Shear Zone II by this model results in sinistral strike-slip offset across a northerly-

trending, steeply west-dipping shear zone. This orientation and sense of offset are not easily explained in either an oceanic crustal or an obduction or post-obduction setting. In addition, Model 2 relies on localized recumbent folding. Recumbent folding has not been observed in other portions of the ophiolite massifs or in the underlying rocks of the Humber Arm Supergroup. It is likely that if this type of folding had occurred on North Arm Mountain, other examples would be found in the area.

Model 1 and Model 3 are both reasonable possibilities. Model 3 is slightly more satisfactory because it results in three out of six zones forming as axis-parallel, inward-facing normal and oblique-normal structures (versus two out of six for Model 1), and because five out of six of the original orientations are inward facing (this includes axis-oblique and axis-parallel structures), which is the more common sense of offset across ridge-bounding normal faults. The upright folding called for in Model 3 is similar to large-scale folding of the North Arm massif (Williams, 1973; Casey and Kidd, 1981), folding observed in the sedimentary rocks of the Humber Arm allochthon (Bosworth and Idleman, 1984), and to folding of the basal thrust of the Coastal Complex south of Trout River (B. Idleman, pers. comm., 1985).

Figure 4.33

Hypothetical cross sections of the southern half of the North Arm Mountain massif. Lithologic contact orientation after Casey (1980).

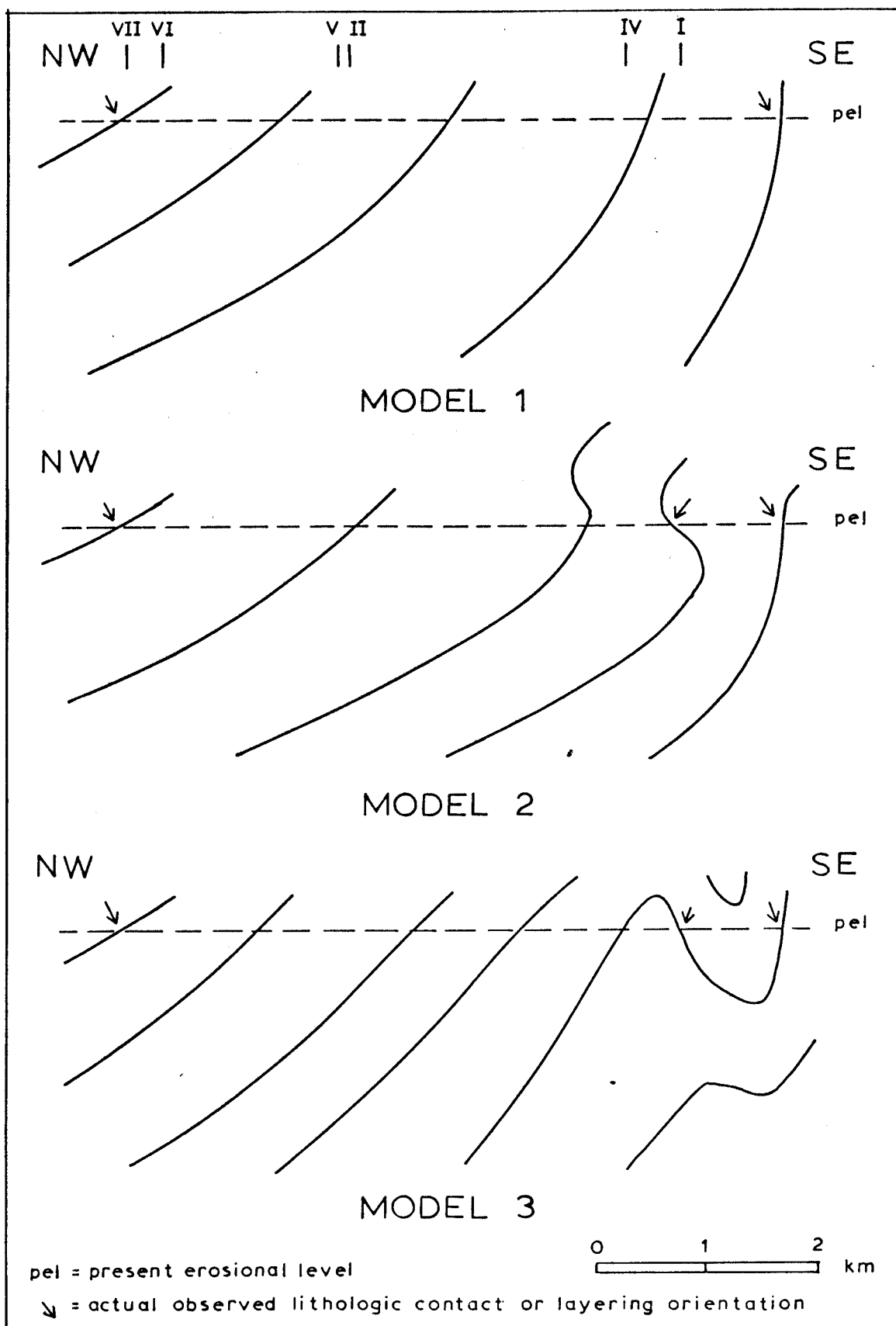


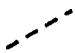

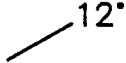
Table 4.2

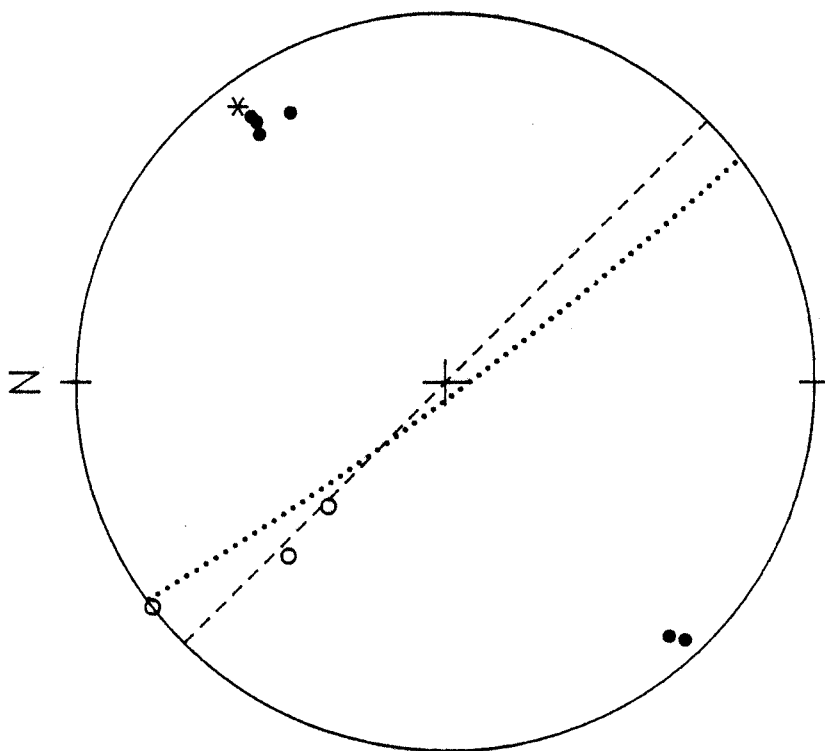
Amount and sense of rotation about a NE-trending, horizontal axis for each shear zone for each model. Sense of rotation facing NE indicated by arrow, i.e., 45° = 45° rotation clockwise about the axis.

Shear Zone	Model I	Model II	Model III
I	$\uparrow 80$	$\uparrow 122$	$58^\circ \uparrow$
II	$\uparrow 68$	$\uparrow 55$	$\uparrow 40$
IV	$\uparrow 75$	$\uparrow 87$	$\uparrow 58$
V	$\uparrow 68$	$\uparrow 51$	$\uparrow 40$
VI	$\uparrow 29$	$\uparrow 30$	$\uparrow 25$
VII	$\uparrow 25$	$\uparrow 25$	$\uparrow 25$

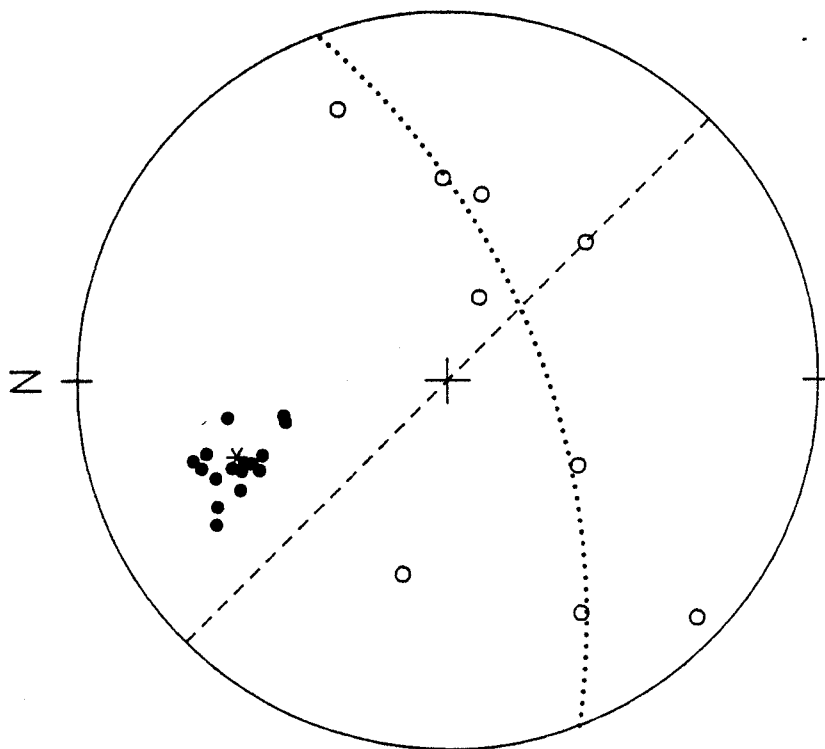
Figure 4.34

Stereographic (lower hemisphere projection) representations of actual lineation and foliation orientations, and orientations resulting from unfolding according to Models 1, 2, and 3.

-  dike orientation (average for area)
- poles to foliation
- * average foliation (pole)
-  average foliation plane
- lineation
- ⊕ slip direction
- U/D side up/side down
-  12° rotation axis, sense, and amount of rotation

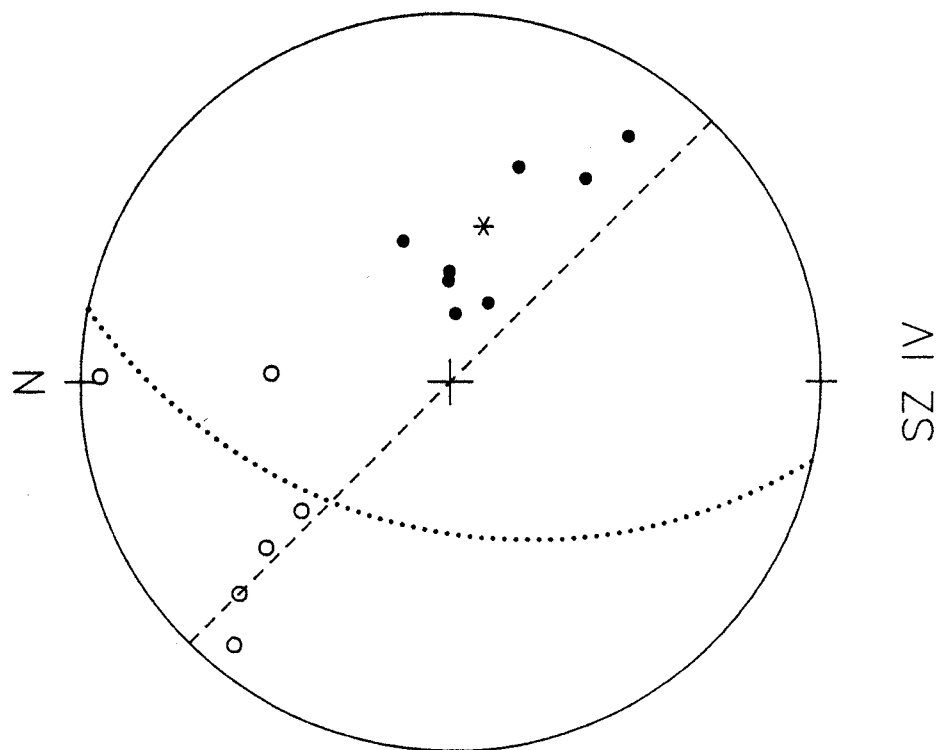
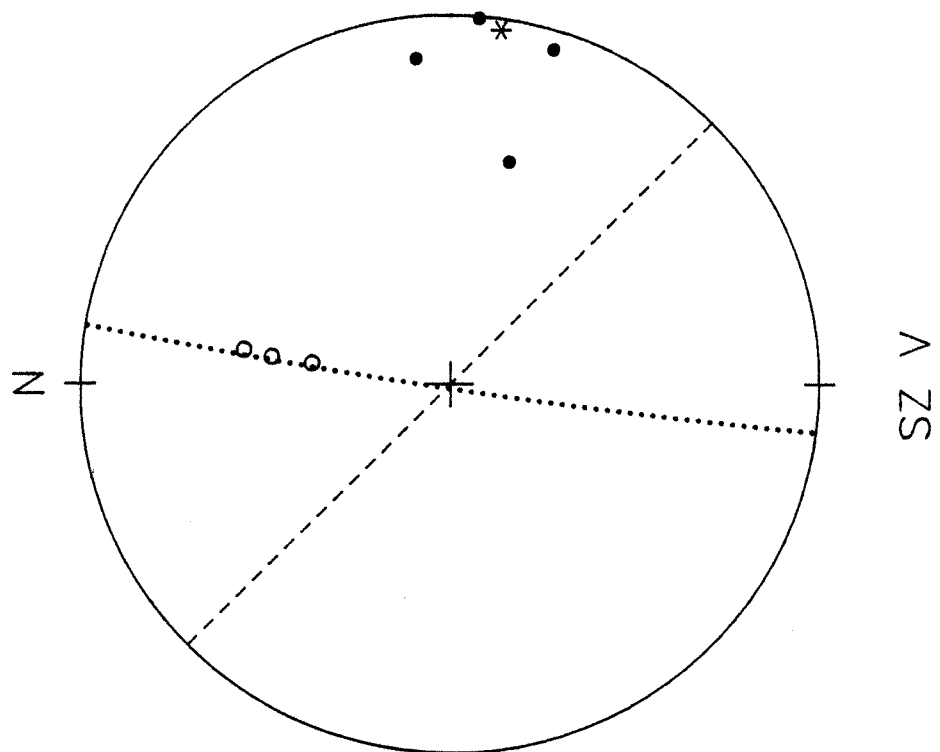


SZ II

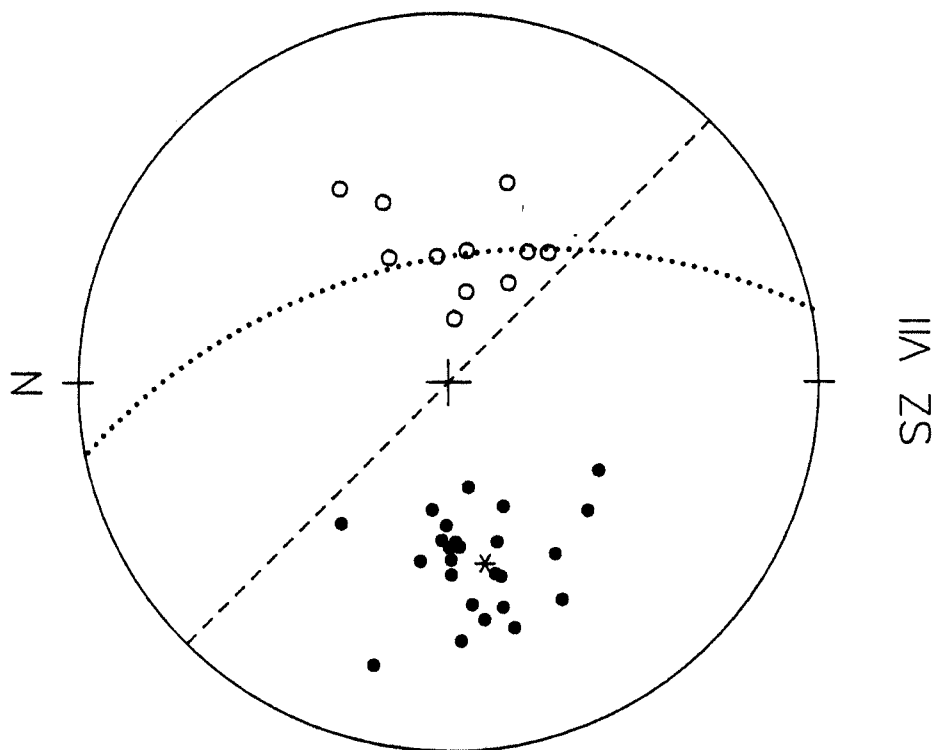
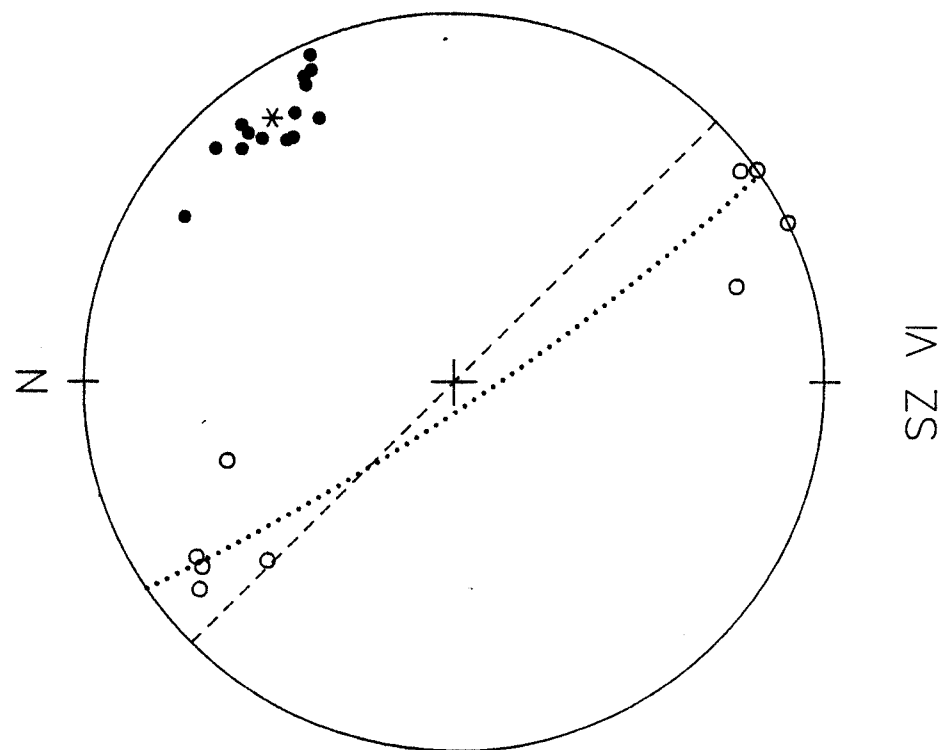


SZ IA+B

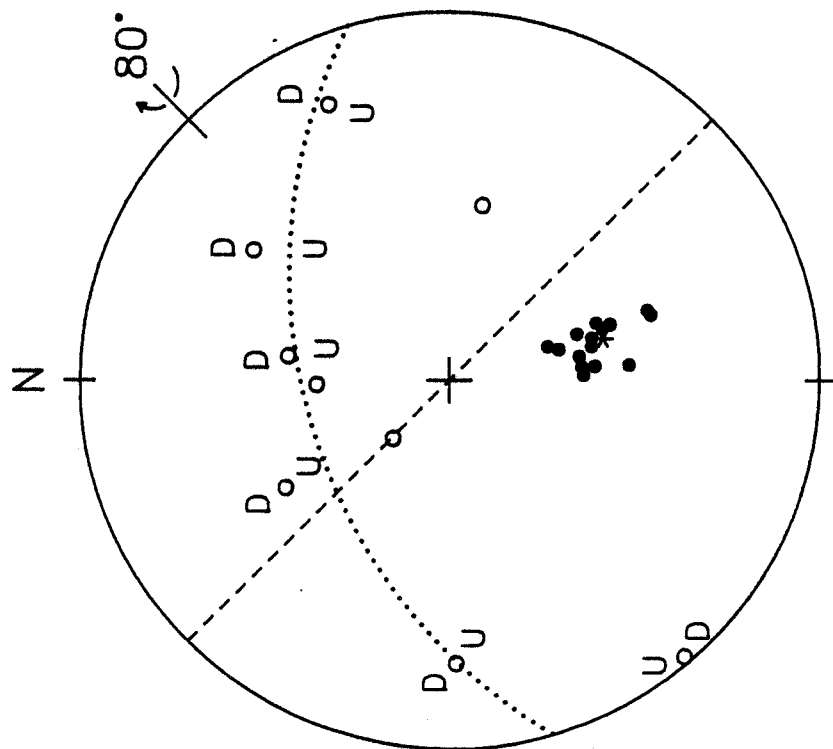
Present Orientation



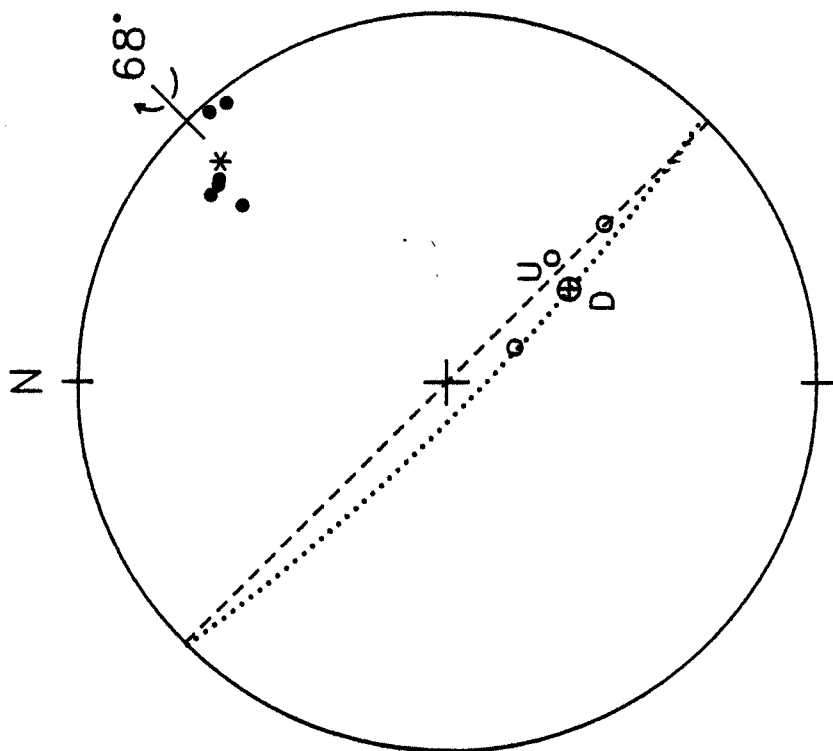
Present Orientation



Present Orientation

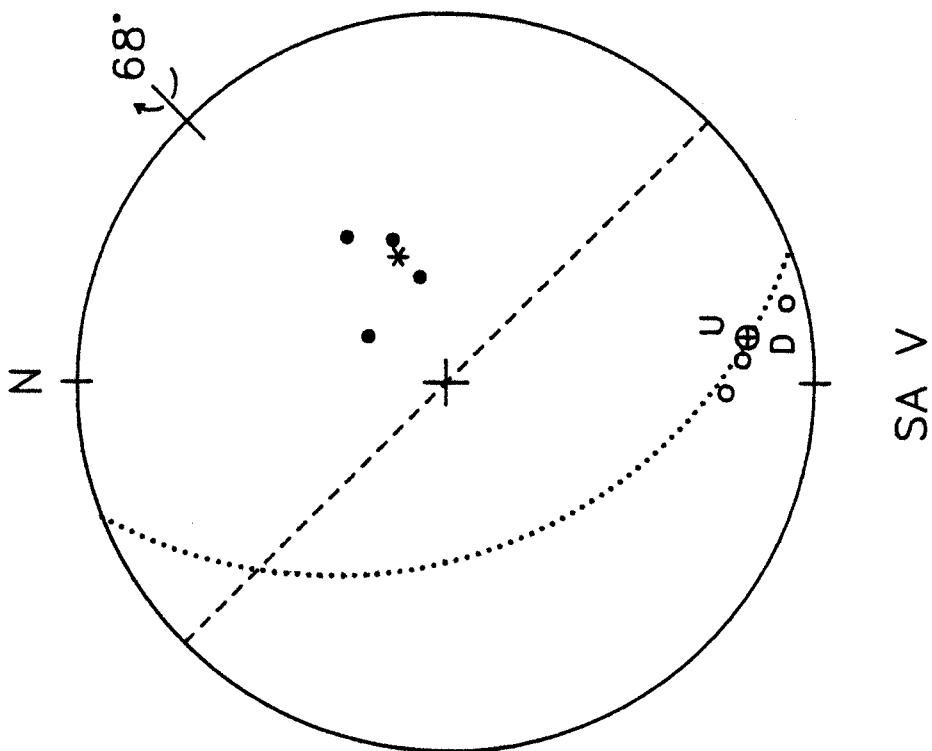
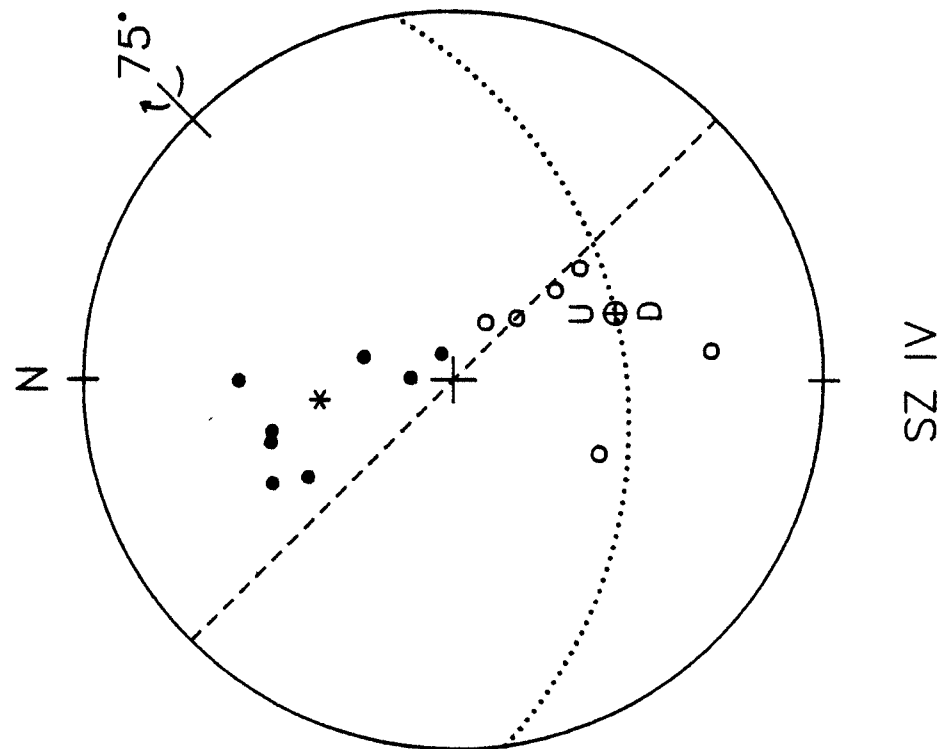


SZ IA+B

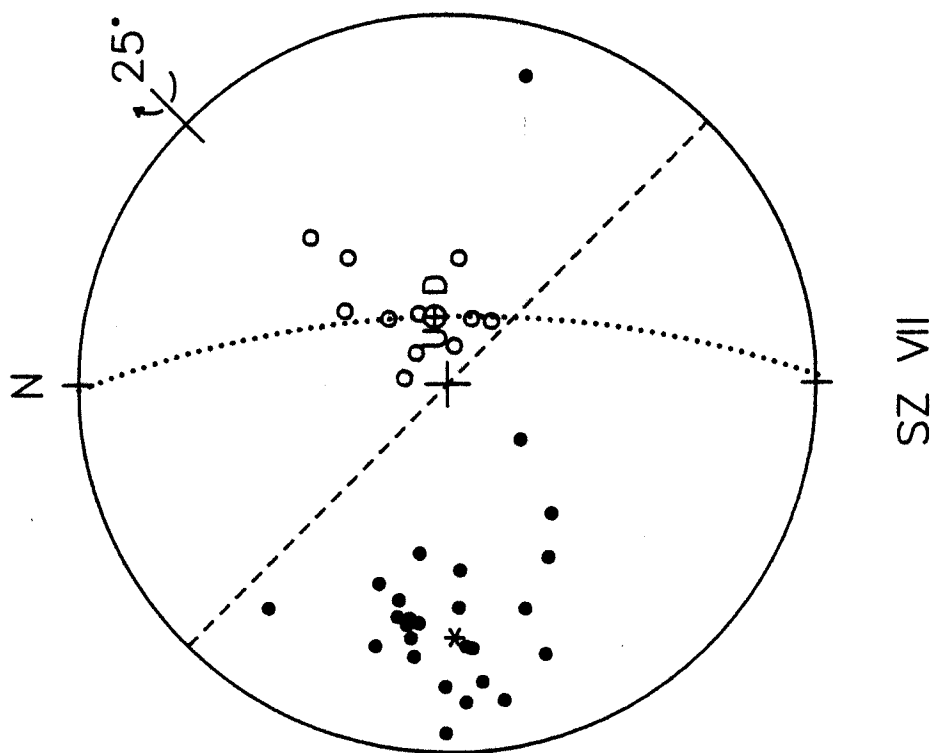
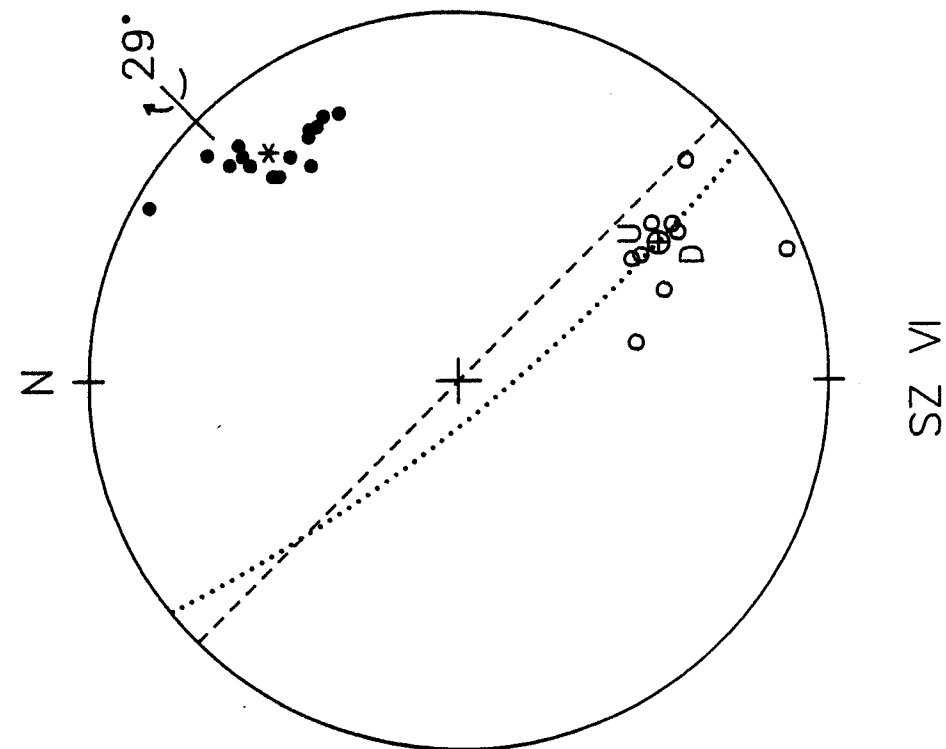


SZ II

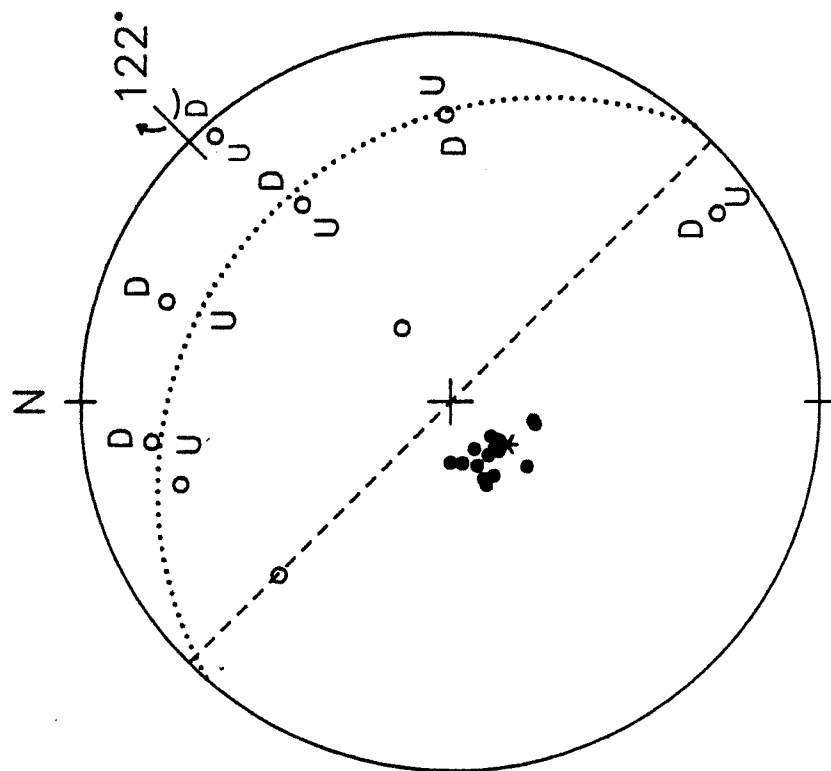
Model 1



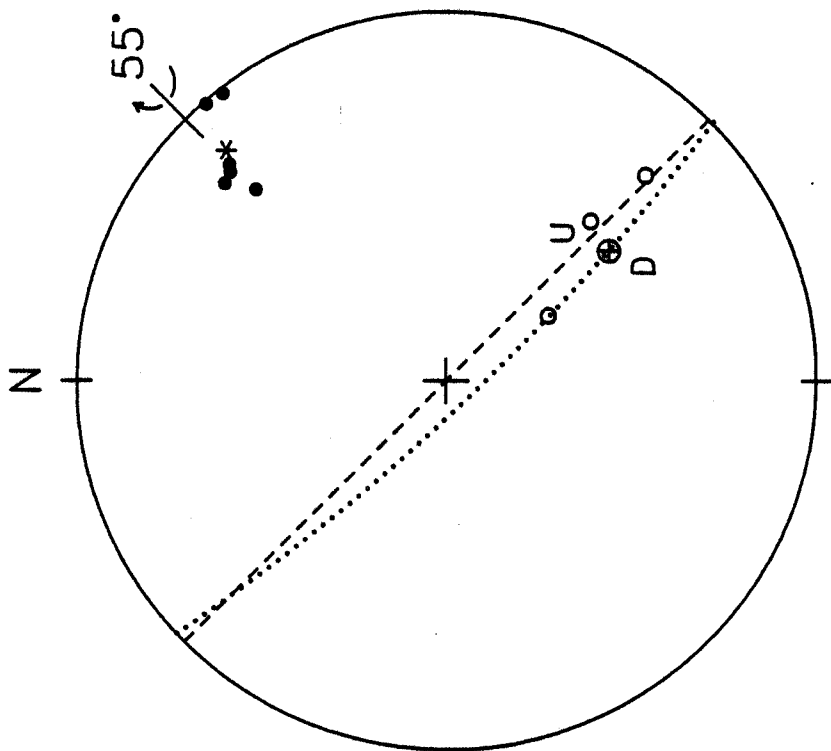
Model 1



Model 1

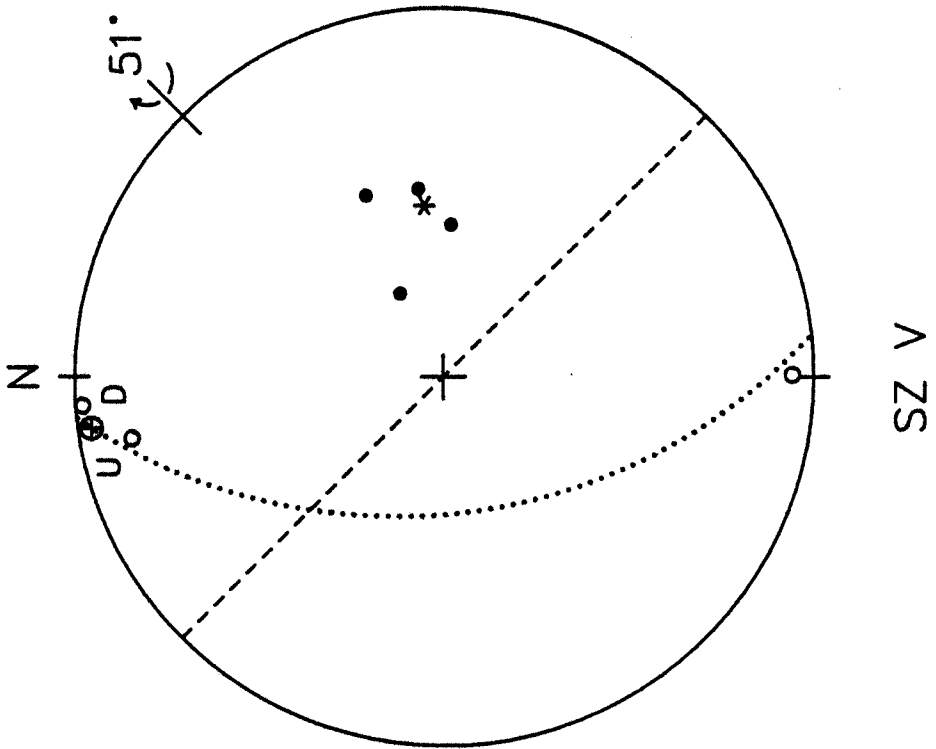
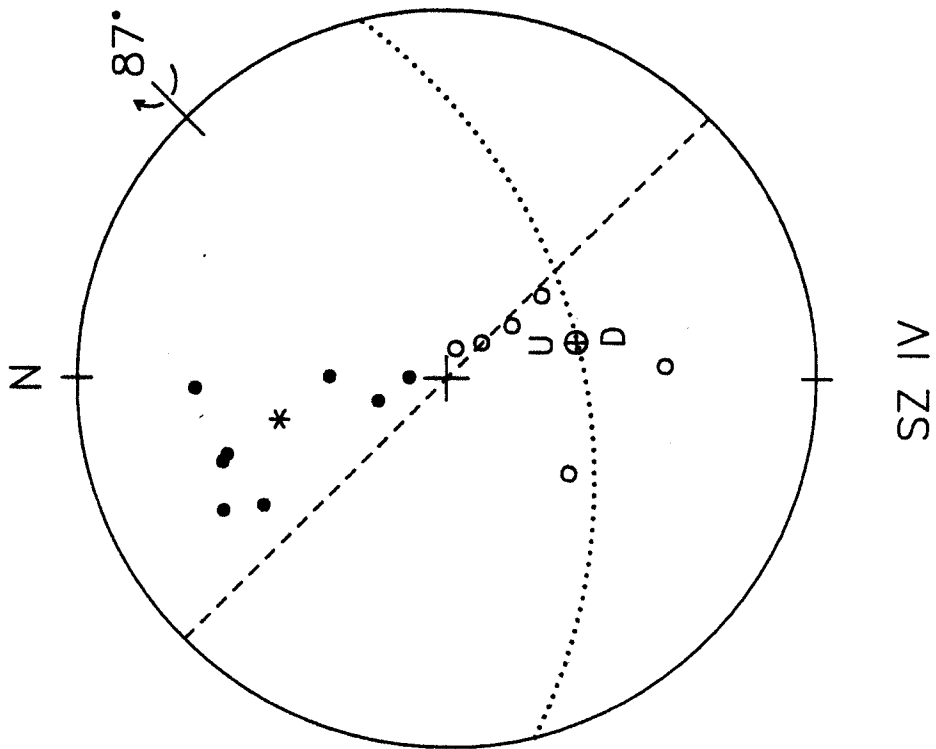


SZ IA+B

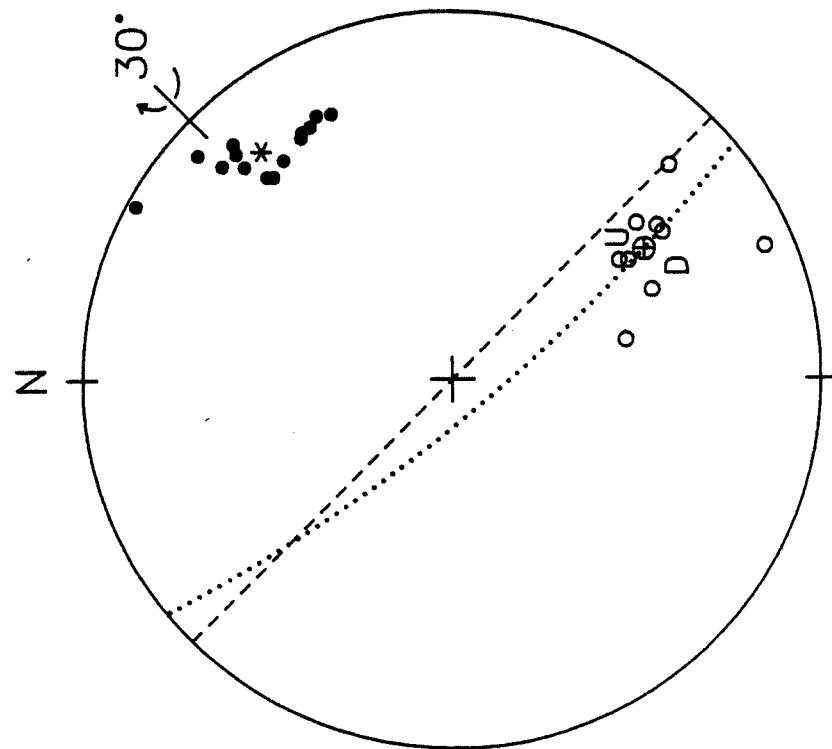


SZ II

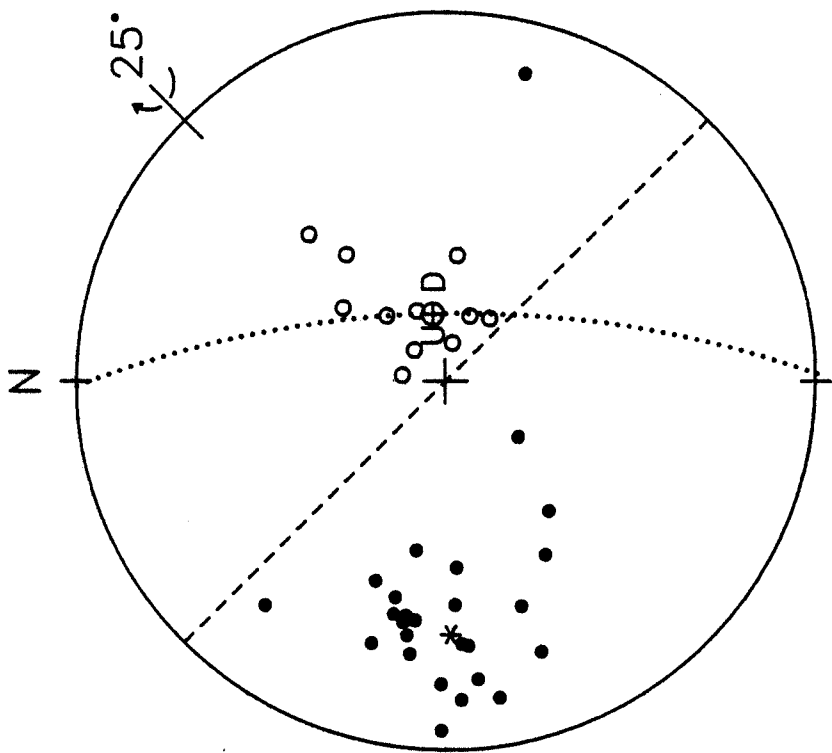
Model 2



Model 2

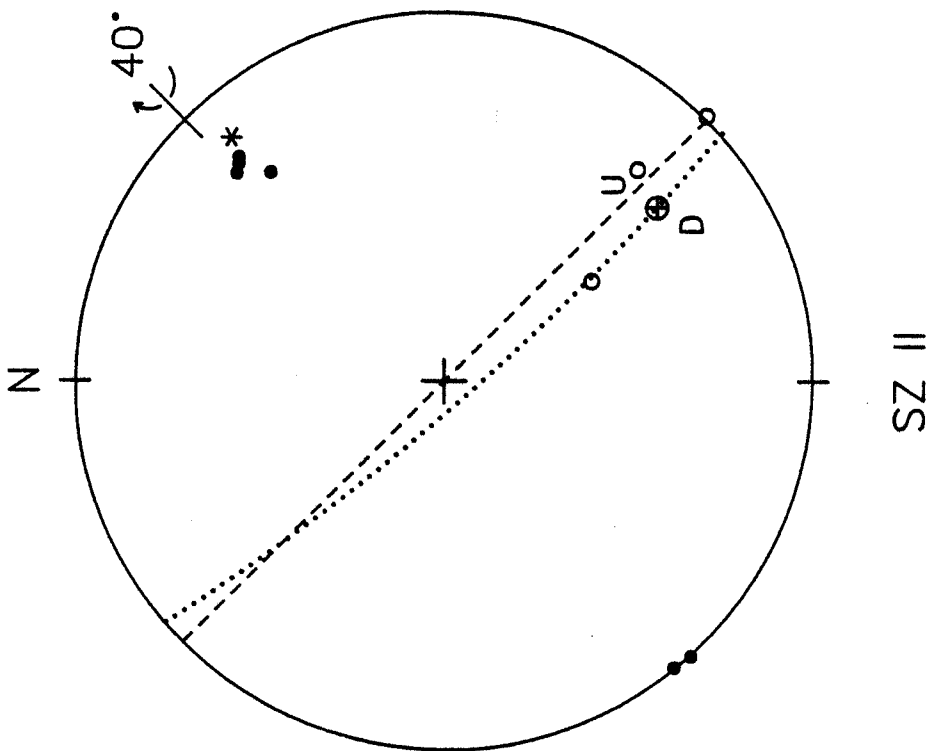


SZ VI

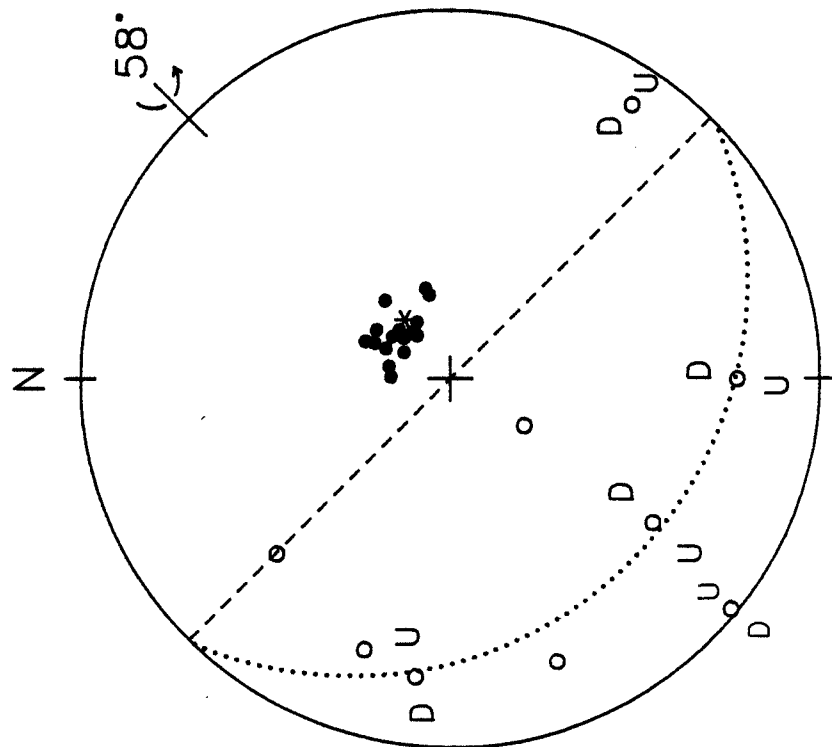


SZ VII

Model 2

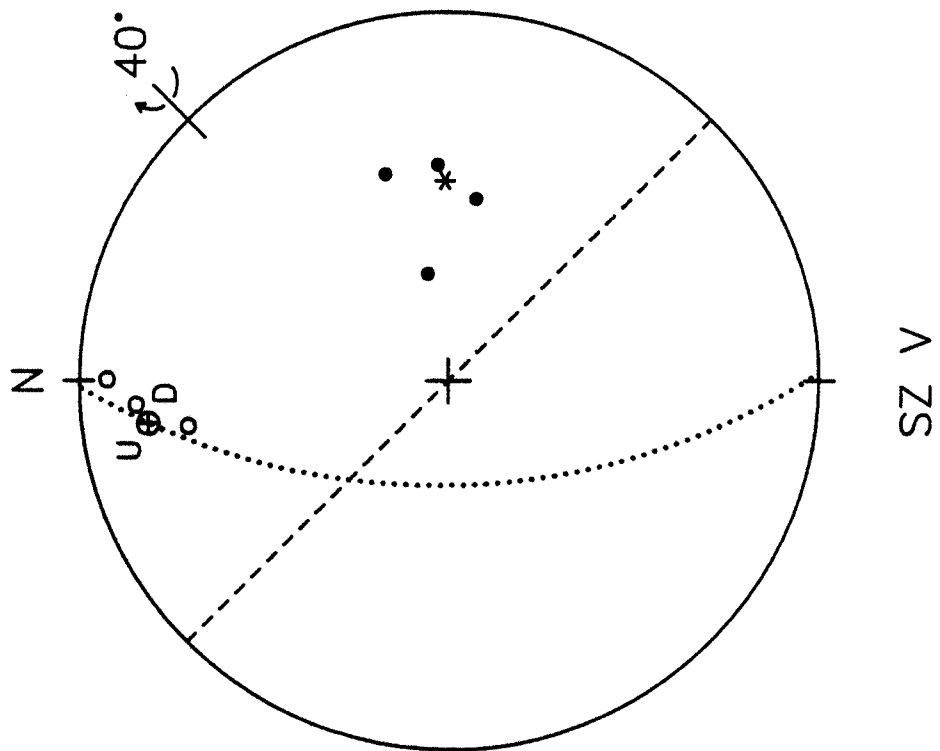
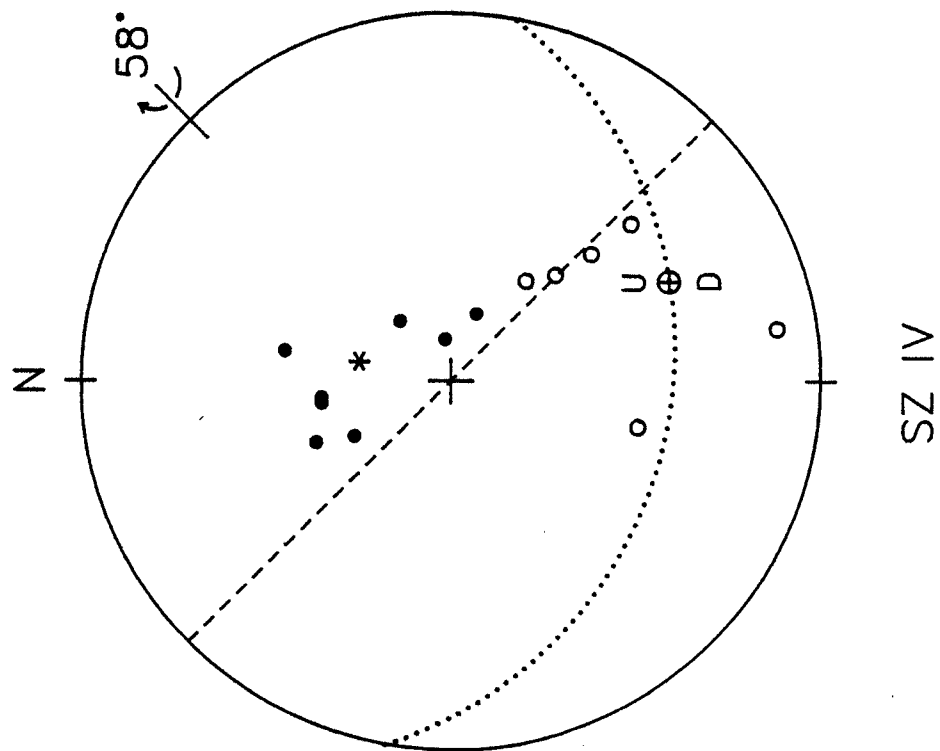


SZ II

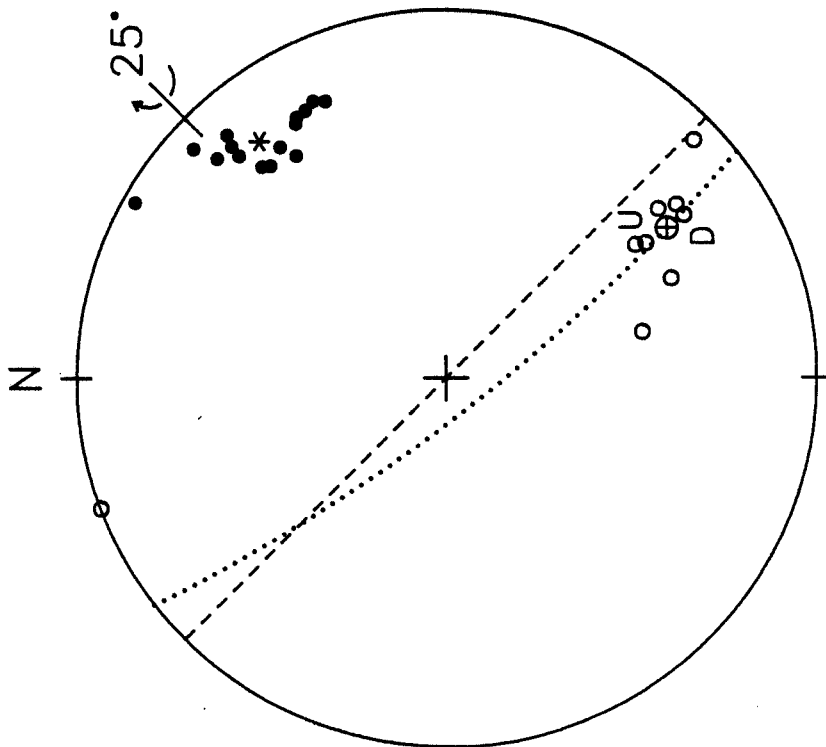


SZ IA+B

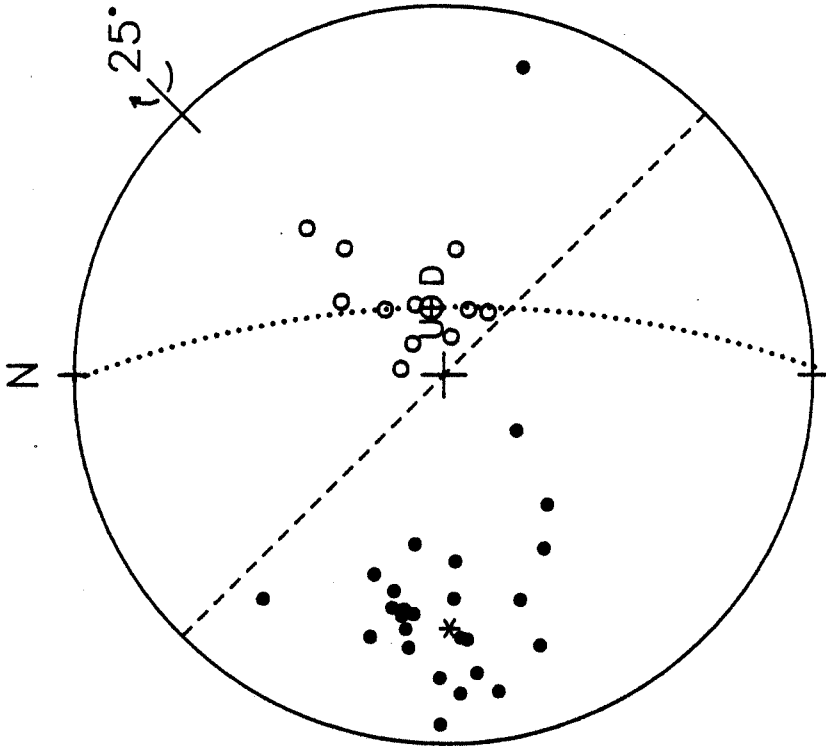
Model 3



Model 3



SZ VI



SZ VII

Model 3

Table 4.3

Model 1

- SZ: I Moderately dipping, axis-oblique normal (?) fault.
 II Steeply dipping, axis-parallel, inward-facing, oblique-slip normal fault.
 IV Moderately dipping, axis-oblique normal fault (inward-facing).
 V Moderately dipping, axis-oblique, oblique-slip normal fault (inward-facing).
 VI Steeply dipping, axis-parallel, inward-facing, oblique-slip normal fault.
 VII Steeply dipping, axis-oblique normal fault (outward-facing).

Model 2

- SZ: I Gently dipping, outward-facing, axis-parallel normal (?) fault.
 II Steeply dipping, inward-facing, axis-parallel, oblique-slip normal fault.
 IV Moderately dipping, axis-oblique normal fault (inward facing).
 V Moderately dipping, axis-oblique strike-slip fault (sinistral).
 VI Steeply dipping, axis-parallel, inward-facing, oblique-slip normal fault.
 VII Steeply dipping, axis-oblique normal fault (outward-facing).

Model 3

- SZ: I Gently dipping, inward-facing, axis-parallel fault of uncertain displacement.
 II Steeply dipping, inward-facing, axis-parallel, oblique-slip normal fault.
 IV Moderately dipping, axis-oblique, oblique-slip normal fault (inward-facing).
 V Steeply dipping, axis-oblique, oblique-slip normal fault (inward-facing).
 VI Steeply dipping, axis-parallel, inward-facing, oblique-slip normal fault.
 VII Steeply dipping, axis-oblique, outward-facing normal fault.

CHAPTER 5. METAMORPHISM

The mineral assemblages of the shear zones were studied to help distinguish whether the shear zones formed during formation and evolution of the oceanic crust, or during obduction-related or later phases of deformation. Oceanic crustal deformation that occurred within the plutonic section in the vicinity of the ridge axis is likely to be high temperature, ductile deformation, while structures interpreted as obduction and emplacement-related or later include brittle faults and open folds (Casey, 1980; Rosencrantz, 1980; see Chapter 2 for discussion).

A. Analytical Technique

Observations of thin sections were made with a petrographic microscope. Electron microprobe analyses of one sample from each shear zone and one undeformed sample were made on an ETEC Autoprobe using energy dispersive x-ray analysis. Approximate spot diameter was 2 μm .

Amphibole analyses were recalculated to thirteen cations, excluding K, Na, and Ca. This recalculation, suggested by Robinson et al. (1982) for calcic amphiboles, is based on known chemical and crystal-chemical limits observed in calcic amphiboles. After "cation normalization", cations were assigned to crystallographic sites, again according to Robinson et al. (1982). Any analyses which did not meet site assignment criteria were rejected.

B. Shear Zone Mineral Assemblage

The most common phases present in the shear zone samples are amphibole (mainly actinolitic hornblende and magnesio-hornblende) and

calcic plagioclase. Clinopyroxene, sphene, chlorite, opaques, and quartz are present in minor to trace amounts. One grain of epidote was probed in one sample. This is the only occurrence of epidote observed. This assemblage is typical of amphibolites which have been described by many researchers in both experimental and field studies (Miyashiro, 1958; Liou et al., 1974; Laird, 1980; Maruyama et al., 1982, 1983; Moody et al., 1983).

The amphibole present in the fresh samples of the country rock is late magmatic, brown to red-brown magnesio-hastingsite (Fig. 5.1b, classification after Leake, 1978). In the shear zone samples, amphiboles are not zoned, and they range in color from almost completely colorless, through pale green to deep green and blue green. These color variations are partly due to compositional differences and optical orientation, and in some cases due to variations in thin section thickness. Because amphibole compositions encompass such a large range, it is not possible to accurately identify amphiboles by optical means. For this reason several samples were analyzed with an electron microprobe as described above. The microprobe results are summarized in Figure 5.1 a and b, where they are plotted according to the classification scheme of Leake (1978). Most of the analyses fall within the actinolitic hornblende and magnesio-hornblende field.

It is interesting to note that within each sample there is a significant range of amphibole composition. In most slides there is complete overlap in the composition of coarse grained amphiboles and fine grained, recrystallized amphiboles. Sample 121 // L is an exception. In this sample most of the analyses in both fine grained, recrystallized amphiboles, amphibole porphyroclasts, and coarse grained,

Figure 5.1

A) and B) Amphibole analyses plotted according to classification scheme of Leake (1978). Individual samples and shear zones from which they were taken are listed below.

	SZ
□ sample 33A	I
● sample 7011L	II
x sample 23A	IV
△ sample 961L	VI
○ sample 12111L	VII
▲ sample 34A (undeformed)	I

$(\text{Na}+\text{K})_A < 0.50; \text{Ti} < 0.50$

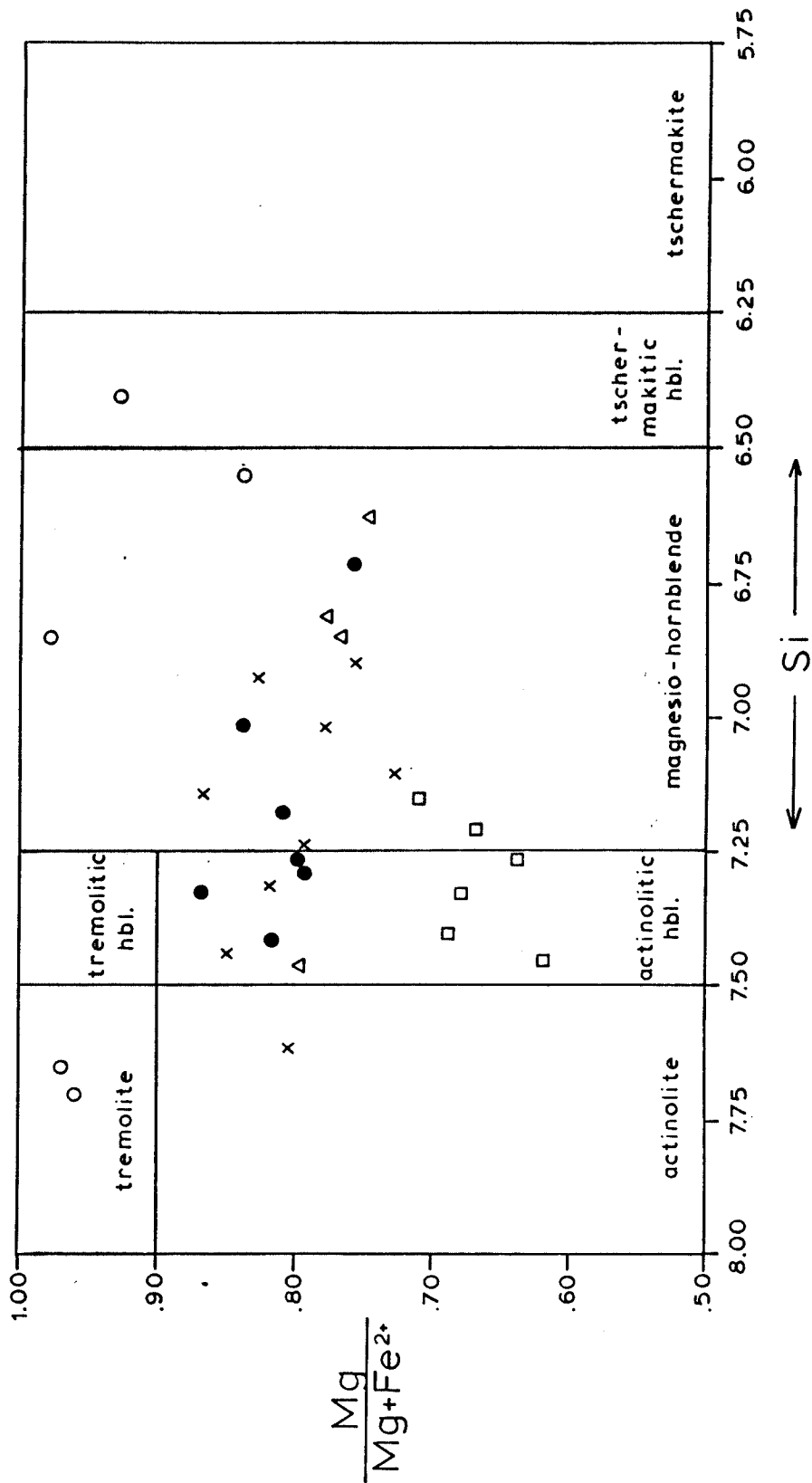


Figure 5.1 A

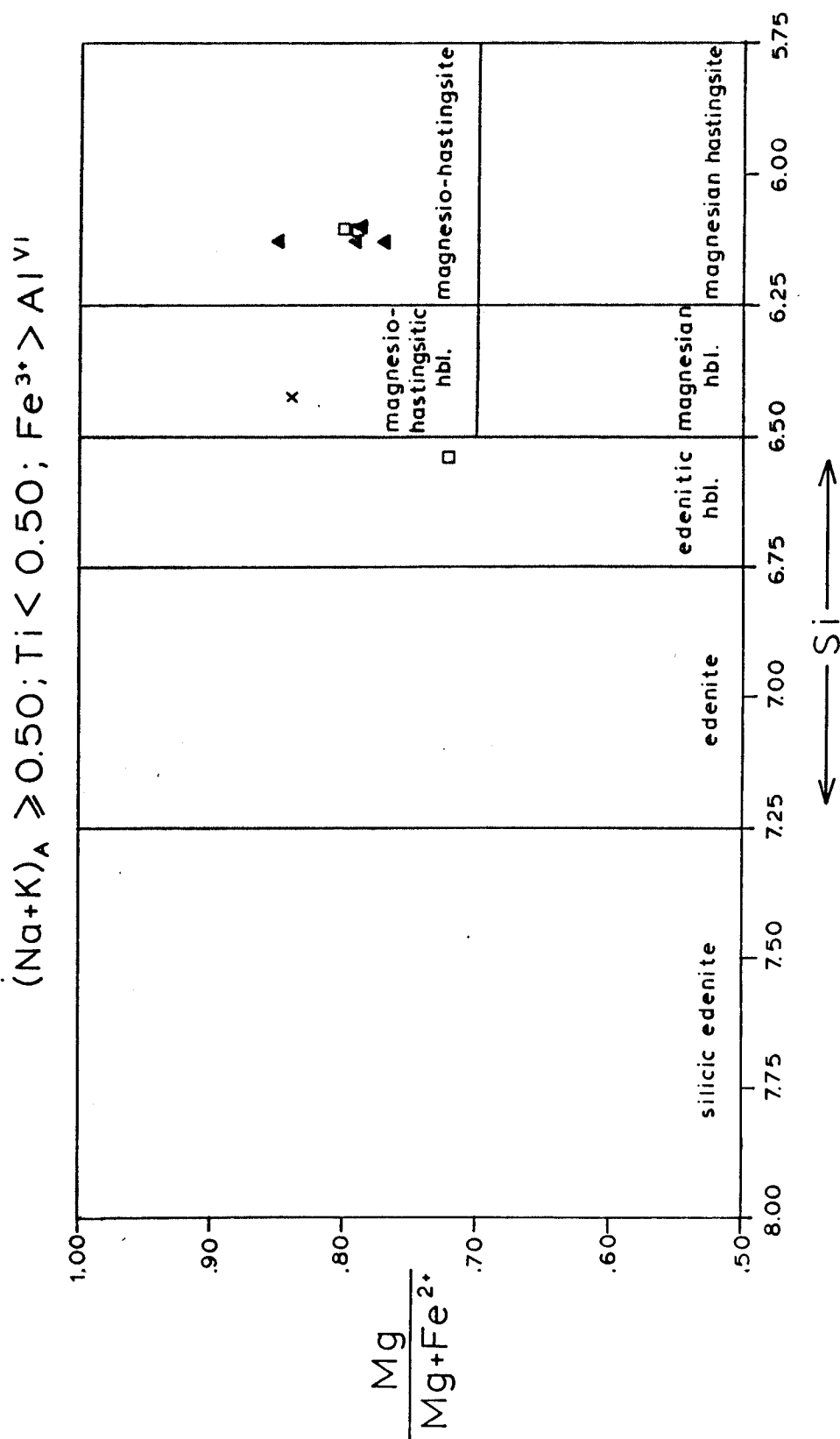


Figure 5.1 B

undeformed amphiboles plot in hornblende fields (several 10 second qualitative analyses verifying this were done on the microprobe - these results are not plotted in Fig. 5.1). However, in one location in the slide fine grained, colorless tremolite blades are present within a coarse magnesio-hornblende grain. The magnesio-hornblende grain is within a coarse grained, relatively undeformed zone which is surrounded by narrow, fine grained, highly deformed zones. The tremolite blades within it are randomly oriented. It is not possible to state with certainty whether these tremolite blades grew during or after movement across the shear zone, although their orientation and the lack of tremolite within fine grained, recrystallized areas suggests that they may have formed afterwards.

Probe analyses of plagioclases within an undeformed sample (34 A) indicate compositions ranging from An_{75} to An_{80} (bytownite). In deformed samples the compositions of plagioclase ranged from An_{31} to An_{94} (andesine to anorthite). The distribution of compositions is shown in Figure 5.2a. No zoning is apparent optically or with the aid of the microprobe. Overall, recrystallized plagioclase tends to be slightly less calcic than porphyroclastic plagioclase. The range of plagioclase compositions varies from sample to sample (Fig. 5.2b). No systematic changes (i.e. relative to position in the section) are apparent.

Clinopyroxenes in the country rock and, where present, in the shear zones, are unzoned augites and salites which plot towards the diopside corner of the pyroxene quadrilateral (Fig. 5.3). Where clinopyroxene is found in shear zone samples it is usually rimmed by amphibole and it often has a dusty look to it due to the growth of fine grained alteration products. This alteration may be so intense that

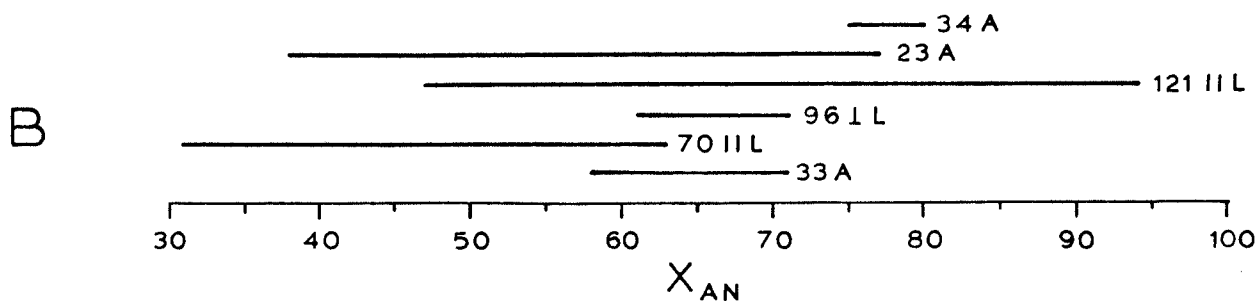
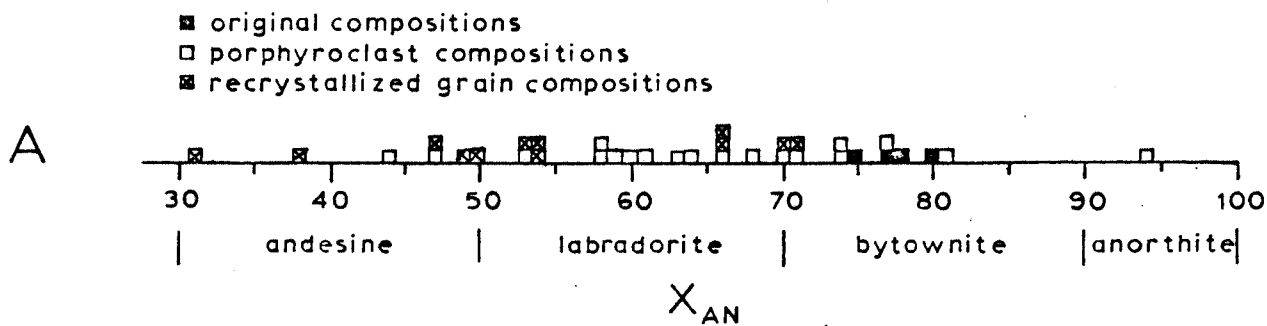


Figure 5.2

A) All analyzed plagioclase compositions. B) Range of plagioclase compositions for each sample.

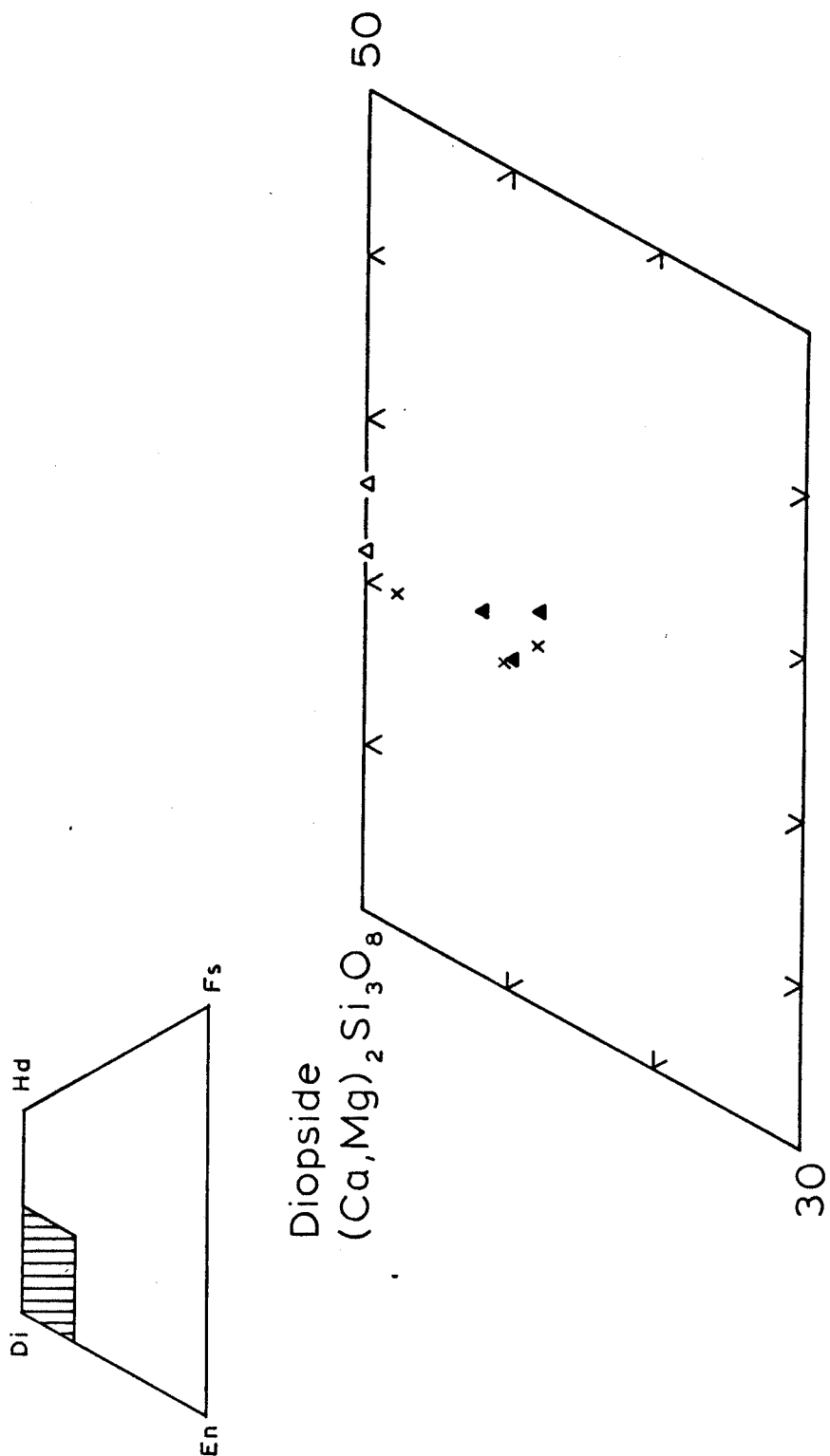


Figure 5.3

Plot of pyroxene compositions. Symbols are the same as those in Figure 5.1.

the grains in which it occurs are almost opaque. In some samples there are plagioclase + clinopyroxene \pm amphibole rich zones where clinopyroxene looks very fresh; it lacks dusty alteration and amphibole rims. Outside these zones within a given sample more typical dusty alteration of clinopyroxenes may be seen. It may be that portions of given shear zones where clinopyroxene is fresh deformed under conditions where clinopyroxene was a stable phase.

Sphene is a widespread accessory mineral. The grains which are present are almost all anhedral. Sphene was only observed in samples from within the shear zones.

Chlorite is found in both the country rock and shear zone samples as vein material. In the shear zones it is also occasionally found in large diffuse masses. In several samples the chlorite masses are elongate parallel to the foliation. They may have been deformed, or, more likely, post-kinematic alteration may have spread preferentially along the the foliation planes.

Several grains of quartz were probed in fine grained, recrystallized zones of one of the samples. It is possible that minor amounts of quartz are present in other samples, but that due to the similarities in the optical properties of plagioclase and quartz they were not identified.

C. Interpretation

Several characteristics of the mineral assemblage within the shear zone samples suggest that they formed under lower amphibolite facies conditions. These include the absence of albite, the wide range of Al_2O_3 concentrations within analyzed amphiboles, and the presence of

sphene.

The composition of all plagioclase grains probed was greater than An_{30} (Fig. 5.2). In addition, approximately fifty ten-second qualitative analyses of plagioclase grains were made. These "spot checks", which are not plotted in Figure 5.2, revealed only calcic plagioclase. These results suggest that plagioclase was deforming and recrystallizing at temperatures above the closure of the peristerite solvus. The temperature at which this solvus closes is extremely sensitive to pressure. At 2 kb a consolute temperature of 420 °C is estimated (Marayuma et al., 1982), while at 3.5 - 5.7 kb the consolute temperature is approximately 525 °C (Crawford, 1966; Nord et al., 1978; Spear, 1980; see Figure 5.4).

Most of the amphibole analyses fall within the actinolitic hornblende and magnesio-hornblende fields of Leake (1978) (Fig. 5.1). Figure 5.5 is a plot of stoichiometric Si vs. weight percent Al_2O_3 . From this plot it can be seen that there is a wide range of Al_2O_3 content within the shear zone amphiboles, even within a single sample. In some samples there are apparent gaps in Al_2O_3 content. Only one of these actually reflects the existence of two amphiboles (sample 121 // L), while in the others the lack of a sufficient number of analyses (96 // L) or the presence of relict brown magmatic amphibole (sample 33A, three high Al points) results in apparent compositional gaps. Overall, then, there tends to be a continuum of Al_2O_3 compositions. This indicates that the minimum temperature of shear zone formation was within the lower amphibolite facies, based on the work of Marayuma et al. (1983). They delineated a gap in Ca-amphibole compositions which closes with increasing temperature, and which is reflected

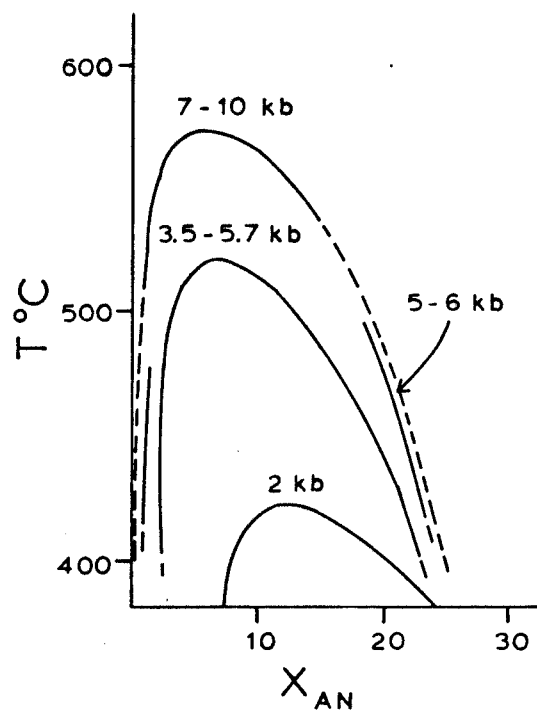


Figure 5.4

Peristerite solvus at low, medium, and high pressure, after Marayuma (1982), Spear (1980), Nord (1978), Crawford (1966).

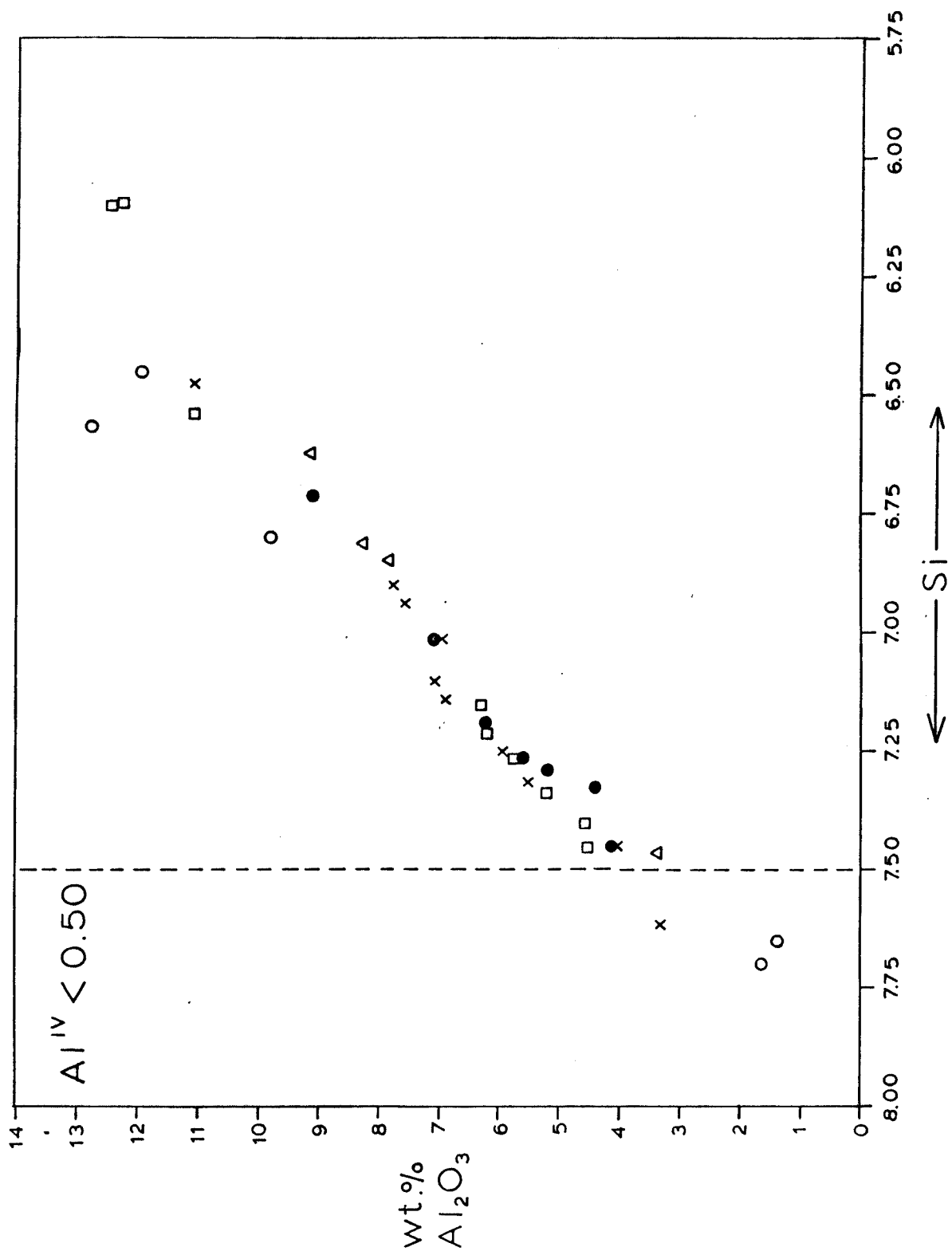


Figure 5.5

Stoichiometric Si vs. wt. % Al_2O_3 . Symbols are the same as those used in Figure 5.1.

in Al_2O_3 contents (such a gap has been recognized for years, for example see Miyashiro, 1958; Spear, 1981). Figure 5.6 is a diagram showing this compositional gap plotted against mineral assemblages of increasing grade. At low pressures (approximately 2 kb) this gap closes at approximately 420 °C. Increasing pressure increases the temperature of closure (Marayuma et al., 1983). Once the compositional gap has closed, the range of Al_2O_3 content within individual samples narrows, and steadily increases with increasing temperature.

The temperature of closure of the compositional gap in amphiboles may vary considerably, depending on bulk rock composition, fo_2 , and $\text{P}_{\text{H}_2\text{O}}$. The temperature estimate made by Marayuma et al., (1983) is lower than that of Apter and Liou (1983), Liou et al. (1974), and Moody et al. (1983), and is considered to represent a minimum estimate.

Al_2O_3 content and the range of plagioclase compositions provide minimum temperature estimates for the observed mineral assemblage. The widespread occurrence of sphene within shear zone samples offers an approximate upper temperature limit which virtually coincides with lower limit estimates. Sphene-reducing reactions take place within (Moody et al., 1983) or just beyond (Marayuma et al., 1983) the low pressure greenschist-amphibolite transition zone. At higher temperatures sphene is replaced by ilmenite. The presence of sphene suggests that lower amphibolite conditions (420 °C and just above at pressures around 2 kb) are the highest temperature conditions under which shear zone formation occurred.

The mineral assemblage discussed above is not diagnostic for pressure. A minimum pressure estimate can be calculated assuming that shear zone formation took place in the oceanic crust. With a 3 km

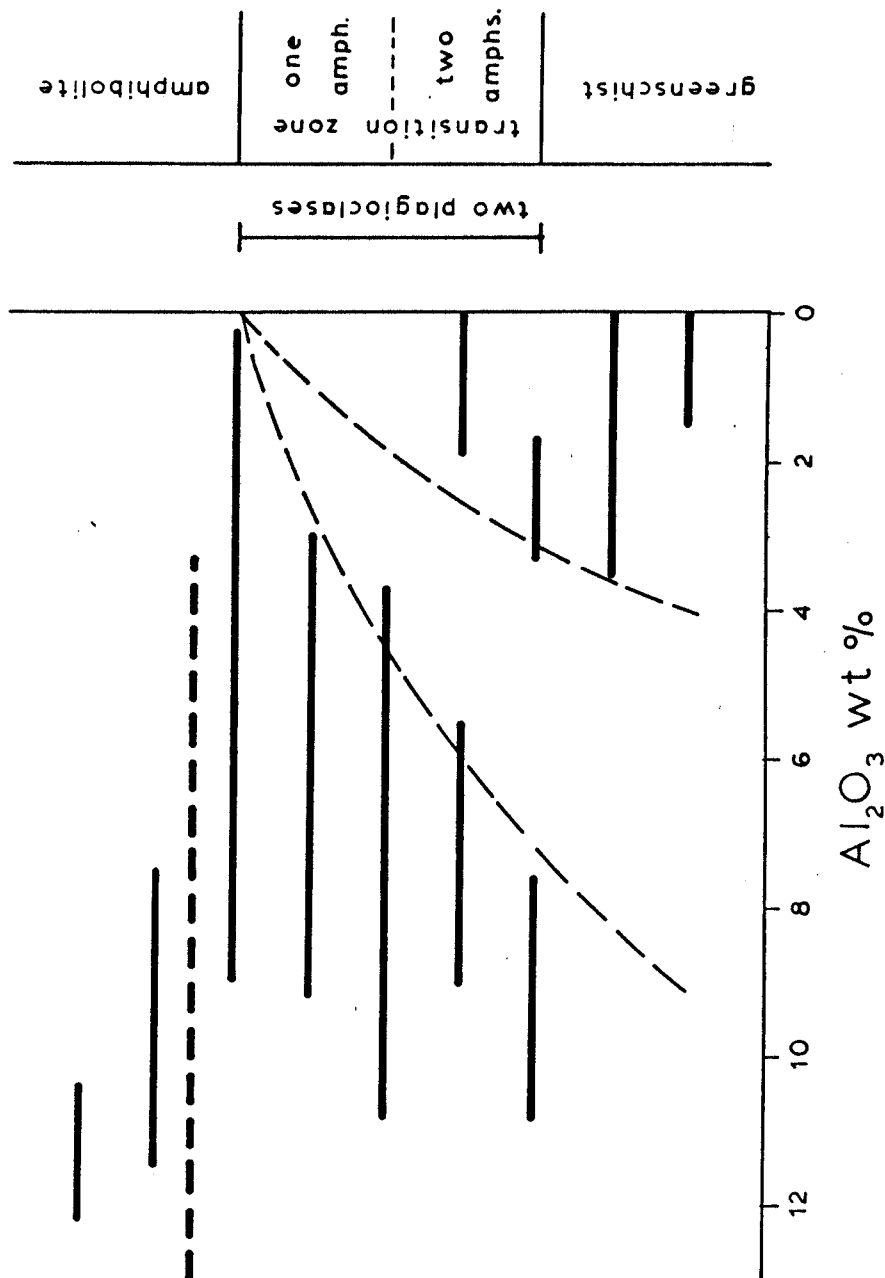


Figure 5.6

Ca-amphibole compositional gap illustrated on a plot of wt. % Al_2O_3 vs. metamorphic grade (increasing temperature at constant pressure). Thick lines indicate Al_2O_3 compositions of coexisting amphiboles from progressively higher metamorphic zones, from Marayuma et al.(1983). Thick dashed line gives range of amphibole compositions from this study.

column of water, a 2 km thick sequence of sediments, pillow lavas, and sheeted dikes, and a 4 km thick gabbroic sequence, the pressure at the base of the sheeted dikes (location of shear zones VI and VII) would be approximately 1.0 kb, and the pressure at the base of the gabbroic section (location of shear zones I and IV) would be up to 2.3 kb. If shear zone formation occurred during obduction, pressures may have been somewhat higher, although still within the low to medium pressure range discussed above.

CHAPTER 6. CONCLUSIONS AND DISCUSSION

The main conclusions which can be drawn regarding the shear zones in this study are listed here, and discussed below:

(1) The shear zones are s-c mylonites (Berthé et al., 1979) in which the c-surfaces define the main mylonitic foliation. The main foliation is parallel to the shear zone boundaries.

(2) The main mylonitic foliation is cut in several locations by brittle "mini-faults" and narrow cataclastic zones, and by undeformed, post-kinematic veins. Vein minerals include zeolites, chlorite, clinozoisite, smectite, and prehnite.

(3) Shear zone VII is cut by an undeformed diabase dike. Assuming that the dike did not result from off-axis volcanism, this relationship constrains location of shear zone formation to within a half a magma chamber's width of the ridge axis.

(4) Reconstruction of the paleo-orientations of the shear zones, coupled with sense of shear deduced mainly from microstructural criteria, indicate that the shear zones originated as paleo-axis-parallel or axis-oblique, inward- or outward-facing normal faults.

(5) The mineral assemblage of the shear zones, calcic plagioclase + hornblende + sphene, indicates that the shear zones formed under a minimum of lower amphibolite facies temperatures. At low pressures, a minimum temperature of formation of 420° C is estimated. Higher pressure estimates would increase minimum temperature estimates.

Several lines of evidence suggest that the shear zones observed in this study are likely to have formed as deep level expressions of mid-ocean ridge, axis-bounding, inward- and outward-facing normal faults,

rather than as obduction, emplacement, or later features. One of the main arguments in favor of shear zone formation within pre-obduction oceanic crust is that ductile deformation dominates, and the mineral assemblage within the shear zones indicates a minimum temperature of deformation of approximately 420 °C. Thermal modelling of the oceanic crust suggests that the 500 °C isotherm would be below the base of the oceanic crust within 30 kilometers of a slow-spreading ridge (half rate = 1 cm yr⁻¹), and within approximately 100 kilometers of a fast spreading ridge (half rate = 6 cm yr⁻¹) (Kusznir, 1980). Considering that at least 20 million years had elapsed between time of formation of the Bay of Islands ophiolites (486 ± 1.9 ma, Dunning and Krogh, 1983) and the time of obduction (469 ± 5 ma, Dallmeyer and Williams, 1975; this represents an estimate of the youngest age of obduction (Casey and Dewey, 1984)), oceanic crust formed at a fast spreading ridge axis would be 1.2×10^3 kilometers away from the ridge axis by the time of obduction, while material formed at a slow spreading ridge would be 200 kilometers away from the axis. Both of these estimates allow more than sufficient time and distance from the ridge axis to allow lower amphibolite facies metamorphism to occur within any portion of the oceanic crust.

The amphibolitized shear zones are cut by post-kinematic veins. Typical vein minerals include zeolites, chlorite, clinozoisite, smectite, and prehnite. These are low grade phases very different from the shear zone amphibolites. Vein formation must have occurred after substantial cooling of the oceanic crust, either far from the ridge axis or during obduction/emplacement.

Shear Zone VII is cut by an undeformed diabase dike. No diabase

dikes are seen below the uppermost isotropic gabbros within the ophiolites, nor do any dikes cut the sediments of the Humber Arm Supergroup which structurally underlie the ophiolite massifs; there is therefore no evidence for off-axis or post-emplacement volcanism. This suggests that Shear Zone VII definitely formed within the oceanic crust, and that it had formed before the crust had passed out of the zone of intrusion of dikes. In the case of a steady state magma chamber, maximum magma chamber half widths of 8-10 kilometers have been estimated (Sleep, 1975; Kusznir, 1980; Casey and Karson, 1981). This provides the maximum distance from the ridge axis at which Shear Zone VII could have formed.

When the shear zones are returned to their original orientations by unfolding of the North Arm Mountain massif following Model 3 it is found that three formed as paleo-axis parallel, and that three formed oblique to the ridge axis. When sense of shear across the zones is considered, the axis-parallel zones are shown to be inward- and outward-facing, oblique-slip and down-dip normal faults. Sense of shear information also suggests offsets in a normal sense across zones which formed oblique to the paleo-ridge axis.

These results are compatible with faulting observed on present day mid-ocean ridge systems. In addition, normal displacements suggest an extensional environment. If these faults were obduction or post-obduction features, reverse senses of offset would be expected.

Rosencrantz (1980) noted extensive fracturing and fissuring within the sheeted dikes of the northern half of North Arm Mountain. These zones of deformation grade, along strike, into zones of amphibolitized and deformed upper level gabbros. The deformed areas intersect the

diabase/gabbro contact at a high angle. Many of the observed zones are cut by undeformed diabase dikes. Rosencrantz (1980, 1982; Casey et al., 1981) proposed that these zones formed as oceanic crustal structures, with intense fracturing and fissuring occurring at shallow levels, and ductile deformation and amphibolitization occurring at deeper levels. The shallow level zones observed in this study have many characteristics in common with the zones described by Rosencrantz (1980), while the deeper level zones may offer some insight into the nature of deformation occurring at depth.

Shear zones VI and VII, near the top of the isotropic gabbros, are at a high angle to the diabase/gabbro contact. The deeper level Shear Zone I intersects paleo-horizontal at a lower angle. This suggests that, with depth, flattening may occur, and that steeply dipping, shallow level faults may become listric with depth in this section. The shear zones observed in this study are not continuous features that cut across the entire crustal section. Rather, they are discontinuously exposed examples of structures which are likely to have all formed in response to similar conditions, each taking up a portion of oceanic crustal deformation.

Shear zones within the lower portions of the gabbroic sections of Blow-me-Down Mountain and Table Mountain were studied by Girardeau and Mevel (1982). The widths, textures, and syn- and post- kinematic mineral assemblages within those shear zones are very similar to the features of the shear zones observed in this study. Girardeau and Mevel (1982) discerned two generations of shear zone formation. The first shear zones are 0.5 - 1.5 meters wide and layering-parallel. These shear zones formed at a low angle to paleo-horizontal. This

generation of zones are cut by narrow (< 0.15 meters wide), layering-oblique zones which formed at a high angle to paleo-horizontal. Girardeau and Mevel (1982) propose that the wide, layering-parallel shear zones formed due to magma chamber floor subsidence (Dewey and Kidd, 1977), in response to lithospheric necking (Tapponier and Francheteau, 1978), or asthenospheric flow in the upper mantle. Casey and Karson (1981) have proposed that the Bay of Islands ophiolite complex formed at a steady state magma chamber, based on compositional layering attitudes within the North Arm Mountain and Lewis Hills massifs. This led to the inference that the spreading rate at the paleo-ridge axis was moderately fast. This model makes it unnecessary to invoke magma chamber floor subsidence to account for observed layering orientations, and it makes it unlikely that significant lithospheric necking (suggested as a mechanism for axial valley formation at slow spreading ridges) occurred. Since only gabbros in the lowest part of the section were studied, it is possible that asthenospheric flow may have contributed to the formation of structures in that part of the section, or that they may have formed as the deepest level extensions of listric normal faults, a possibility which Girardeau and Mevel (1982) did not consider.

Girardeau and Mevel (1982) did not consider shear zones in the upper portion of the gabbroic section, and they did not look at sense of offset across the shear zones. This information would have been useful in determining whether oceanic crustal faulting may have been responsible for shear zone formation, and is an appropriate topic for future study.

Figure 6.1 is a schematic cross section of oceanic crust based on

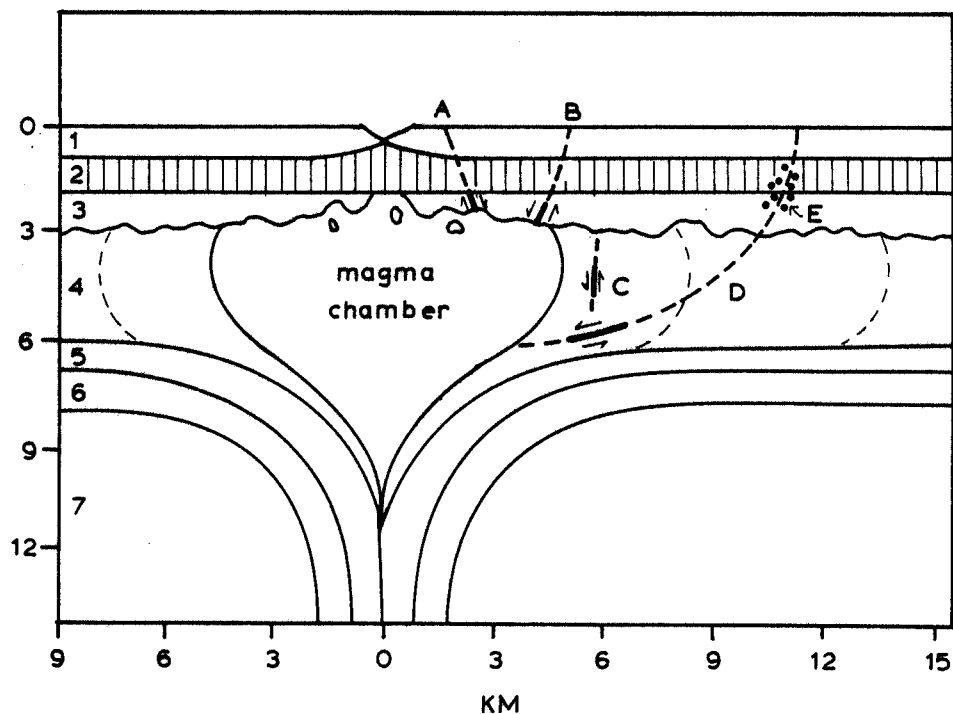


Figure 6.1

Hypothetical cross section of oceanic crust showing setting of shear zone formation. A, B, C, and D show possible extents of shear zones VII, VI, II, and I, respectively, as dashed lines. Position of shear zone in the section is shown with a heavy solid line. E represents the amphibolitized zones observed by Rosencrantz (1980, 1982). Small arrows show sense of shear results. Lithologies: (1) pillow lavas, (2) diabase dikes, (3) isotropic gabbros, (4) layered gabbros - fine dashed lines = layering orientations, (5) interlayered gabbroic and ultramafic rocks of magmatic origin, (6) ultramafic rocks of magmatic origin, (7) ultramafics.

the North Arm Mountain massif. In it are shown hypothetical locations of formation of shear zones I-VII. It is likely that larger structures such as shear zone I may have formed as the deepest portion of a once continuous structure. Lack of outcrop and limited extent of exposure of the gabbroic section prevent the tracing of the structure into higher level units of the ophiolite. If it were possible to reliably trace shear zone I to its shallowest level, it might be seen to grade into one of the broad, amphibolitized zones of Rosencrantz (1980), or perhaps be cross cut by later ocean floor, obduction-related, or other structures. The narrower, shorter zones (i.e., shear zones II and V) do not necessarily represent portions of structures which cut across the entire crust. They are likely to have formed in response to the same conditions (i.e., extension) which formed the larger, through-going structures, but they may terminate in zones of diffuse deformation, rather than cutting from the top of the crustal section to the magma chamber.

The argument that the shear zones may represent deep-level expressions of axis-bounding normal faults would be strengthened by continued study of shear zones within ophiolite massifs. It is important that the overall structure of the massifs be well known in order to be able to determine the original orientation of shear zones and other features within the oceanic crust which cannot be studied by conventional ocean floor work. Continued careful mapping is therefore important. A more extensive sampling of shear zones present between the tectonized portions of the lower crust and the shallowest crustal levels would allow comparison of shear zone orientation, conditions of deformation, and sense and amount of offset. Understanding the forma-

tion of individual structures or groups of structures furthers our understanding of the formation and evolution of oceanic crust.

REFERENCES CITED

- Allmendinger, R.W., and F. Riis, 1979, The Galapagos rift at 86°W, 1. Regional morphological and structural analysis, *J. Geophys. Res.*, v. 84, n. B10, p. 5379-5389.
- Apted, M.J., and J.G. Liou, 1983, Phase relations among greenschist, epidote-amphibolite, and amphibolite in a basaltic system, *Amer. Jour. Sci.*, v. 283A, p. 328-354.
- Ballard, R.D., J. Francheteau, T. Juteau, C. Rangin, and W. Normark, 1981, East Pacific Rise at 21°N: the volcanic, tectonic, and hydrothermal processes at the ridge axis, *Earth Planet. Sci. Lett.*, v. 55, p. 1-10.
- Ballard, R.D., and T.J. van Andel, 1977, Morphology and tectonics of the inner rift valley at lat. 36°50'N on the mid-Atlantic ridge, *Geol. Soc. Amer. Bull.*, v. 88, p. 507-530.
- Bergstrom, S.M., J. Rive, and M. Kay, 1974, Significance of conodonts, graptolites, and shelly faunas from the Ordovician of western and north-central Newfoundland, *Can. J. Earth Sci.*, v. 11, p. 1625-1660.
- Berthé, D., P. Chouckroune, and P. Jegouzo, 1979, Orthogneiss, mylonite, and non-coaxial deformation of granites: the example of the South Armorican Shear Zone, *J. Struc. Geol.*, v. 1, p. 31-42.
- Bird, J.M., and J.F. Dewey, 1970, Lithosphere plate-continental margin tectonics and the evolution of the Appalachian orogen, *Geol. Soc. Amer. Bull.*, v. 81, p. 1031-1060.
- Bonatti, E., J. Honnorez, P. Kirst, and F. Rodicati, 1975, Metagabbros from the Mid-Atlantic Ridge at 06°N: contact hydrothermal-dynamic metamorphism beneath the axial valley, *J. Geol.*, v. 83, p. 61-73.
- Bosworth, W. and B. Idleman, 1984, Structural style and sequence in the Humber Allochthon, western Newfoundland, *N.E. Geol. Soc. Amer. Prog. with Abstr.*, v. 16, n. 1, p. 4.
- Bradley, D.C., 1982, Subsidence in late Paleozoic basins in the northern Appalachians, *Tectonics*, v. 1, n. 1, p. 107-123.
- Brückner, W.D., 1966, Stratigraphy and structure of west-central Newfoundland, in *Guidebook, Geology in parts of Atlantic Provinces*, ed. W.H. Poole, Ann. Meeting, Geol. Assoc. Can., Min. Assoc. Can., p. 137-151.
- Casey, J.F., 1980, Geology of the southern half of North Arm Mountain Massif, Bay of Islands ophiolite complex, southwestern Newfoundland, Ph.D., State University of New York at Albany, 620 pp.

- Casey, J.F., and J.F. Dewey, 1984, Initiation of subduction zones along transform and accreting plate boundaries, triple junction evolution, and fore-arc spreading centres - implications for ophiolite geology and obduction, in "Ophiolites and Oceanic Lithosphere", eds. I.G. Gass, S.L. Lippard, and A.W. Shelton, Blackwell Scientific Publications, Oxford, p. 269-290.
- Casey, J.F., and J.A. Karson, 1981, Magma chamber profiles from the Bay of Islands ophiolite complex: implications for crustal level magma chambers at mid-ocean ridges, *Nature*, v. 292, p. 295-301.
- Casey, J.F., J.F. Dewey, P.J. Fox, J.A. Karson, and E. Rosencrantz, 1981, Heterogeneous nature of oceanic crust and upper mantle: a perspective from the Bay of Islands ophiolite complex, in "The Sea: Ideas and Observations on Progress in the Study of the Seas", v. 7, ed. C. Emiliani, John Wiley and Sons, New York, p. 305-338.
- Casey, J.F., D.L. Elthon, F.X. Siroky, J.A. Karson, J. Sullivan, 1985, Geochemical and geologic evidence bearing on the origin of the Bay of Islands and Coastal Complex ophiolites of western Newfoundland, *Tectonophysics*, in press.
- Casey, J.F., J.A. Karson, D. Elthon, E. Rosencrantz, and M. Titus, 1983, Reconstruction of the geometry of accretion during formation of the Bay of Islands ophiolite complex, *Tectonics*, v. 2, n. 6, p. 509-528.
- Casey, J.F., and W.S.F. Kidd, 1981, A parallochthonous group of sedimentary rocks unconformably overlying the Bay of Islands ophiolite complex, North Arm Mountain, Newfoundland, *Can. J. Earth Sci.*, v. 18, n. 6, p. 1035-1050.
- CLIPPERTON Scientific Team, 1983, EPR near 11-13°N: geology of new hydrothermal fields, *Science*, v. 219, p. 1321-1324.
- Crane, K., 1978, Structure and tectonics of the Galapagos inner rift, 86°10' W, *J. Geol.*, v. 86, p. 715-730.
- Crane, K., and R.D. Ballard, 1981, volcanics and structure of the FAMOUS Narrowgate rift: evidence for cyclic evolution: AMAR 1, *J. Geophys. Res.*, v. 86, n. B6, p. 5112-5124.
- Crawford, M.L., 1966, Composition of plagioclase and associated minerals in some schists from Vermont, U.S.A., and S.W. New Zealand, with inferences about peristerite solvus, *Contrib. Mineral. Petrol.*, v. 13, p. 269-294.
- CYAMEX, 1981, First manned submersible dives on the East Pacific Rise at 21°N (Project Rita): general results, *Mar. Geophys. Res.*, v. 4, p. 345-379.

- Dallmeyer, R.D., and H. Williams, 1975, $^{40}\text{Ar}/^{39}\text{Ar}$ ages from the Bay of Islands metamorphic aureole, their bearing on the timing of Ordovician ophiolite obduction, *Can. J. Earth Sci.*, v. 12, p. 1685-1690.
- Dewey, J.F., M.J. Kennedy, and W.S.F. Kidd, 1983, A geotraverse through the Appalachians of northern Newfoundland, in *Profiles of Orogenic Belts*, *Geodyn. Ser.*, v. 10, ed. N. Rast and F.M. Delany, AGU, Washington D.C., p.
- Dewey, J.F., and W.S.F. Kidd, 1977, Geometry of plate accretion, *Geol. Soc. Amer. Bull.*, v. 88, p. 960-968.
- Dunning, G.R., and T.E. Krogh, 1983, Tightly clustered, precise U/Pb (zircon) ages of ophiolites from the Newfoundland Appalachians, *N.E. Geol. Soc. Amer. Abstr. with Prog.*, v. 15, n. 3, p. 136.
- Ewing, M., and B. Heezen, 1956, Some problems of Antarctic submarine geology, in *Antarctica in the International Geophysical Year*, eds. A. Crary, L.M. Gould, E.O. Hurlbut, H. Odishaw, and W.E. Smith, *Amer. Geophys. Union, Geophys. Monogr.* 1, p. 75-81.
- Fahraeus, L.E., 1970, Conodont-based correlations of lower and middle Ordovician strata in western Newfoundland, *Geol. Soc. Amer. Bull.*, v. 81, p. 2061-2076.
- Fox, P.J., and D.G. Gallo, 1984, A tectonic model for ridge-plate boundaries: implications for the structure of oceanic lithosphere, *Tectonophysics*, v. , p.
- Francheteau, J., and R.D. Ballard, 1983, The East Pacific Rise near 21°N , 13°N , and 20°S : inferences for along-strike variability of axial processes of the mid-ocean ridge, *Earth Planet. Sci. Lett.*, v. 64, p. 93-116.
- Girardeau, J., and C. Mevel, 1982, Amphibolitized sheared gabbros from ophiolites as indicators of the evolution of the oceanic crust: Bay of Islands, Newfoundland, *Earth Planet. Sci. Lett.*, v. 61, p. 151-165.
- Heezen, B., 1960, The rift in the ocean floor, *Sci. Amer.*, v. 203, p. 98-110.
- Helmstaedt, H., and J.M. Allen, 1977, Metagabbro norite from DSDP hole 334: an example of high-temperature deformation and recrystallization near the mid-Atlantic ridge, *Can. J. Earth Sci.*, v. 14, p. 886-898.
- Jacobsen, S.B., and G.J. Wasserburg, 1979, Nd and Sm isotopic study of the Bay of Islands ophiolite complex and the evolution of the source of mid-ocean ridge basalts, *J. Geophys. Res.*, v. 84, p. 7429-7445.

- Karson, J.A., 1977, Geology of the northern Lewis Hills, western Newfoundland, Ph.D., State University of New York at Albany, 474 pp.
- Karson, J.A., and H.J.B. Dick, 1983, Tectonics of ridge-transform intersections at the Kane Fracture Zone, *Mar. Geophys. Res.*, v. 6, p. 51-98.
- Karson, J.A., and J.F. Dewey, 1978, Coastal complex, western Newfoundland: an early Ordovician oceanic fracture zone, *Geol. Soc. Amer. Bull.*, v. 89, p. 1037-1049.
- Kidd, W.S.F., and B. Idleman, 1982, Field relations and regional significance of the volcanics of Woods Island, Newfoundland, *N.E. Geol. Soc. Amer. Abstr. with Prog.*, v. 14, n. 1, 2, p. 30.
- Kindle, C.H., and H.B. Whittington, 1959, Some stratigraphic problems of the Cow Head area in western Newfoundland, *Trans. N.Y. Acad. Sci.*, ser. II, v. 22, p. 7-18.
- Klitgord, K.D., and J.D. Mudie, 1974, The Galapagos spreading center: a near-bottom geophysical survey, *Geophys. J. Roy. Astron. Soc.*, v. 38, p. 563-587.
- Kusznir, N.J., 1980, Thermal evolution of the oceanic crust, its dependence on spreading rate and effect on crustal structure, *Geophys. J. R. astron. Soc.*, v. 61, p. 167-181.
- Laird, J., 1980, Phase equilibria in mafic schist from Vermont, *J. Petrol.*, v. 21, p. 1-37.
- Leake, B.E., 1978, Nomenclature of amphiboles, *Amer. Mineral.*, v. 63, p. 1023-1052.
- Lilly, H.D., 1967, Some notes on stratigraphy and structural style in central west Newfoundland, *Geol. Soc. Can. Spec. Paper no. 4*, p. 201-211.
- Liou, J.G., S. Kuniyoshi, and K. Ito, 1974, Experimental studies of the phase relations between greenschist and amphibolite in a basaltic system, *Amer. Jour. Sci.*, v. 274, p. 613-632.
- Lister, G.S., and A.W. Snoke, 1984, S-C mylonites, *J. Struc. Geol.*, v. 6, n. 6, p. 617-638.
- Lock, B.E., 1969, The lower Paleozoic geology of western White Bay, Newfoundland, Ph.D. thesis, Cambridge Univ., Cambridge, England, 343 pp.
- Lonsdale, P., 1977a, Structural geomorphology of a fast-spreading rise crest: the EPR near 3°21'S, *Mar. Geophys. Res.*, v. 3, p. 251-293.
- Lonsdale, P., 1977b, Regional shape and tectonics of the equatorial East Pacific Rise, *Mar. Geophys. Res.*, v. 3, p. 295-315.

- Luyendyk, B.P., and Macdonald, K.C., 1977, Physiography and structure of the inner floor of the FAMOUS rift valley: observations with a deep tow instrument package, *Geol. Soc. Amer. Bull.*, v. 88, p. 648-663.
- Macdonald, K.C., 1977, Near bottom magnetic anomalies, asymmetric spreading, oblique spreading and tectonics of the MAR at lat. 37°N, *Geol. Soc. Amer. Bull.*, v. 88, p. 541-555.
- Macdonald, K.C., 1982, Mid-ocean ridges. Fine scale tectonic, volcanic, and hydrothermal processes within the plate boundary zone, *Ann. Rev. Earth Planet. Sci.*, v. 10, p. 155-190.
- Macdonald, K.C., and P.J. Fox, 1983, Overlapping spreading centers: new accretion geometry on the East Pacific Rise, *Nature*, v. 301, n. 5903, p. 55-58.
- Macdonald, K.C., and Luyendyk, B.P., 1977, Deep-tow studies of the structure of the mid-Atlantic ridge crest near lat. 37°N, *Geol. Soc. Amer. Bull.*, v. 88, p. 621-636.
- Macdonald, K.C., B.P. Luyendyk, J.D. Mudie, and F.N. Speiss, 1975, Near bottom geophysical study of the Mid-Atlantic Ridge median valley near lat. 37°N: preliminary observations, *Geology*, v. 3, p. 211-215.
- Malpas, J., 1979, The dynamothermal aureole of the Bay of Islands ophiolite suite, *Can. J. Earth Sci.*, v. 16, p. 2086-2101.
- Marayuma, S., J.G. Liou, and K. Suzuki, 1982, The peristerite gap in low-grade metamorphic rocks, *Contrib. Mineral. Petrol.*, v. 81, p. 268-276.
- Marayuma, S., K. Suzuki, and J.G. Liou, 1983, Greenschist-amphibolite transition equilibria at low pressures, *J. Petrol.*, v. 24, n. 4, p. 583-604.
- Mattinson, J.M., 1975, Early Paleozoic ophiolite complexes of Newfoundland: isotopic ages of zircons, *Geology*, v. 4, p. 181-183.
- Mattinson, J.M., 1976, Ages of zircons from the Bay of Islands ophiolite complex, western Newfoundland, *Geology*, v. 4, p. 393-394.
- Miyashiro, A., 1958, Regional metamorphism of the Gosaisyo-Takanuki district in the central Abukuma Plateau, *Jour. of the Faculty of Sci., Univ. of Tokyo, sec. II*, v. 1, n. 2, p. 219-272.
- Moody, J.B., D. Meyer, and J.E. Jenkins, 1983, Experimental characterization of the greenschist/amphibolite boundary in mafic systems, *Amer. Jour. Sci.*, v. 283, p. 48-92.
- Nelson, K.D., and J.F. Casey, 1979, Ophiolitic detritus in Upper Ordovician flysch of Notre Dame Bay and its bearing on the tectonic evolution of western Newfoundland, *Geology*, v. 7, p. 27-31.

- Nord, G.L., J. Hammarstrom, and E. Zen, 1978, Zoned plagioclase and peristerite formation in phyllites in southwestern Massachusetts, *Amer. Mineral.*, v. 63, p. 947-955.
- OTTER Scientific Team, 1984, The geology of the Oceanographer Transform: the ridge-transform intersection, *Mar. Geophys. Res.*, v. 6, p. 109-141.
- Pringle, I.R., J.A. Miller, and D.M. Warrell, 1971, Radiometric age determinations of the Long Range Mountains, Newfoundland, *Can. J. Earth Sci.*, v. 8, p. 1325-1330.
- Ramberg, I.B., D.F. Gray, and R.G.H. Reynolds, 1977, Tectonic evolution of the FAMOUS area of the MAR, lat. $35^{\circ}50'$ to $37^{\circ}20'$, *Geol. Soc. Amer. Bull.*, v. 88, p. 609-620.
- Ramsay, J.G., and R.H. Graham, 1970, Strain variation in shear belts, *Can. Jour. Earth Sci.*, v. 7, p. 786-813.
- Rea, D.K., and R.J. Blakely, 1975, Short-wavelength magnetic anomalies in a region of rapid sea floor spreading, *Nature*, v. 255, p. 126-128.
- Robinson, P., J.C. Schumacher, and F.S. Spear, 1982, A general review of metamorphic amphibole compositions, in *Reviews in Mineralogy*, Vol. 9B: Amphiboles: petrology and experimental phase relations, eds. D.R. Veblen and P.H. Ribbe, *Mineral. Soc. of Amer.*, p. 3-42.
- Rodgers, J., and E.R.W. Neale, 1963, Possible "Taconic" klippen in western Newfoundland, *Amer. J. Sci.*, v. 261, p. 713-730.
- Rosencrantz, E., 1980, The geology of the northern part of North Arm Massif, Bay of Islands ophiolite complex, Newfoundland: with application to upper oceanic crust lithology, structure, and genesis, Ph.D., State University of New York at Albany, 318 pp.
- Rosencrantz, E., 1982, Formation of uppermost oceanic crust, *Tectonics*, v. 1, p. 471-494.
- Rosendahl, B.R., R.W. Raitt, L.M. Dorman, and L.D. Bibee, 1976, Evolution of oceanic crust, 1. A physical model of the East Pacific Rise crest derived from seismic refraction data, *J. Geophys. Res.*, v. 81, p. 5294-5304.
- Schuchert, C., and C.O. Dunbar, 1934, Stratigraphy of western Newfoundland, *Geol. Soc. Amer. Mem.* 1, 123 pp.
- Shelton, J.W., 1984, Listric normal faults: an illustrated summary, *Amer. Assoc. Petrol. Geol. Bull.*, v. 68, n. 7, p. 801-815.
- Simpson, C., and S.M. Schmid, 1983, An evaluation of criteria to deduce the sense of movement in sheared rocks, *Geol. Soc. Amer. Bull.*, v. 94, p. 1281-1288.

- Sleep, N.H., 1975, Formation of oceanic crust: some thermal constraints, *J. Geophys. Res.*, v. 80, p. 4037-4042.
- Spear, F.S., 1980, NaSi = CaAl exchange equilibrium between plagioclase and amphibole, *Contrib. Mineral. Petrol.*, v. 72, p. 33-41.
- Spear, F.S., 1981, An experimental study of hornblende stability and compositional variability in amphibolite, *Amer. Jour. Sci.*, v. 281, p. 697-734.
- Steiger, R.H., and E. Jager, 1977, Subcommittee on geochronology: convention on the use of decay constants in geo- and cosmo-chronology, *Earth Planet. Sci. Lett.*, v. 36, p. 359-362.
- Stevens, R.K., 1970, Cambro-Ordovician flysch sedimentation and tectonics in west Newfoundland and their possible bearing on a proto-Atlantic Ocean, *Geol. Assoc. Can. Spec. Pap. n. 7*, p. 165-177.
- Stevens, R.K., 1976, Lower Paleozoic evolution of western Newfoundland, Ph.D. thesis, Memorial Univ. of Newfoundland.
- Strong, D.F., 1974, Plateau lavas and diabase dikes of northwestern Newfoundland, *Geol. Mag.*, v. 111, p. 501-574.
- Strong, D.F., and H. Williams, 1972, Early Paleozoic flood basalts of northwestern Newfoundland: their petrology and tectonic significance, *Geol. Assoc. Can. Proc.*, v. 24, n. 2, p.
- Stukas, V., and P.H. Reynolds, 1974, ⁴⁰Ar/³⁹Ar dating of the Long Range dikes, Newfoundland, *Earth. Planet. Sci. Lett.*, v. 22, p. 256-266.
- Sykes, L.R., 1967, Mechanism of earthquakes and nature of faulting on the mid-oceanic ridges, *J. Geophys. Res.*, v. 72, n. 8, p. 2131-2153.
- Tamayo Tectonic Team, 1984, Tectonics at the intersection of the East Pacific Rise with Tamayo Transform Fault, *Mar. Geophys. res.*, v. 6, p. 159-185.
- Tapponnier, P., and J. Francheteau, 1978, Necking of the lithosphere and the mechanics of slowly accreting plate boundaries, *J. Geophys. Res.*, v. 83, p. 3955-3970.
- van Andel, T.J., and R.D. Ballard, 1979, The Galapagos rift at 86°W: volcanism, structure, and evolution of the rift valley, *J. Geophys. Res.*, v. 84, p. 5390-5406.
- Weidner, D., and K. Aki, 1973, Focal depth and mechanism of mid-ocean ridge earthquakes, *J. Geophys. Res.*, v. 78, p. 1818-1831.
- White, S.H., D.J. Evans, and D.L. Zhong, 1982, Fault rocks of the Moine Thrust Zone: microstructures and textures of selected mylonites, *Tex. and Microstruc.*, v. 5, p. 33-61.

- Whittington, H.B., and C.H. Kindle, 1963, Middle Ordovician Table Head Formation, western Newfoundland, Geol. Soc. Amer. Bull., v. 74, p. 745-758.
- Williams, H., 1973, Bay of Islands map area, Newfoundland, Geol. Surv. Pap., Geol. Surv. Can., p. 34-72, 7 pp., and map.
- Williams, H., 1975, Structural succession, nomenclature, and interpretation of transported rocks in western Newfoundland, Can. J. Earth Sci., v. 12, p. 1874-1894.
- Williams, H., and W.R. Smyth, 1973, Metamorphic aureoles beneath ophiolite suites and Alpine peridotites: tectonic implications with west Newfoundland examples, Amer. J. Sci., v. 273, p. 594-621.
- Williams, H., and R.K. Stevens, 1969, Geology of Belle Isle - northern extremity of the deformed Appalachian miogeosynclinal belt, Can. J. Earth Sci., v. 6, p. 1145-1157.
- Williams, P.F., 1983, Large scale transposition by folding in northern Norway, Geol. Rund., v. 72, n. 2, p. 589-604.
- Wilson, J.T., 1966, Did the Atlantic close and then re-open?, Nature, v. 211, p. 676-681.